TARGETED KILLING OF BACTERIA BY CONJUGATION OF A SOLUBLE PHOTOSENSITIZER TO AN ANTIMICROBIAL PEPTIDE: PRINCIPLES AND MECHANISMS

A Dissertation

by

GREGORY ANDREW JOHNSON

Submitted to the Office of Graduate Studies of
Texas A&M University
in partial fulfillment of the requirements for the degree of

DOCTOR OF PHILOSOPHY

Approved by:

Chair of Committee,	Jean-Philippe Pellois
Committee Members,	Gregory Reinhart
	Timothy Devarenne
	Robert Burghardt
Head of Department,	Gregory Reinhart

August 2013

Major Subject: Biochemistry

ABSTRACT

Antimicrobial peptides (AMPs) and photosensitizers (PS) have gained attention as potential alternatives to traditional antibiotics for the treatment of microbial infection due to the decreased likelihood for acquired resistance. However, many AMPs and PS suffer from insufficient activity, specificity, or a combination thereof. AMPs can require high concentrations for effective activity, leading to non-specific side effects and increased costs. PS, on the other hand, are quite active, but are typically hydrophobic and suffer from non-specific binding and damage to host tissues. To solve these problems, we report a novel PS-AMP construct of the soluble PS eosin Y conjugated to the selective AMP $(KLAKLAK)_2$. Eosin Y has a high singlet oxygen quantum yield, which is suitable for photodynamic activity, although the solubility of eosin Y results in poor binding and activity toward membranes on its own. On the other hand, the specificity of $(KLAKLAK)_2$ is high for an AMP, but could still benefit from enhanced activity at lower concentrations. The killing activity and binding specificity of eosin-$(KLAKLAK)_2$ toward both bacteria and mammalian cells was assessed using microbiology, biochemistry, and fluorescence microscopy techniques. Additionally, the mechanism of eosin-$(KLAKLAK)_2$ activity was investigated using liposome models to determine factors involved in binding and membrane disruption. Furthermore, novel applications of transmission electron microscopy (TEM) methods were employed to observe the photodynamic effects of eosin-$(KLAKLAK)_2$ against bacteria.

The PS-AMP conjugate eosin-$(KLAKLAK)_2$ displays synergistic activity between PS and AMP in model liposome systems, and is capable of killing several clinically relevant bacteria, including the multi-drug resistant *Acinetobacter baumannii* AYE strain. Furthermore, bacterial killing is achieved in the presence of red blood cells (RBCs) and other mammalian cell lines without significant toxicity. Liposome models reveal that the lipid composition of bacteria is a potential factor responsible for the observed binding specificity and corresponding activity. Additionally, TEM methods show that eosin-$(KLAKLAK)_2$ causes extensive membrane damage to both Gram positive *Staph aureus* and Gram negative *Escherichia coli*, indicating a primary cause of cell death. A model is proposed where the activities of the PS and AMP, respectively, facilitate the activity of one another, leading to enhanced membrane disruption, and effective antibacterial activity while maintaining cell selectivity.

DEDICATION

To my wife and son, Sally and Dean, to my parents, James and Mary Della, and to my grandparents, James and Orlene. Without a childhood of encouragement, support, and guidance I may not have arrived in graduate school. Once here, the love and joy from my wife and son has made the journey considerably more pleasant.

ACKNOWLEDGEMENTS

I would like to thank Dr. Jean-Philippe Pellois and my committee members Dr. Gregory Reinhart, Dr. Timothy Devarenne, and Dr. Robert Burghardt for their helpful insight, instruction, and guidance throughout my time here at Texas A&M University. I would like thank past and present members of the Pellois lab, for helping me grow as a student and making the lab an enjoyable place to work and learn. I must also thank our collaborators for their contributions, including Dr. Hansoo Kim, and particularly Dr. E. Ann Ellis, without whose talents, the specialized electron microscopy work may not have become a reality. I would also like to thank Dr. Ryland Young and Dr. Jason Gill for use of the *Acinetobacter baumannii* AYE strain and their lab space. I would also like to thank Julius Stuart and Kyle Bruner who each spent a summer working with me in the lab while undergraduates.

I have many friends to thank, especially Roston Elwell, whose generosity has benefited me on many occasions, including when he applied his machine working skills to one of my projects. I'm also grateful to my colleagues for their insight and the department faculty and staff who were always happy to help answer questions.

I will always be indebted to my wife Sally, my parents James and Mary Della, my sister Andrea, my brother Randy, my grandparents James and Orlene, and my in-laws Jim and Christy. Thank you for all of your support.

NOMENCLATURE

PS	photosensitizer(s)
ROS	reactive oxygen species
UV	ultra-violet
VIS	visible
IR	infrared
(a)PDT	(antimicrobial) photodynamic therapy
PDI	photodynamic inactivation
PEI	polyethyleneimine
(A-)AMP(s)	(amphipathic)-antimicrobial peptide(s)
RBC(s)	red blood cell(s)
FDA	Food and Drug Administration
EM	electron microscopy
(S)TEM	(scanning) transmission electron microscopy
EDS	electron dispersive x-ray spectroscopy
DAB	3,3,-diaminobenzidine
Ce6	chlorin e6
MB	methylene blue
HaCaT	human keratinocyte cell line
COLO-316	human ovarian carcinoma
COS-7	African green monkey kidney cells

TAT	transactivator of transcription peptide
ATCC	American Tissue Culture Collection
FWHM	full width, half maximum
EMCCD	electron multiplying charge coupled device
DMEM	Dulbecco's Modified Eagle Medium
RNO	p-nitrosodimethylaniline
NBT	nitro blue tetrazolium
LUV	large unilamellar vesicle
PC	1-stearoyl-2-oleoyl-sn-glycero-3-phosphocholine
Chol	cholesterol
SM	choline sphingomyelin
PE	phosphatidyl ethanolamine
PG	phosphatidyl glycerol
CA	cardiolipin
MIC	minimum inhibitory concentration
RI	retro inverso

TABLE OF CONTENTS

Page

LIST OF FIGURES

1. INTRODUCTION

1.1 History and description of photosensitizers

Photosensitizers (PS) are dyes that are typically non-toxic in the dark, but upon light excitation, can react with oxygen in the local environment to form reactive oxygen species (ROS). The production of ROS can lead to the damage of biological molecules including proteins, lipids, and nucleic acids. This has led to the study of PS for various therapeutic applications.[1] Although the damaging effects of ROS have potential for therapeutic use, there are significant concerns related to non-specific damage.[2] Methods to enhance PS specificity would thus be a valuable improvement for therapeutic applications or for studying biochemical responses to acute ROS production.

The earliest observation that photodynamic action required light, oxygen, and a photosensitizing molecule was made by Downes and Blunt in 1877, who saw that bacterial growth was prevented in certain solutions only when exposed to both light and air.[3] However, the broadly used term in the field, "*photodynamische wirkung*" (loosely translated "photodynamic activity") was not coined until 1900 when H. von Tappeiner's student, Oscar Raab, mixed the fluorescent dye acridine orange with bacteria that subsequently died in the presence of light and oxygen.[4] Another early discovery of note came from Friedrich Meyer-Betz in 1913, who self-administered a dose of hematoporphyrin, an acid hydrolysis product of hemoglobin. After exposure to sunlight for ten minutes, an inflammatory response occurred in his skin followed by pealing, with photosensitivity remaining for weeks afterward.[5, 6]

Over a century after these early discoveries, there is an extensive list of characterized PS, with a variety of maximum excitation wavelengths ranging across the ultraviolet (UV), visible (VIS), and near infrared (IR) spectrum.[7] The excitation wavelength may be particularly important for certain applications. For example, a PS excited by IR is generally preferable for achieving a certain degree of tissue penetration.[8] However, PS with excitation wavelengths in the visible range may be more convenient to monitor in laboratory assays, and for use with more traditional light sources.[9,10]

Structurally, PS are generally composed of conjugated ring systems that are typical of light-absorbing and fluorescent molecules.[11] Some common fluorophores also have an appreciable photosensitizing activity, although they may not be typically used as PS.[7] Common antimicrobial PS include porphyrins, chlorins, pthalocyanines, xanthenes, or phenothiazines.[1] Depending on the atoms inherent to the PS structure, charged groups are often added to aid solubility in aqueous solutions.[12] Their photodynamic activity also typically correlates with their lipophilicity and effective photosensitizers often have a high propensity to bind and damage biological membranes.[13, 14]Hydrophobicity, however, can have both beneficial and negative impacts upon the photodynamic activity of a PS.[15,16] Hydrophobicity can lead to aggregation and a decreased PS availability for binding to intended targets. Another common structural modification is halogenation, found commonly with fluorescein-based PS derivatives. Halogenation typically results in a greater triplet state quantum yield for these structures, thus enhancing the photodynamic activity.[7] Halogenation also conveys protection to the PS against damage

caused by the ROS that the PS itself produces. Protection from the ROS will then increase the useful lifetime of the molecule in the context of its photodynamic activity.[17]

1.1.1 Development of photosensitizers as antimicrobial agents

The general use of PS for therapeutic purposes has been broadly termed photodynamic therapy (PDT), although this particular term is most often associated with the killing of cancer cells.[11] Applications of PS range from targeted killing of cancer cells, to dermatological treatments (e.g. acne[1, 18-20] and psoriasis[21, 22]), to antifungal[8, 23, 24] and antibacterial treatments (e.g. blood decontamination[25-27] and oral infection[28]). The use of PS for the specific application of killing bacteria or other microbes is called either antibacterial or antimicrobial PDT (aPDT), or alternatively, photodynamic inactivation (PDI). One of the most promising signs for PDI is the observation that attempts by some groups to promote an acquired bacterial resistance to PDI in the laboratory using repeated sub-lethal treatments, have failed to produce resistant strains.[29] This approach also appears to kill antibiotic resistant strains as effectively as their antibiotic sensitive counterparts.[30,31]

In order to promote targeting of PS to bacteria, modifications have been made to the structures of PS, generally increasing positive charge, to promote attraction to the negatively charged surface of bacterial membranes. This approach has had some success using addition of amino group substituents, or attachment of the PS to poly-lysine chains, or certain positively charged peptides.[32-34] The photodynamic efficacy of PS towards Gram-negative bacteria has been improved by addition of cationic compounds

such as poly-lysines and poly-ethyleneimine (PEI).[35-37] The size of the polymer conjugate is an important determinant of the efficacy with which bacterial photoinactivation is achieved.[12] For instance, *Escherichia coli* was not photo-inactivated efficiently by a PS conjugated to small molecular weight pL (i.e. 8 lysines).[12] However, a larger pL conjugate (i.e. 37 lysines) was more phototoxic, presumably because of the increased propensity of the large polycationic compound to disrupt the outer membrane of Gram-negative bacteria.[38] On the other hand, large pL complexes might not permeate the surface layer of Gram-positive bacteria as efficiently as smaller analogs because of a molecular-sieving effect.[12, 39] Consequently, increasing the size of a pL-PS conjugate might increase activity against Gram-negative bacteria but reduce the photoinactivation efficiency achieved against Gram-positive strains. As one might expect, modifications such as these are especially helpful for those PS with low inherent solubility.[40] Another approach to circumvent the hydrophobicity of some PS has been to use liposome or micelle delivery platforms.[41, 42] While these approaches have had some success, some considerable hurdles still exist for PDI.

1.1.2 Proposed mechanisms of PS in antimicrobial applications

The mechanism for the photodynamic activity of PS is well understood today. A PS undergoes a process resembling phosphorescence, where absorption of light leads to transition of an electron from its ground state (S0) to an excited state (S1), followed by intersystem crossing to the triplet state (T1). Instead of phosphorescing, however, a PS achieves photodynamic activity through one of two competing pathways originating in

the triplet state. A PS can either react: 1) in an *electron* transfer mechanism with molecular oxygen (O_2), other substrates, or solvent, or 2) in an *energy* transfer mechanism with molecular oxygen.

The classification of these PS reactions are not always consistent in the literature.[6,43,44] For this work, I will use the most commonly used definition in the PS field.[45] According to this classification, a Type I photosensitizing mechanism involves electron transfer via hydrogen atom or lone electron. Examples of Type I reactions include: 1) the formation of superoxide ($O_2^{\cdot -}$) by electron transfer from a PS, or 2) lipid radical formation after removal of a hydrogen atom by the PS. A Type II mechanism is defined by resonant energy transfer from the excited PS to ground state molecular oxygen (triplet state, $^3O_2$), resulting in the formation of an excited state singlet oxygen ($^1O_2$). This last process is unique in that the ROS produced is an excited state molecule which can decay to its ground state without necessarily undergoing a secondary reaction with other substrates. This characteristic may impart a greater degree of spatial restriction to the activity of singlet oxygen. Conversely, other ROS ($O_2^{\cdot -}$, $HO\cdot$, and H_2O_2) persist in their chemical states until they react with another molecule.[46]

The ROS produced can result in a network of damaging reactions to biological molecules, such as lipids, proteins, and nucleic acids. In the lipid membrane, ROS can produce lipid hydroperoxides (LOOH), which can lead to subsequent rounds of radical lipid peroxidation.[47] Low levels of ROS-mediated lipid damage may be tolerable, but sufficient damage can lead to irreparable damage and cell death.[48]

1.1.3 Present problems with PS treatments

Achieving specific targeting may be the single greatest problem facing the use of PS in therapeutic applications.[1] When trying to target cancer cells, bacteria, or fungi for *in vivo* PDI, non-specific damage to healthy cells can occur with detrimental effects. For example, earlier attempts in mouse models to accelerate wound healing after bacterial infection using a porphyrin derivative, actually delayed healing compared to mice not treated with PDI, since the skin was injured by the treatment[49] This result may not be that surprising, considering the affinity that porphyrins typically have for mammalian tissue, exemplified by the persistence of sensitization from porphyrins in patients.[6] Recently, however, some notable successes for topical infections in mice have been demonstrated with the fullerene BF6 and the phthalocyanine derivative RLP068.[40, 50] Hamblin and co-workers have shown that the binding of pL-PS conjugates to microbial cells is very rapid while the endocytic uptake of these compounds into human cells is slower.[12, 37, 51] In principle, it is therefore possible to target and kill bacteria selectively by controlling the time cells are exposed to the conjugates. However, moieties that can target bacteria while inducing minimum endocytic uptake in human cells might provide a better selectivity between these different cell types and be more practical in general.

Another inherent limitation to PS treatments is the requirement of light. Penetration of visible light into tissue is generally on the order of 1 mm, while near infrared (e.g. 750 nm) may penetrate up to 10 mm.[52] This prevents the use of PS in more internal locations unless the region can be surgically accessed, which can be undesirably invasive. The other side of this problem, as exemplified by porphyrins again, is not being

able to turn the light off (or go out in the sun), requiring patients to carefully cover their skin.

While acquired resistance to PDI has not been seen, Gram negative bacteria appear to have a naturally increased resistance to PDI treatments compared to Gram positive counterparts. Higher concentrations of PS or light dose are usually required to kill Gram negative strains to the same extent as Gram positive strains. These effects are likely due to the additional physical barrier presented by their outer membrane, and the additional targets in the outer membrane that can prevent ROS reaching the cell membrane or cellular interior.[53]

1.2 History of antimicrobial peptides (AMPs)

The antimicrobial peptide (AMP) magainin, was first discovered in the African clawed frog *Xenopus laevis*, when surgical incisions repeatedly failed to produce infection, even though the frogs were placed back into non-sterile water after stitching the incisions.[54] Extracts of the skin revealed that two peptides (magainin 1 & 2) with closely related sequences were responsible for the antimicrobial activity. This discovery opened up the field to a vast number of peptides with analogous function, along with the realization that these peptides were a part of the innate immune system of all multicellular organisms.[55] The assortment of AMPs discovered generally fall into a few conserved structural classes, including helical, β-sheet, and extended structures.[56]

1.2.1 Development of AMPs as antimicrobial agents

Regardless of class, AMPs are most often characterized by positive and hydrophobic residues, providing for electrostatic attraction to the negatively charged surface of bacteria, and an affinity for the lipid membrane. Association of AMPs with the membranes of bacteria leads to membrane disruption, leakage, and cell death. This activity has brought much attention to AMPs as potential therapeutic agents for antibiotic-resistant bacteria.[57] The therapeutic potential for AMPs was particularly supported by a report in 2006, which demonstrated the requirement of 600-700 bacteria culture passages before resistance was noted.[58] The first clinical trial for an AMP was with a modified analog of the original Magainin peptide, which showed comparable activity to a traditional antibiotic in the treatment of foot ulcers. However, the Food and Drug Administration (FDA) did not approve the treatment because of its lack of improvement over existing therapies.[57, 59, 60] To date, there are still no AMPs approved for therapeutic use, although several AMPs and synthetic structural analogs are in clinical development.[57, 61] An increased understanding of the mechanisms involved in membrane disruption may allow for sufficient improvements in design for such peptides to become therapeutics in the near future.

1.2.2 Proposed mechanisms of AMPs in antimicrobial applications

To complement the negative surface charge of bacteria, most AMPs are positively charged and electrostatically attracted to the bacterial surface. Cellular targets include lipid A in Gram negative bacteria, the peptidoglycan layer of Gram positive

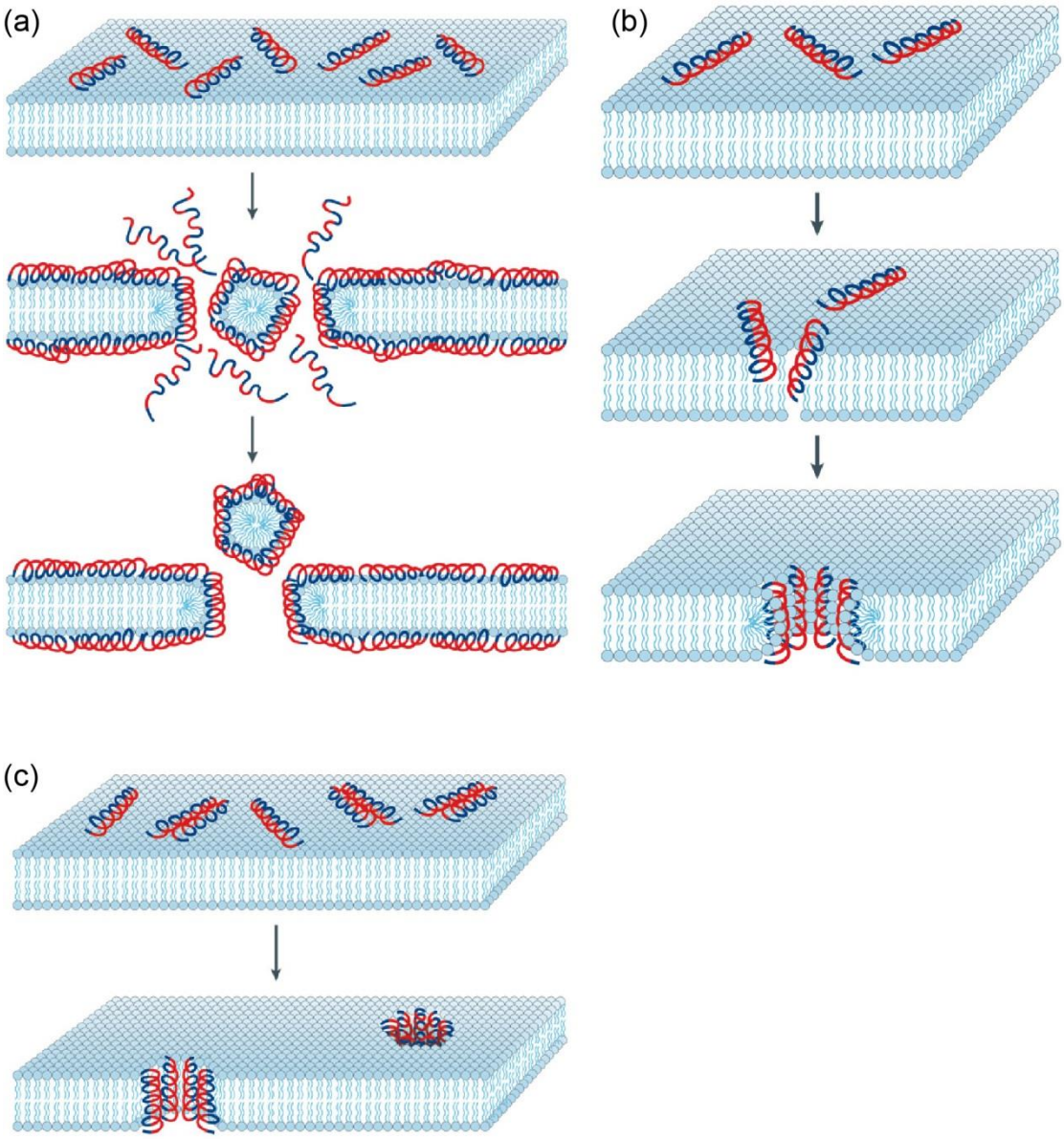

Figure 1-1 Models of membrane disruption by AMPs. Carpet (a), toroidal pore (b), and barrel stave (c) models. Used by permission.[62]

bacteria, negatively charged phospholipids, and even intracellular targets for some AMPs.[63, 64] There are differing and disputed mechanisms for different AMPs, which generally consist of a membrane disrupting activity.[56, 65] Helical amphipathic AMPs (A-AMPs) are the most frequently modeled in the literature, typically using model liposome systems. A-AMPs are easily synthesized, and are not dependent on disulfide chemistry like certain AMP classes, making A-AMPs easier to handle.

The most common membrane disruption models are depicted in Figure 1, which include the toroidal pore, barrel stave, and carpet models. Each of these mechanisms relies upon a threshold concentration of AMP bound to the membrane before stable pore formation can take place.[62] Using liposome models, an early binding phase is observed with membrane thinning increasing with AMP concentration. A threshold is then reached where pore formation occurs, with the membrane width remaining constant thereafter.[66] In the context of PDI, such pore formation is toxic to the bacteria. Therefore, understanding the chemical properties and structural features required to enhance this activity, while also maintaining sufficient specificity to bacterial membranes, is of great importance to the field.

1.2.3 Potential problems of AMP-based treatments

To achieve bacterial killing, a high concentration of AMPs can be required for sufficient activity, leading to undesirable non-specific side effects.[65] The membrane disruption activity of AMPs is also thought by some to be equally disruptive to mammalian cells under the conditions where the same amount of peptide is bound.

However, these conditions are usually avoided due to a more favorable attraction to bacterial cells.[65] Improvements to cell specificity with synthetic mimics could decrease side effects and lower the costs of treatment, making synthetic AMP mimics an area of increasing interest.[61]

A major concern for the use of AMPs as therapeutic agents has been the evidence for resistance mechanisms in several bacteria strains against AMP activity. These mechanisms include charge modification of Lipid A and cell membrane phospholipids, efflux pumps for peptide export, peptidase activity, modification of intracellular targets, and DNA mutations among others.[63] If AMPs are to become legitimate therapeutic treatments, it will be necessary to recognized resistance mechanisms over time and continue to develop AMPs or mimics with improved activity.

1.3 The use of PS-peptide conjugates: current successes and shortfalls

Within only the last year, two groups have published on conjugates of porphyrin derivatives with AMPs as targeting agents, one of which was submitted during the same time as our own work described herein.[67, 68] The first was an AMP with specific affinity for LPS, using protoporphyrin IX as a PS.[67] This work demonstrated successful killing of four Gram negative strains, with preferential binding to bacteria over Jurkat cells. While this construct was effective, it is presumably limited to use on Gram negative bacteria. Since PDI treatments are likely to require killing of both Gram negative and positive bacteria, a compound with activity against both Gram types is preferable. The second work mentioned above used the AMP Apidaecin 1b (from the honey bee), also

with a porphyrin derivative attached.[68] Apidaecin 1b does not disrupt bacterial membranes, but instead achieves its antimicrobial activity by binding intracellular targets. For that construct then, it serves only as a targeting agent. This construct was able to kill Gram negative *E. coli*, although killing of the Gram positive *S. aureus* was limited even at relatively high concentrations around 15 μM.

Apart from AMPs, other peptides have been used to target PS to bacteria. One group conjugated the arginine-rich cell-penetrating peptide TAT to the porphyrin derivative, TPP.[33] While this construct was shown to kill both Gram positive and Gram negative bacteria *in vitro*, bacteria killing experiments were not performed in the presence of other cell types, nor was the conjugate tested for hemolytic activity towards RBCs. TAT has been shown to have extensive endocytic uptake by mammalian cells, so one could envision that the specificity for the TAT-TPP construct is likely non-existent, or even biased towards targeting of mammalian cells. Furthermore, conjugation of TAT to the otherwise innocuous fluorophore, tetramethylrhodamine, has been shown to be highly toxic to mammalian cells, as TAT places TMR in sufficient proximity to membrane targets to cause extensive membrane blebbing and cell death.[69] Although the TAT-TPP conjugate might conceivably be used outside the body, these two works assert the caution that must be taken when choosing a method to target PS to bacteria, as well as the extent of testing that should be performed to determine the suitability for certain antibacterial applications.

A general concern for the conjugation of a PS to a targeting agent is that certain photosensitizers have poor solubility, such as hematoporphyrin. PS with low solubility

can lead to non-specific retention of the free PS in tissues, and lengthened patient sensitivity to light. One can envision then, that the use of an AMP to target a hydrophobic PS might be successful initially, but if the AMP were to be degraded by proteases, then the free PS might create problems similar to those with hematoporphyrin. Additionally, and perhaps more importantly, the hydrophobic nature of a PS conjugated to the AMP might significantly reduce the binding specificity of the peptide, making the treatment less effective overall.

1.4 A possible solution for increasing specificity and activity of PS: targeting a soluble PS by conjugation to a selective AMP

One approach to achieve broad spectrum bacterial killing (both Gram positive and negative) while sparing other cells, might be to choose an AMP as a PS-targeting agent, which has demonstrated such bacteria killing and selectivity on its own. One example of such an AMP is $(KLAKLAK)_2$, which shows similar killing towards both *E. coli* and *S. aureus*, while having low red blood cell lysis and low toxicity to mammalian cells.[70] This type of targeting agent could potentially participate in the membrane disruption process during PDI, since the peptide itself has membrane lytic properties. If the AMP could participate in the membrane lysis event, this might lead to a bacteria killing efficiency greater than the sum of the two entities alone.

The choice of a PS with high solubility could also be advantageous, since the PS would not be expected to interfere with the targeting and membrane interaction of the

AMP. Furthermore, if the AMP were to be degraded, the soluble PS would not bind to cells on its own, and might simply be eliminated from the body.

1.5 The goal of my study

Although both PS and AMPs have found some successful applications, there are significant limitations for their therapeutic use, due to either non-specific effects or the requirement for unreasonably high concentrations. A recent development has successfully targeted a PS to Gram negative bacteria,[67] however, to our knowledge, an agent for broad spectrum targeting of PS to bacteria has not been established prior to separate works of another group[68] and our own.[10] We reasoned that the broad spectrum activity of the model AMP $(KLAKLAK)_2$ might convey broad spectrum targeting for a soluble PS if it were conjugated to the AMP. To this end, I used the PS-AMP conjugate eosin-$(KLAKLAK)_2$ to study the general principle of targeting a PS to bacteria using an AMP. I tested this hypothesis and studied the mechanisms of the conjugate activity using both *in vitro* and *in cellulo* approaches. This work serves as a proof of concept and lays the groundwork for the rational design of photosensitizing compounds with greater efficiency and targeting specificity.

2. EOSIN-$(KLAKLAK)_2$ IS AN EFFICIENT ANTIBACTERIAL AGENT WITH HIGH SPECIFICITY FOR A BROAD SPECTRUM OF BACTERIA*

2.1 Introduction

In this section I tested whether an amphiphilic antimicrobial peptide (A-AMP) might serve as an attractive tool to target PS to bacterial membranes.[71] While A-AMPs are typically cationic, they nonetheless contain fewer positive charges than poly-lysine or CPPs. Consequently, their endocytic uptake into mammalian cells is expected to be comparatively reduced. Overall, our hypothesis was therefore that an A-AMP would improve the antimicrobial photodynamic effect of a PS while inducing little damage toward mammalian cells.

To test this hypothesis, a conjugate between the antimicrobial peptide $(KLAKLAK)_2$ and the photosensitizer eosin Y was used (eosin-$(KLAKLAK)_2$).[70, 72] On one hand, $(KLAKLAK)_2$ is a prototypical A-AMP with minimum inhibitory concentration (MIC) values of approximately 6 μM for *E. coli*, *P. aeruginosa, and S. aureus*.[70, 73] Moreover, hemolytic concentrations and sublethal concentrations to 3T3 cells are two orders of magnitude greater than MIC values.[70] On the other hand, eosin Y is a photosensitizer that, despite a high quantum yield of singlet oxygen (Φ~0.6), is not very phototoxic on its own.[13] This can be attributed in part to the fact that eosin Y is

* Reprinted with permission from "Photoinactivation of Gram positive and Gram negative bacteria with the antimicrobial peptide $(KLAKLAK)_2$ conjugated to the hydrophilic photosensitizer eosin Y" by Johnson, G.A., Muthukrishnan, N., Pellois, J.P., 2013. *Bioconjugate Chemistry*, 24, 114-123, Copyright 2013 American Chemical Society.

relatively hydrophilic and that it does not significantly partition into membranes.[13] We were therefore interested in testing whether $(KLAKLAK)_2$ could enhance the photodynamic activity of this singlet oxygen generator by bringing it in proximity to bacterial membranes. The choice of a PS with low intrinsic phototoxicity might seem surprising as a starting point. However, we were concerned that a more photoactive but more lipophilic PS might significantly compromise the targeting specificity of the A-AMP conjugate. Indeed, many PS are too lipophilic to distinguish between human and bacterial bilayers. With eosin-$(KLAKLAK)_2$ however, we anticipated that the A-AMP would dictate binding specificity with minimal interference by the conjugated PS.

2.2 Results

2.2.1 Design of a light irradiation apparatus for high throughput of photosensitizing samples

In order to efficiently process light-irradiated samples in a 96-well plate, we designed an apparatus that could provide an even distribution of light over all wells, depicted in Figure 2-1. This design consisted of an inexpensive 600 W halogen lamp (Utilitech #0320777) purchased from a local hardware store. The selection of filters available in the size required for a 96-well plate is limited in both quantity and spectral selectivity. Fortunately, we managed to find a 5 x 7 inch green filter (Edmund Optics cat. no. NT46-624, 470 - 550 nm FWHM) having a transmittance which aligned with the absorbance spectrum of eosin Y and eosin-$(KLAKLAK)_2$ (Figure 2-2). Although the green filter does show additional transmittance at longer wavelengths, this region is not

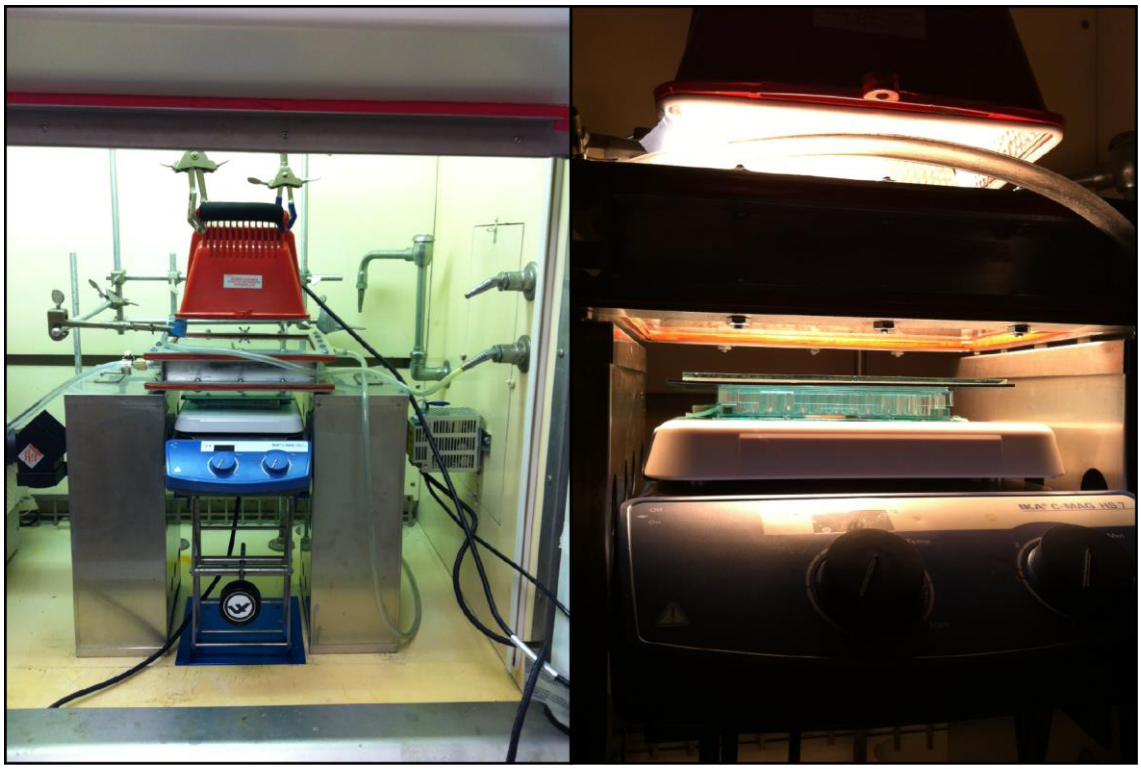

Figure 2-1: Light irradiation setup designed for excitation of photosensitizers in a high throughput 96-well plate format. (At left) An air hose was used for direct cooling of the lamp to prevent overheating, and water lines to and from a flowing water filter (steel box directly below lamp). (At right) Sample irradiation in a 96-well plate with lid, color filter, and diffusing glass, always performed with the room darkened.

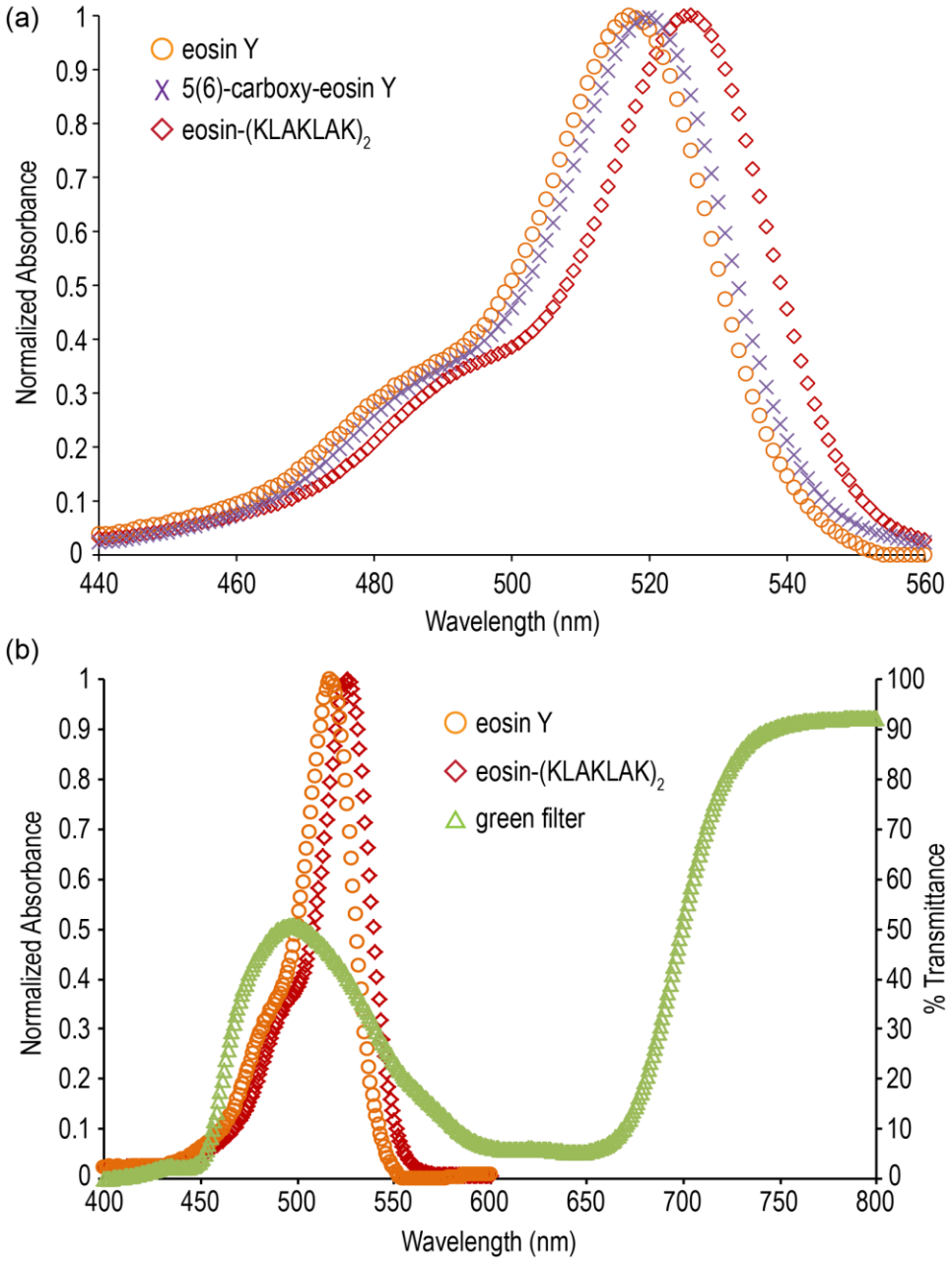

Figure 2-2: Absorbance and transmittance spectra of reagents and filter used for photosensitizing assays. (a) Normalized absorbance spectra for eosin Y, 5(6)-carboxy-eosin Y, and eosin-$(KLAKLAK)_2$. (~5 µM for each sample) (b) Overlay of eosin Y and eosin-$(KLAKLAK)_2$ absorbance (left axis) with the green filter transmittance (right axis).

absorbed by eosin Y (Figure 2-2), nor did light alone without reagents have any significant effects in any experiment performed. It is interesting to note that the addition of a carboxylic acid to eosin Y results in a small shift in the maximum from 517 to 520 nm. However, the conjugation of 5(6)-carboxy-eosin Y to the N-terminus of $(KLAKLAK)_2$ results in a larger shift from 520 to 526 nm, indicating a more significant alteration of absorbance properties after conjugation to the peptide. The spectral output of the lamp through the water filter, or in addition to green or red filters is shown in Figure 2-3. The red filter (Edmund Optics cat. no. NT46-622, cut-on 625 nm) was applied for the PS chlorin e6 (Ce6), used for an experiment discussed later in section 3. The spectral analyzer in our possession could only measure from 500-800 nm, so it was not possible to quantify how much infrared light was absorbed by the water filter. However, sample temperature remained relatively constant over the 30 min irradiation, rising only ~4-5 degrees Celsius, with a range of ~25-29 degrees Celsius over the duration of the experiment. In comparison, the lamp itself after the experiment is very hot and cannot be touched without being burned, indicating that the sample is protected from the large majority of heat produced by the lamp.

2.2.2 Eosin-$(KLAKLAK)_2$ kills Gram-negative and Gram-positive bacteria upon light irradiation

The photodynamic activity of eosin-$(KLAKLAK)_2$ was tested against *A. baumannii*, *P. aeruginosa*, and *E. coli* (Gram negative) as well as *S. aureus*, and *S. epidermidis* (Gram positive). Eosin Y was used as an unconjugated control. The

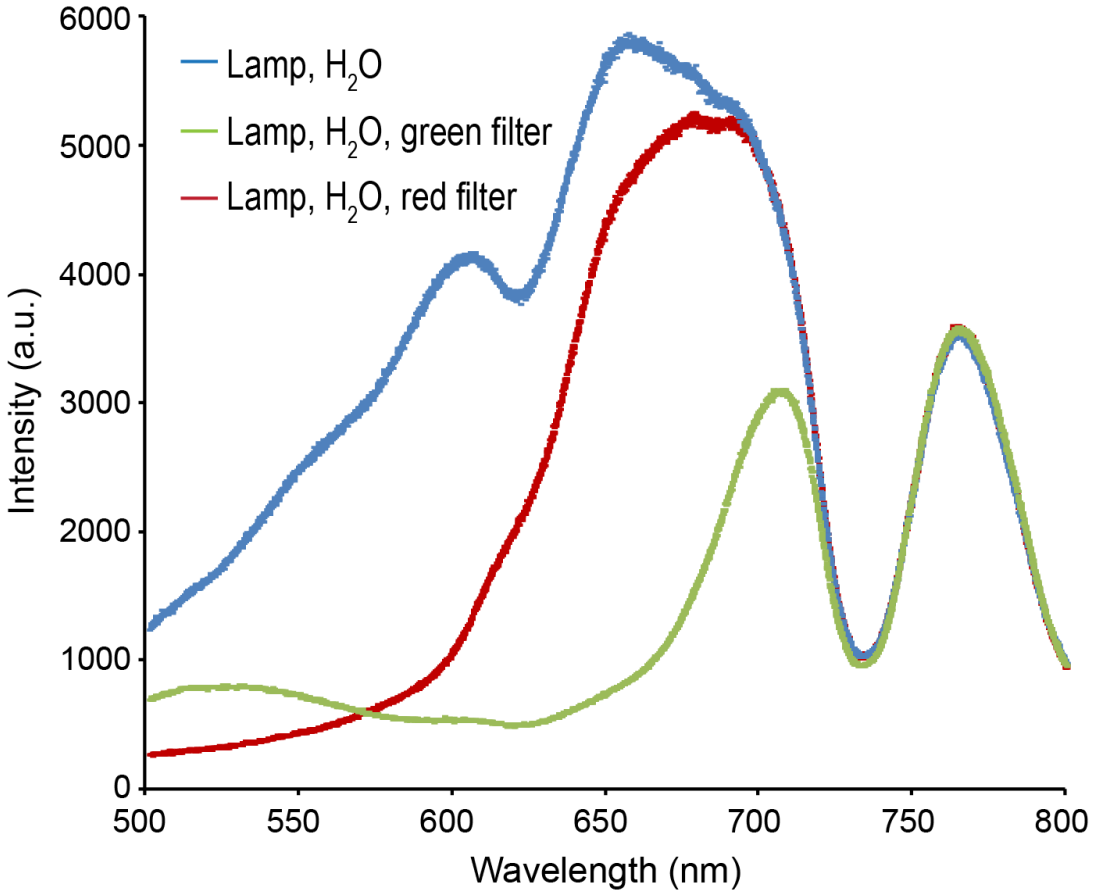

Figure 2-3: Spectra of quartz-halogen lamp in the presence and absence of light filters used for different PS. Spectra represent light after passage through the water filter and diffusing glass, shown with and without green and red filters in place.

bactericidal activity of the tested compounds was determined both in the dark and after irradiation at 525 nm for 30 min (525 nm corresponds to the excitation maximum of eosin Y). As shown in Figure 2-4, eosin Y alone or $(KLAKLAK)_2$ alone had no significant effects on cell viability at 10 μM in the absence or presence of light. Similarly, eosin-$(KLAKLAK)_2$ had little activity toward *S. aureus or E. coli* in the dark below 10 μM. However, the antimicrobial activity of eosin-$(KLAKLAK)_2$ towards both strains was greatly enhanced with irradiation at 525nm, as the peptide killed 99.9 to 99.999% of bacteria at 1 μM. As expected for a light-induced process, the extent of photoinactivation was dependent on the irradiation time and increasing light exposure increased killing (Figure 2-4d). Similar results were obtained with *A. baumannii*, *P. aeruginosa*, and *S. epidermidis* (Figure 2-5). Dark toxicity of Eosin-$(KLAKLAK)_2$ against the Gram negative strains *E. coli* and *Ps. aeruginosa* occurred at 10 μM or less (Figures 2-1b and 2-2a). Even greater dark toxicity was observed towards the Gram negative *A. baumannii*, with 99% killing at 1 μM, a greater extent of killing than observed from $(KLAKLAK)_2$ alone for this strain (Figure 2-2b).

2.2.3 Eosin-$(KLAKLAK)_2$ associates with bacteria to a greater extent than eosin Y

In order to investigate a potential cause for the difference in activity between eosin Y and eosin-$(KLAKLAK)_2$, the association of these two compounds with bacteria was characterized. Eosin-$(KLAKLAK)_2$ and eosin Y were incubated with 10^8 CFU/mL of *E. coli* or *S. aureus* under conditions identical to those used for photoinactivation

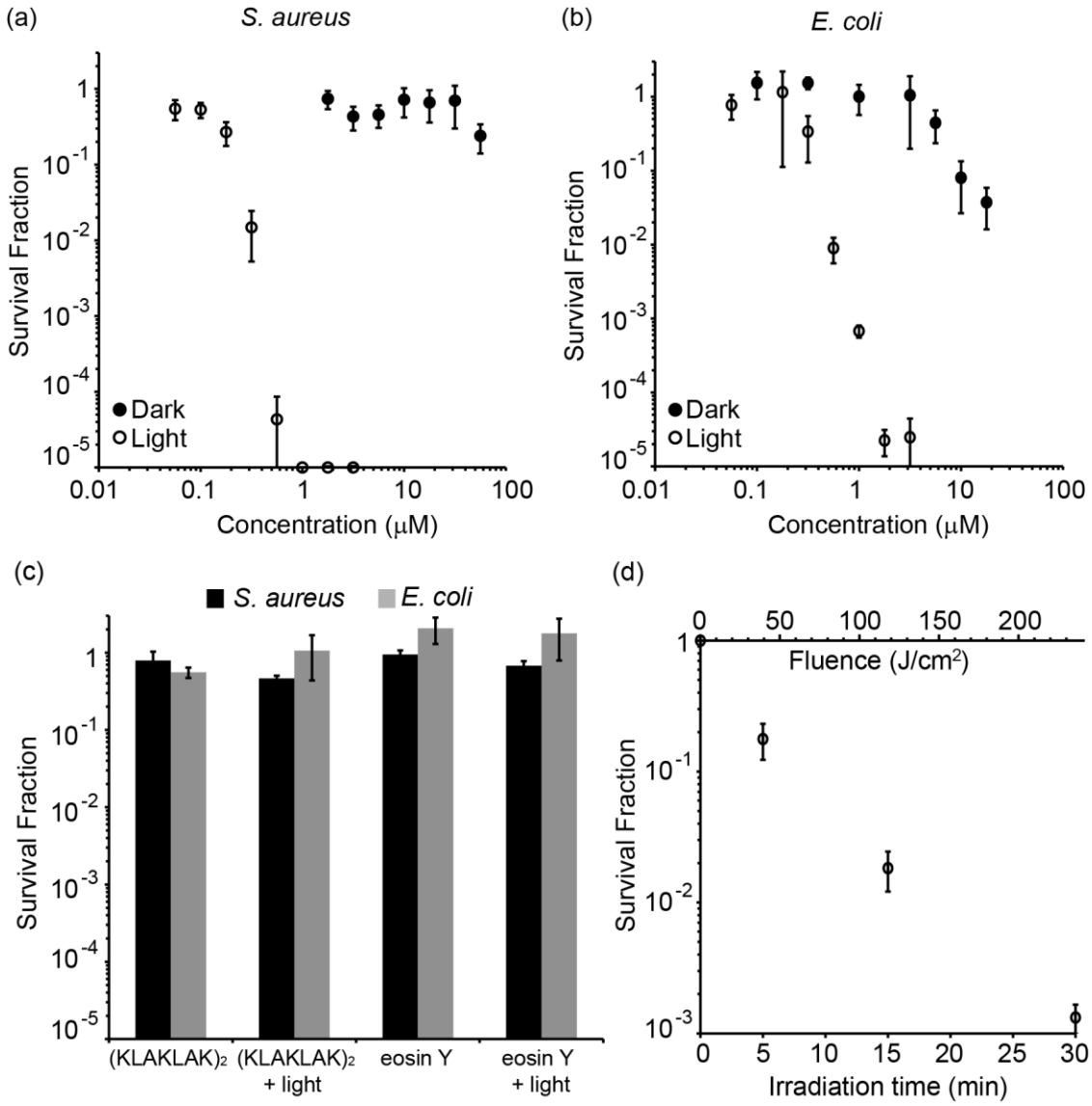

Figure 2-4: Eosin-$(KLAKLAK)_2$ kills bacteria upon light irradiation while eosin Y does not. (a) Survival fraction of *S. aureus* (10^8 CFU/mL) after exposure to eosin-$(KLAKLAK)_2$ in the dark or irradiated with visible light for 30 min. (b) Identical experiment performed with *E. coli* (10^8 CFU/mL). (c) Effects of $(KLAKLAK)_2$ (10 μM) or eosin Y (10 μM) on the survival of *S. aureus* or *E. coli* after 30 min incubation in the absence or presence of light. (d) Photoinactivation of *E. coli* (10^8 CFU/mL) by eosin-$(KLAKLAK)_2$ (1 μM) as a function of irradiation time and fluence.

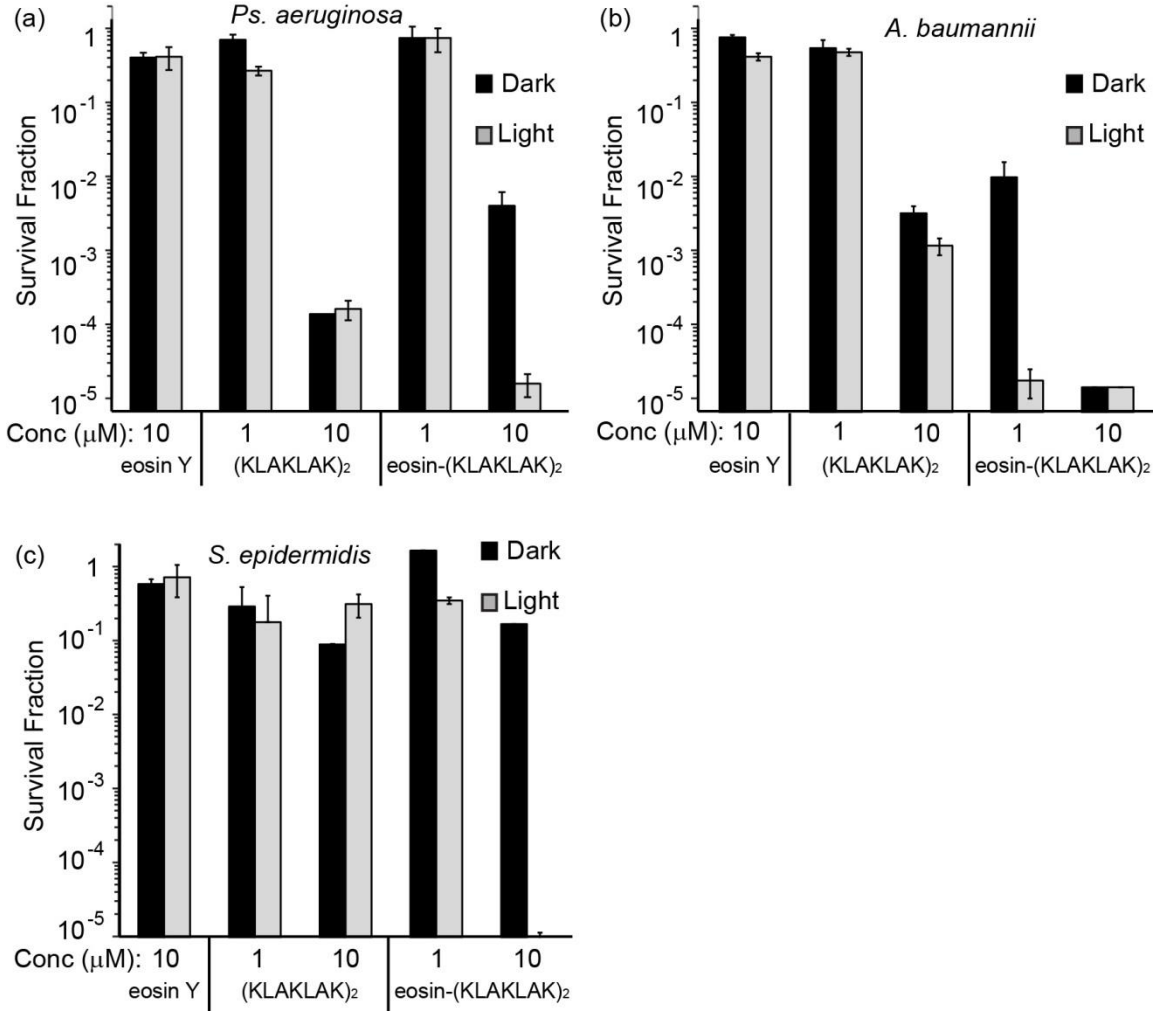

Figure 2-5: Eosin $(KLAKLAK)_2$ kills a broad spectrum of bacteria. Survival fraction of *Ps. aeruginosa* (a), *A. baumannii* (b), and *S. epidermidis* (c) (10^8 CFU/mL for each) after exposure to eosin-$(KLAKLAK)_2$ in the dark or irradiated with visible light for 30 min.

assays. The mixtures were centrifuged to separate the molecules present in solution (soluble fraction) to those bound to bacteria (pellet fraction). The amount of eosin-$(KLAKLAK)_2$ or eosin Y associated with bacteria was then determined by measuring the fluorescence present in the pellet fraction. The concentrations tested were in the range of 0.1 to 1 μM for eosin-$(KLAKLAK)_2$ and 0.1 to 10 μM for eosin Y. These conditions correspond to peptide to bacteria ratios at which no killing is detected in the dark. The signal detected is therefore proportional to the binding of eosin-$(KLAKLAK)_2$ or eosin Y to live bacteria as opposed to the binding of these compounds to dead cells.

As shown in Figure 2-6, eosin-$(KLAKLAK)_2$ associates with *E. coli* or *S. aureus* to a greater extent than eosin Y. For instance, eosin-$(KLAKLAK)_2$ partitions equally between soluble and bacteria-bound fractions at 1 μM while eosin Y is mostly present in solution at this concentration (Figure 2-6a). These data therefore suggest that $(KLAKLAK)_2$ enhances the binding of eosin Y to bacteria. Moreover, the amount of eosin-$(KLAKLAK)_2$ bound to *E. coli* at 1 μM is equivalent to that obtained for eosin Y at 10 μM (Figure 2-6b). It is interesting to note that, at these respective concentrations, eosin-$(KLAKLAK)_2$ photo-inactivates 99.9% of bacteria while eosin Y has no photo-induced activity (see Figure 2-4). These results therefore suggest that $(KLAKLAK)_2$ enhances the photodynamic activity of the photosensitizer.

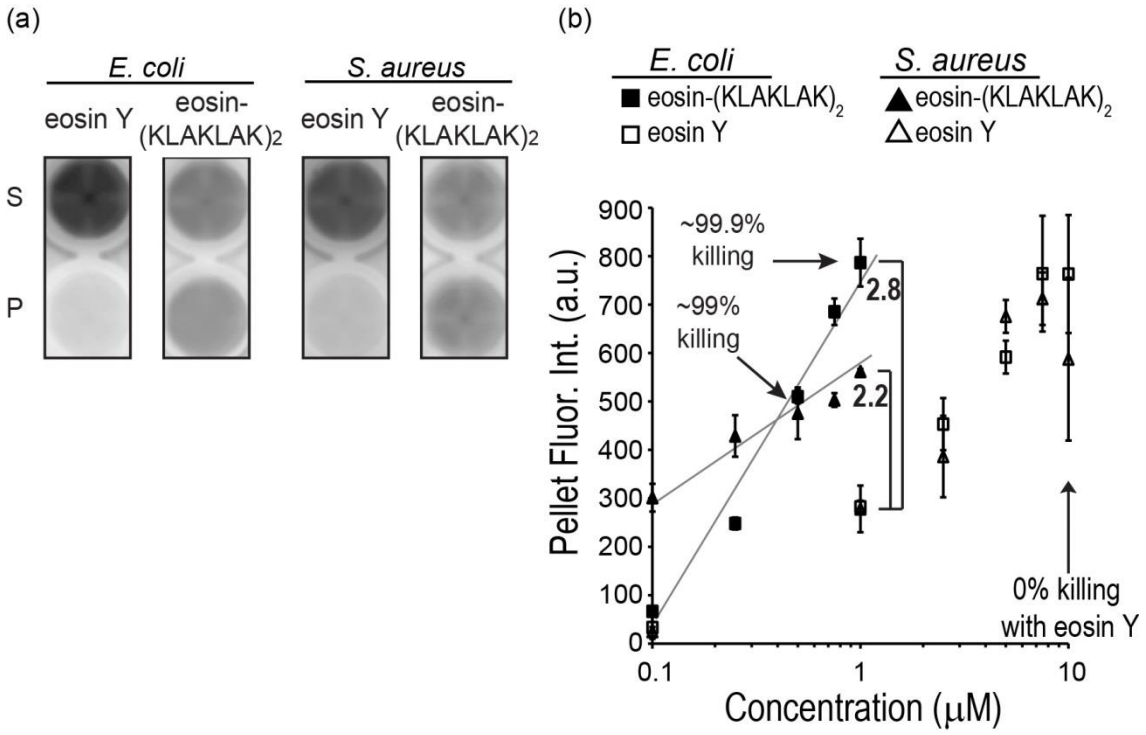

Figure 2-6: Eosin-(KLAKLAK)$_2$ has a higher propensity to bind to bacteria than eosin Y. (a) Partitioning of eosin Y and eosin-(KLAKLAK)$_2$ between soluble (S) and bacteria-bound (pellet, P) fractions. Bacteria (10^8 CFU/mL) were incubated with 1 μM of eosin Y or eosin-(KLAKLAK)$_2$. The samples were centrifuged to separate the S and P fractions and placed in a multi-well plate. The fluorescence of each fraction was imaged on a fluorescence scanner. The fluorescence image obtained is represented as an inverted monochrome (dark contrast = bright fluorescence). (b) Fluorescence intensity associated with bacteria (pellet fraction) as a function of eosin-(KLAKLAK)$_2$ or eosin Y concentration. *E. coli* (■ eosin-(KLAKLAK)$_2$, □ eosin Y) and *S. aureus* (▲ eosin-(KLAKLAK)$_2$, Δ eosin Y) were used at 10^8 CFU/mL and the fluorescence intensities reported are those obtained when the samples are kept in the dark (no bacterial killing is obtained under these conditions). The percentage of killing achieved when the same samples are exposed to light for 30 min are highlighted with arrows (these numbers correspond to the results obtained in Figure 1-1). Numbers depicted at 1 μM indicate difference in fluorescence from eosin Y, relative to *E. coli* and *S. aureus*.

2.2.4 Eosin-$(KLAKLAK)_2$ photoinactivates bacteria without causing significant photohemolysis

In order to test the specificity of the compounds between bacterial and mammalian cells, the photo-hemolytic activities of eosin-$(KLAKLAK)_2$ and eosin Y were assessed. For these assays, RBC suspensions containing 2.5 million cells per milliliter were used (this corresponds to a 2000-fold dilution of the concentration of lipid to eosin- $(KLAKLAK)_2$ ratios similar to that expected in the bacterial inactivation assays (see discussion for details). The photosensitizers Chlorin e6 (Ce6) and methylene Blue (MB) were also used for comparison. Ce6 (Φ_Δ ~0.65)[7] photolyses RBCs readily and this compound was therefore was used as a positive control.[74] MB (Φ_Δ ~0.52) [7] on the other hand, is not significantly photohemolytic and it has been successfully used for blood decontamination.[25] MB was therefore used to assess the stringency of our photohemolysis assay. Ce6 showed approximately 70% and 100% photohemolysis at 1 µM and 10 µM, respectively, while photohemolysis by MB was 20% and 45% at these concentrations. Eosin-$(KLAKLAK)_2$ showed less photohemolysis than MB, with less than 10% photohemolysis at 1 µM or lower, and 40% at 10 µM (Figure 2-7b). Eosin-$(KLAKLAK)_2$ also showed the lowest hemolysis in the dark with only 5% hemolysis at 10 µM. Interestingly, eosin Y gave similar results to eosin-$(KLAKLAK)_2$. These data therefore suggest that conjugation of $(KLAKLAK)_2$ to eosin Y does not significantly increase the photolytic activity of the photosensitizer towards erythrocytes.

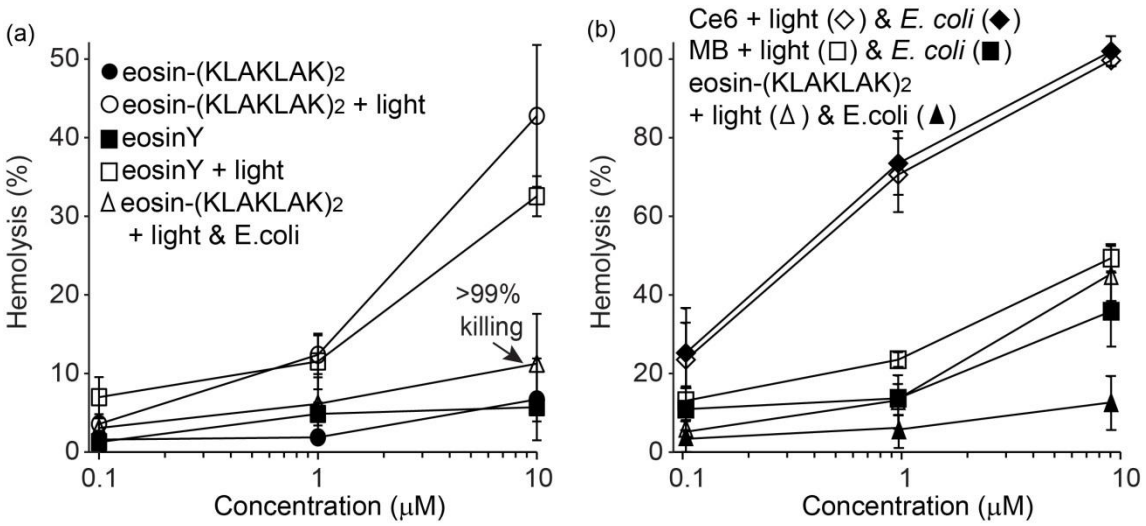

Figure 2-7: Eosin-(KLAKLAK)$_2$ shows a better response to the presence of bacteria in photohemolysis assays than the most promising PS for blood decontamination, methylene blue. (a) Hemolytic activities of eosin-(KLAKLAK)$_2$ and eosin Y in the dark or after 30 min irradiation with light. Suspensions of RBCs (0.05% by volume) were prepared with or without *E. coli* (10^8 CFU/mL) present. (b) Comparison of eosin-(KLAKLAK)$_2$ hemolytic activity to chlorin e6 (Ce6) and methylene blue (MB). Experiments were performed in the same way as in (a).

In order to address the issue of specificity more directly, a suspension of *E. coli* (10^8 CFU/mL) was added to the RBCs before mixing with PS or peptide conjugate for light irradiation. The photo-hemolytic activity and bacterial photoinactivation were measured after irradiation. As shown in Figure 2-7, the photo-hemolytic activity of eosin-$(KLAKLAK)_2$ was reduced in the presence of *E.coli*. For instance, the photohemolysis obtained at 10 μM eosin-$(KLAKLAK)_2$ was reduced from approximately 40% to 10% in the presence of bacteria. On the other hand, more than99% bacterial photoinactivation was achieved. These results therefore suggest that eosin-$(KLAKLAK)_2$ destroys bacteria preferentially over red blood cells. In order to confirm that the reduction in photohemolysis observed was not a general phenomenon simply caused by the addition of *E. coli*, Ce6 was here again included as a control. It has been shown that *E. coli* does not take up Ce6 at the concentrations used in our assays.[12] We therefore expected that presence of *E. coli* should not affect the photo-hemolytic activity of Ce6. Indeed, no significant change in the photohemolysis activity of Ce6 was observed in the presence of *E. coli* (Figure 2-7b).

In order to test whether the reduced hemolysis by eosin-$(KLAKLAK)_2$ in the presence of *E. coli* and *S. aureus* is caused by the association of the peptide with the bacteria, samples of eosin-$(KLAKLAK)_2$ and cells were examined by microscopy before and after irradiation (Figures 2-8 and 2-9). The fluorescent photosensitizer rose bengal (RB) was also observed with cells in order to compare eosin-$(KLAKLAK)_2$ with a lipophilic PS known to be non-specific in its binding.[75] As shown in Figure 2-8a, the fluorescence signal of eosin-$(KLAKLAK)_2$ is associated with bacteria (also visible in

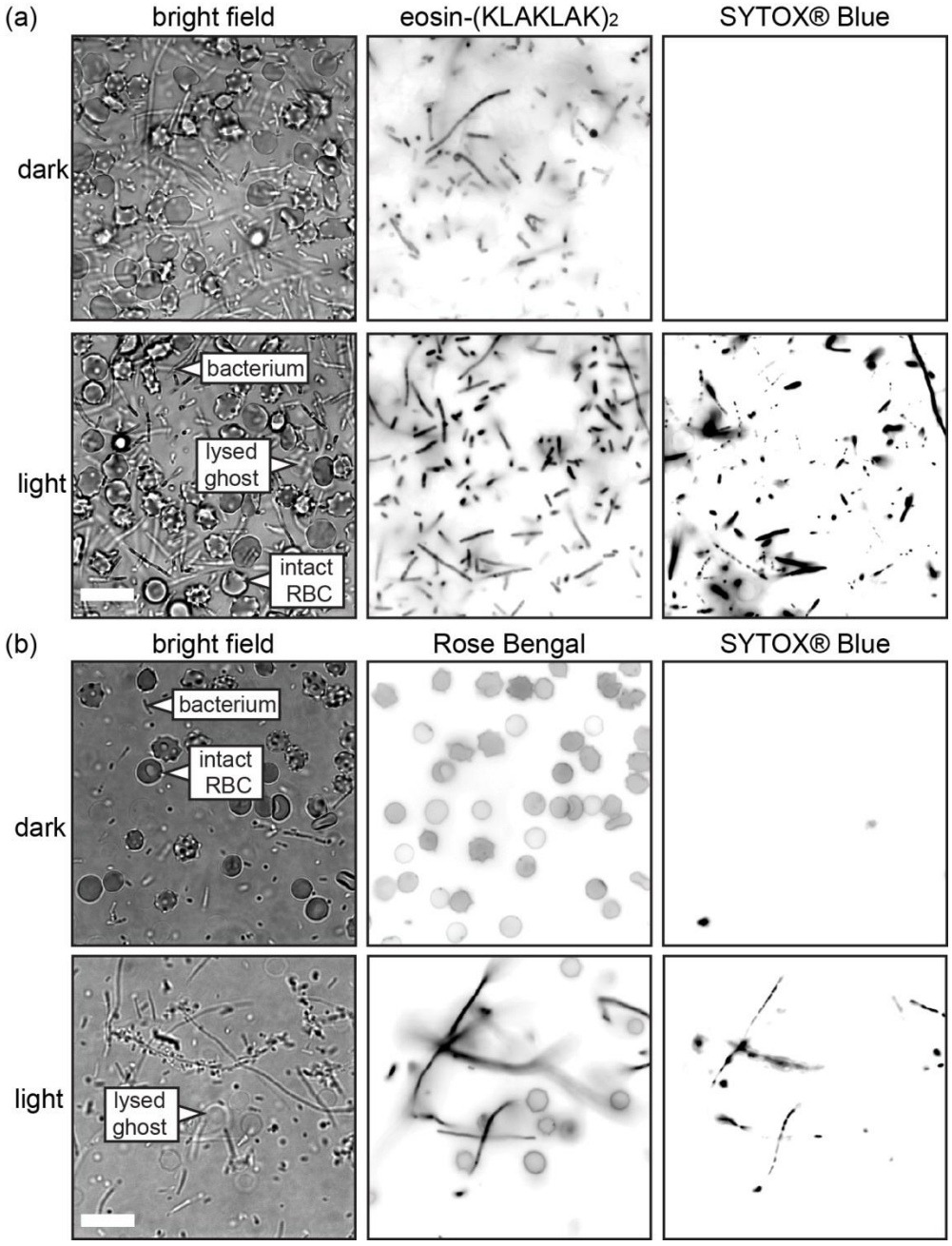

Figure 2-8: Eosin-(KLAKLAK)$_2$ binds more to *E. coli* than RBCs. Bright-field and fluorescence imaging of RBCs (0.05% by volume) mixed with *E. coli* (10^8 CFU/mL) and (a) eosin-(KLAKLAK)$_2$ (1 μM) or (b) Rose Bengal (1 μM). Images were acquired after 30 min incubation in the absence or presence of light. SYTOX Blue was added to the samples afterward to detect dead bacteria. Intact RBCs in the bright field images have a dark contrast while lysed ghosts are transparent and only visible as rings. Scale bar is 10 μm.

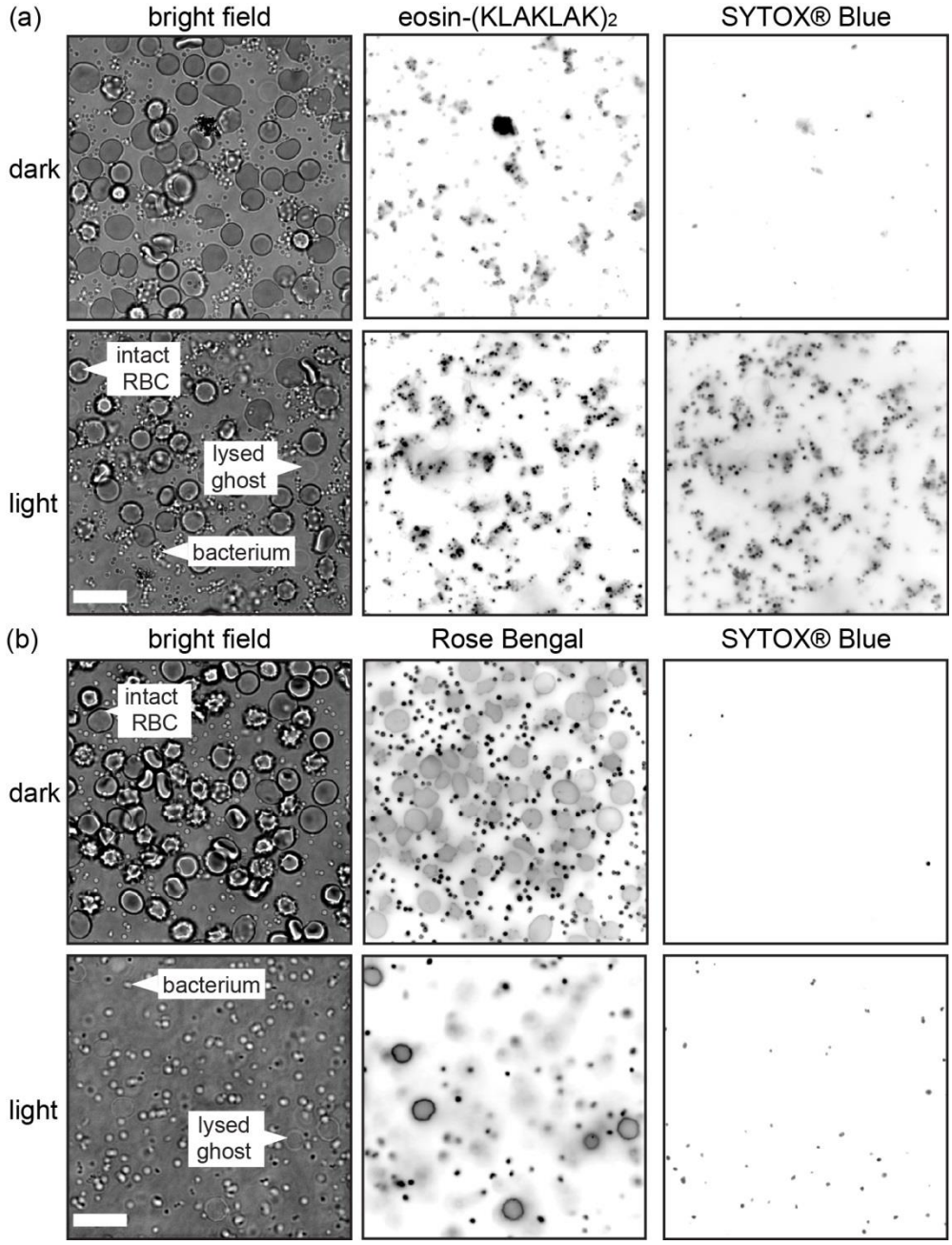

Figure 2-9: Eosin-(KLAKLAK)$_2$ binds more to *S. aureus* than RBCs. Bright field and fluorescence imaging of RBCs (0.05% by volume) mixed with *S. aureus* (10^8 CFU/mL) and (a) eosin-(KLAKLAK)$_2$ (1 μM) and (b) Rose Bengal (1 μM). Images were acquired after 30 min incubation in the absence or presence of light. SYTOX® Blue was added to the samples afterwards to detect dead bacteria. Intact RBCs in the bright field images have a dark contrast while lysed ghosts are transparent and only visible as rings. Scale bar is 10 μm.

bright field image) while RBCs present in the sample are not stained by eosin-$(KLAKLAK)_2$. In comparison, RB stains the plasma membrane of RBCs. This therefore indicates that eosin-$(KLAKLAK)_2$ binds to bacteria to a much greater extent than to RBCs. In addition, most of the RBCs present after irradiation have a dark contrast consistent with these cells being intact and only a few lysed ghosts can be observed (ghosts are transparent but their plasma membrane remains visible). These results therefore confirm that the extent of photohemolysis of RBC in the presence of *E. coli* is limited. Moreover, bacteria were stained by SYTOX® Blue after irradiation but not before. SYTOX® Blue is a nuclear stain that does not penetrate live cells but that can stain cells with a compromised membrane. These data therefore indicate the bacteria present were photo-inactivated. A colony-forming assay after serial dilutions of the sample confirmed that more than 99% of the bacteria were killed. Overall, these data suggest that, while eosin-$(KLAKLAK)_2$ is capable of lysing the membrane of RBCs at certain peptide to cell ratios, the photolytic activity of this compound is more pronounced toward bacteria. In particular, this appears to be consistent with a preferential association of the peptide with bacterial cells over erythrocytes.

2.2.5 Eosin-$(KLAKLAK)_2$ is less phototoxic towards mammalian cells than bacteria

The phototoxicity of eosin-$(KLAKLAK)_2$ was tested with HaCaT (human keratinocytes), COS-7 (monkey fibroblasts) and COLO 316 (human ovarian carcinoma). Cells were incubated with eosin Y, $(KLAKLAK)_2$, and eosin-$(KLAKLAK)_2$ and

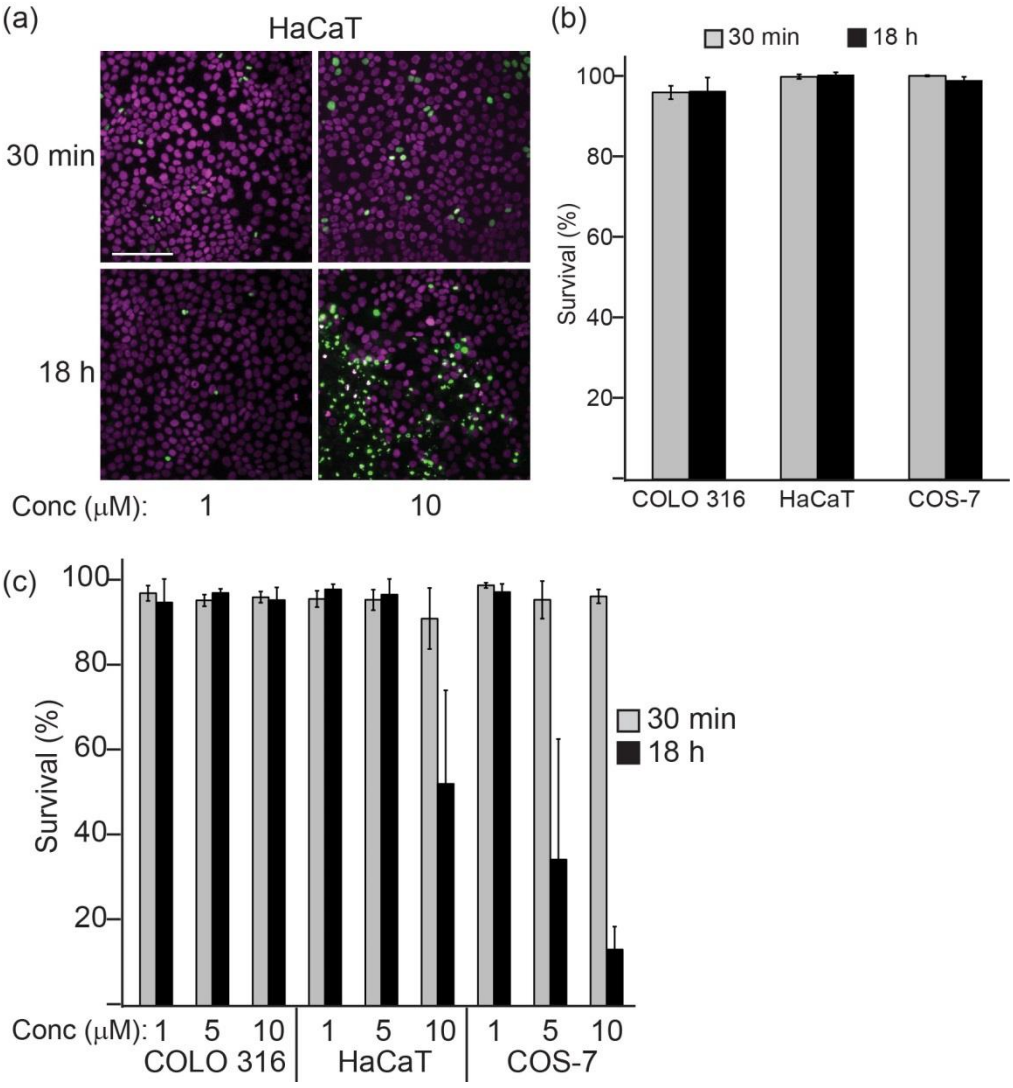

Figure 2-10: Eosin-(KLAKLAK)$_2$ is not phototoxic toward COLO 316, HaCaT, or COS-7 cell lines at concentrations required to kill bacteria. (a) Fluorescence microscopy imaging (20×) of HaCaT cells incubated with eosin-(KLAKLAK)$_2$ (1 or 10 μM) for 30 min with light exposure. Cells were coincubated with Hoescht (pseudo colored purple here) and SYTOX Green dyes immediately following (30 min) or 18 h after illumination. Percent survival of cells was determined by counting the cells with compromised plasma membranes (stained by SYTOX Green) compared to the total (all cells are stained by Hoescht). Scale bar is 100 μm. (b) Survival of COLO 316, HaCaT, and COS-7 cells with eosin-(KLAKLAK)$_2$ (10 μM) in the dark (c) Survival of COLO 316, HaCaT, and COS-7 cells exposed to eosin-(KLAKLAK)$_2$ (1, 5, and 10 μM) for 30 min with light irradiation. Cell viability was assessed 30 min and 18 h after exposure.

irradiated under the same conditions used for bacterial photoinactivation. The viability of cells was assessed before and after irradiation using SYTOX® Green exclusion assays (Figure 2-10a), where the cell-impermeable SYTOX® Green only fluoresces after binding to DNA in cells whose membranes have been compromised, indicating cell death. In the dark the compounds showed no toxicity towards the cells in the range of concentration tested (1 to 10 μM) (Figure 2-10b). In the light some toxicity was observed only at higher concentrations (5 or 10 μM) for COS-7 and HaCaT, while COLO 316 showed no toxicity even at 10μM eosin-$(KLAKLAK)_2$ (Figure 2-10c).

The propensity of eosin-$(KLAKLAK)_2$ to be internalized by mammalians cells was evaluated by fluorescence microscopy (Figure 2-11a). The peptide TAT labeled with eosin- Y (eosin-TAT) was used as a positive control. TAT is an arginine-rich peptide known to be endocytosed efficiently by mammalian cells.[69] After incubation with cells for 30 min, eosin-TAT distributed in a punctate manner inside cells, indicative of the accumulation of the compound inside endocytic organelles (Figure 2-11a). In contrast, a fluorescence signal at least 10-fold less than this intensity was detected for eosin-$(KLAKLAK)_2$ under identical conditions (Figure 2-11b). Together, these data suggest that eosin-$(KLAKLAK)_2$ associates minimally with mammalian cells and that the photodynamic activity of eosin-$(KLAKLAK)_2$ toward mammalian cells is significantly less than that obtained with bacteria.

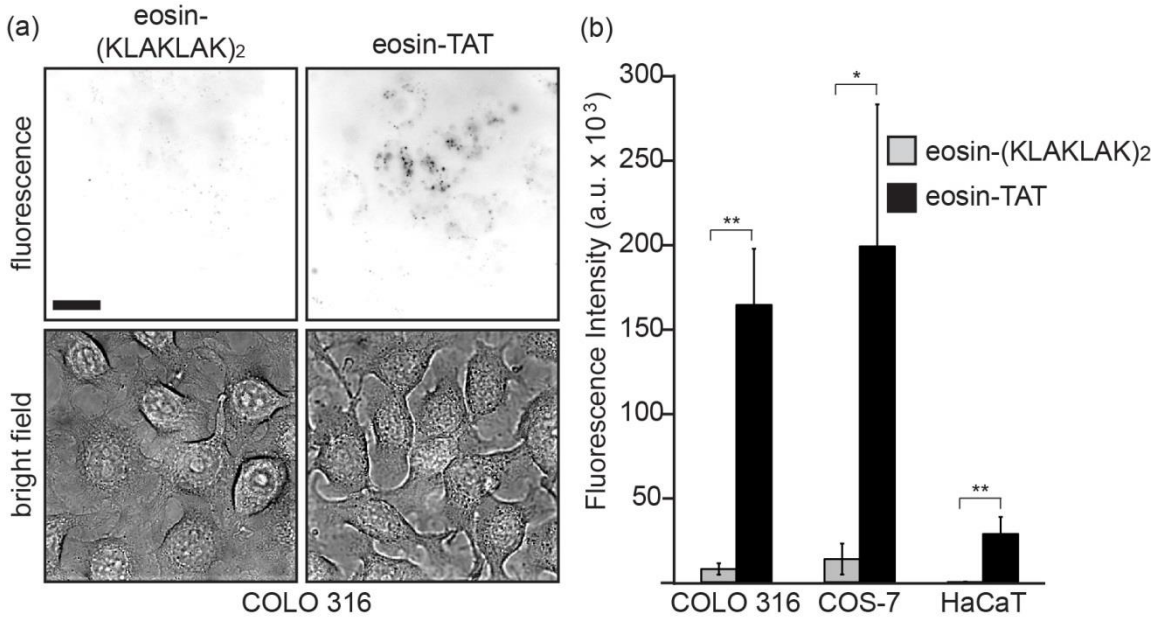

Figure 2-11: Eosin-$(KLAKLAK)_2$ is taken up by cells significantly less than eosin-TAT. (a) Bright-field and fluorescence microscopy imaging of COLO 316 cells (100×) incubated with eosin-$(KLAKLAK)_2$ (1 μM) or eosin-TAT (1 μM) for 30 min. Scale bar is 10 μm. (b) Total fluorescence intensity of cells incubated with eosin-$(KLAKLAK)_2$ or eosin-TAT (1 μM) for 30 min (two-tailed t test, * = $p < 0.05$, ** = $p < 0.01$).

2.3 Discussion

Bacterial photoinactivation assays show that a moderate dose of light can reduce the lethal concentration of eosin-$(KLAKLAK)_2$ towards bacteria by more than 10 fold. The peptide $(KLAKLAK)_2$ greatly enhances the photodynamic activity of eosin Y as this PS is not very phototoxic on its own. Moreover, eosin-$(KLAKLAK)_2$ caused the photoinactivation of Gram-positive and Gram-negative strains to a similar extent. Our results therefore suggest that, unlike what has been observed for other cationic PS, the outer membrane of the gram-negative bacteria might not represent a significant barrier to the penetration of the peptide conjugate.[76-78] This is consistent with the reported MICs of $(KLAKLAK)_2$ being similar for Gram-negative and Gram-positive bacteria.[70] The binding of eosin-$(KLAKLAK)_2$ with *E. coli* and *S. aureus* was greater than that of eosin Y alone, indicating that the peptide promotes the association of the PS to bacteria. The peptide therefore appears to enable the photodynamic activity of the photosensitizer by acting as a targeting agent.

Based on the models proposed in the literature for $(KLAKLAK)_2$ and related antimicrobial peptides, one can envision that eosin-$(KLAKLAK)_2$ binds to bacterial lipid bilayers. At the low concentration at which photoinactivation is achieved, however, the peptide itself is not able to cause the formation of lytic pores, as no antimicrobial activity is detected in the dark. Yet, binding experiments reveal that, with equal amount of eosin-$(KLAKLAK)_2$ and eosin Y bound to bacteria, eosin-$(KLAKLAK)_2$ is able to photo-inactivate bacteria but eosin Y cannot. A possible explanation for this effect might be that $(KLAKLAK)_2$ contributes to destabilizing the bacterial membrane. $(KLAKLAK)_2$

could for example, promote lysis or enhance the damaging effect of ROS generated by the photosensitizer. We envisioned for instance, that the A-AMP-disrupted bacterial membrane might become more susceptible to the ROS produced by the PS agent, while ROS-induced membrane damage might also facilitate membrane disruption by the A-AMP. Another possible explanation involves the idea that $(KLAKLAK)_2$ might position eosin Y in a cellular location that eosin Y alone is not otherwise able to access and that the generation of ROS at this particular location kills cells more effectively. Further studies are required to validate these models and elucidating which of these principles can be exploited should be useful for the design of optimized PDT agents.

An important aspect of antimicrobial PDT is the specificity of the PS toward bacterial cells. Ideally, the photodynamic drug should kill bacteria without damaging host tissues. In order to compare the photodynamic activity of eosin-$(KLAKLAK)_2$ towards bacteria to that obtained with RBCs, photohemolysis assays were performed with human erythrocytes. Under the assumption that a lipid bilayer is a primary target of the photodynamic activity of eosin-$(KLAKLAK)_2$, conditions were chosen to obtain peptide to lipid ratios similar between bacterial photoinactivation and photohemolysis assays. RBCs were, for instance, diluted 2,000-fold in comparison to human blood. One can therefore expect that hemolysis would be more pronounced at the low RBC concentration used than at the high concentration of human blood and that the assays used are relatively stringent. Approximately 10% hemolysis was obtained at 1 μM eosin-$(KLAKLAK)_2$, the concentration required to achieve approximately 99.99% inactivation of *E. coli* or *S. aureus*. Due to the stringent conditions of the hemolysis assays, this low

level of hemolysis accompanied by significant bacterial inactivation therefore suggests that bacterial photoinactivation can be achieved under conditions where RBCs can be spared. Yet, a concern is raised by the observation that photohemolysis increases to 40% as the concentration of eosin-$(KLAKLAK)_2$ is increased to 10 μM. The concentration window at which bacterial killing can be achieved without adverse effects to RBCs might therefore be relatively narrow. Interestingly though, mixing experiments between bacteria and erythrocytes show that eosin-$(KLAKLAK)_2$ associates with bacteria to a greater extent than red blood cells. Eosin-$(KLAKLAK)_2$ binding to bacteria presumably reduces the concentration of compound present in solution or on the surface of RBCs. Consequently, photohemolysis with eosin-$(KLAKLAK)_2$ at 10 μM was reduced to 10% when bacteria were present. More than 99% bacterial killing could be achieved under these conditions, further confirming that eosin-$(KLAKLAK)_2$ can inactivate bacteria before significant damage is observed for a human cell.

To further address the issue of specificity, the photodynamic activity of eosin-$(KLAKLAK)_2$ was tested against epithelial cells, keratinocytes and fibroblasts. As with RBCs, one might expect eosin-$(KLAKLAK)_2$ to possibly interact with the plasma membrane of these cells. In addition, relatively large and amphiphilic molecules like eosin-$(KLAKLAK)_2$ can be endocytosed by cells. As a matter of fact, lysine and arginine-rich peptides, previously used to improve the targeting of PS such as chlorin e6 to bacteria, are well known to be effectively endocytosed by human cells.[79-81] Unfortunately, PS that accumulate in the endocytic pathway can photo-lyse endocytic organelles such as lysosomes and this might in turn cause cell-death.[51, 69, 82] Consistent

with this idea, cells that have endocytosed PS conjugated to lysine or arginine-rich polymers can be killed readily upon irradiation.[51, 69, 83] Moreover, the photolysis of endocytic organelles raises a concern related to the penetration of antimicrobial peptides inside human cells. In particular, it has been shown that antimicrobial peptides that escape the endocytic pathway might gain access to mitochondria, disrupt the membrane of these organelles, and induce apoptosis.[72] For instance, $(KLAKLAK)_2$ causes cellular apoptosis when combined with agents capable of delivering this peptide in the cytoplasm of human cells, although $(KLAKLAK)_2$ is not toxic without these delivery agents.[84, 85] We were therefore concerned that eosin-$(KLAKLAK)_2$ might be taken up into mammalian cells, lyse endocytic organelles upon irradiation, and possibly cause cell death. To test whether eosin-$(KLAKLAK)_2$ would be endocytosed by cells and in order to assess the phototoxicity of the compound, eosin-$(KLAKLAK)_2$ was incubated with different cell lines and uptake was examined by fluorescence microscopy. While internalization of the positive control eosin-TAT could be readily observed, eosin-$(KLAKLAK)_2$ was not significantly internalized by cells. Also, the viability of cells was not significantly affected by irradiation for 30 min with incubation at 1 μM eosin-$(KLAKLAK)_2$ (conditions at which more than 99.9% bacterial photoinactivation is achieved). These results therefore suggest that bacterial cells are more susceptible to the photodynamic activity of eosin-$(KLAKLAK)_2$ than mammalian cells. At higher concentrations (5 or 10 μM), the phototoxicity towards mammalian cells was increased in a cell-dependent manner. In order to design optimal compounds, it will be interesting to determine in future studies what causes the differences observed in phototoxicity.

Nonetheless, these results suggest that the photoinactivation of bacteria without human tissue damage might be achievable. Of course, *in vivo* experiments will be necessary to validate this idea.

Overall, our results establish that the conjugation of eosin Y to the antimicrobial peptide $(KLAKLAK)_2$ increases the photodynamic activity of eosin Y towards *E. coli* and *S. aureus* considerably. A possible advantage of antimicrobial peptides over other polycationic polymers might involve a reduced propensity to be endocytosed by human cells and, consequently, a reduced phototoxicity towards these cells. In addition, it will be interesting to test whether peptides that have a higher antimicrobial activity in the dark would further reduce the concentration of PS-peptide conjugate required to achieve bacterial photoinactivation.

2.4 Materials and methods

Cell culture reagents were purchased from Invitrogen. Peptide synthesis reagents were from Novabiochem. The compound 5,6-carboxy-eosin was purchased from Marker Gene Technologies. All other reagents were from Sigma. COS-7 and COLO 316 were obtained from ATCC. HaCaT cells were a generous gift from Joan Massagué (Memorial Sloan-Keterring Cancer Center). Whole blood was purchased from Gulf Coast Regional Blood Center (Houston, TX).

2.4.1 Spectroscopy

Absorbance and transmission measurements were recorded using a Shimadzu UV-1700 UV-VIS spectrophotometer in conjunction with UV Probe 2.21 software. Samples (150 µl) were placed in Fisherbrand® utlramicro quartz cuvettes with a 1 cm pathlength. Blank readings were performed with solvent only, usually water except for Ce6, which was suspended in phosphate buffer (100 mM NaCl, 10 mM Na_2HPO_4, pH 7.4) to permit solubility. Transmittance spectra of the filters were recorded by positioning the filters in slots directly in front of the detector. Since positioning of the filter required the sample compartment door to be open, both background and filter transmittance measurements were performed in a darkened room to reduce noise to the detector.

2.4.2 Peptide design and synthesis

H_2N-KLAKLAKKLAKLAK-NH_2 ("$(KLAKLAK)_2$") was synthesized by Fmoc solid phase peptide synthesis using rink amide MBHA resin according to previously reported protocols (Novabiochem). Eosin-$(KLAKLAK)_2$ was synthesized by coupling of 5,6-carboxy-eosin Y to the N-terminal residue of the peptide. H_2N-KLAKLAKKLAKLAK-NH_2 and eosin-$(KLAKLAK)_2$ were purified using HPLC and their mass was confirmed by MALDI-TOF. Because possible differences in the eosin Y isomers may produce different membrane affinities, the isomer of the labeled peptide that first eluted from HPLC was used for all experiments. H_2N-KLAKLAKKLAKLAK-

NH_2 expected mass: 1522.08, observed mass: 1523.18. Eosin-$(KLAKLAK)_2$ expected mass: 2198.82, observed mass: 2196.67.

2.4.3 Bacterial strains

Escherichia coli BL21 DE3 was obtained from Agilent. *Pseudomonas aeruginosa* (ATCC 27853), *Staphylococcus aureus* subsp. *aureus* (ATCC 29213), and *Staphylococcus epidermidis* (ATCC 12228) were purchased from the American Type Culture Collection. Multidrug-resistant *Acinetobacter baumannii* AYE strain (ATCC BAA-1710) was a gift from Dr. Ry Young at Texas A&M University Center for Phage Technology. *E. coli* and *S. aureus* were grown in Luria-Bertani broth (LB), *Ps. aeruginosa* and *A. baumannii* were grown in tryptic soy broth, and *S. epidermidis* in nutrient broth. Glycerol stocks were established for each strain and used to streak agar plates. Colonies from plates were used to inoculate overnight cultures which were grown aerobically at 37^{o}C. Fresh cultures were inoculated the next day in a 1:1000 dilution of overnight culture and used for experiments after growth to mid log phase ($O.D._{600}$ ~0.4-0.6).

2.4.4 Bacterial photoinactivation assay

Bacteria were grown as described above in 14 mL round-bottom Falcon® culture tubes in their respective media, then centrifuged at 1500 g for 10 min and resuspended in sterile phosphate buffer (100 mM NaCl, 10 mM Na_2HPO_4, pH 7.4). This wash procedure was repeated a second time and this stock suspension was used to make suspensions at

the OD required for the particular strain to have approximately 10^8 CFU/mL (colony forming units were determined by plating 10-fold serial dilutions of cultures on agar plates as described below). Peptide solutions (10X, 22 μl) were prepared in wells of a 96-well plate before addition of 200 μl of bacteria in phosphate buffer (~10^8 CFU/mL). Samples were allowed to incubate for approximately 3-5 min before irradiation to allow for peptide binding, and micro stir bars (2x2 mm, Cowie® via Fisher) were added for continued aeration during irradiation. The lipid to peptide (L/P) ratio under these conditions is 1:1 when the peptide or PS concentration is approximately 3 μM (these calculations assume 25 x 10^6 lipids per bacteria).

Irradiation was achieved using a homemade setup with a 600 W halogen lamp (Utilitech #0320777). The lamp was suspended by clamps and air-cooled during operation. A homemade water filter was placed below the lamp to filter out IR with continuous exchange of the water supply. A stir plate was placed underneath the water filter to hold the samples for illumination. Samples were placed in a 96-well plate with a lid. A 5x7 inch green filter (Edmund Optics cat. no. NT46-624, 470-550nm FWHM) was placed on top of the lid for excitation of eosin. A single pane of 1/16 inch diffusing glass was placed on top of the green filter to provide an even distribution of light intensity. Experiments detecting the $^1O_2$ production from Rose Bengal via reaction with RNO demonstrated that this setup provides even distribution of light across all 96 wells (data not shown). Samples were stirred at 200 rpm and set at a distance of 20 cm from the light source. Exposure time was 30 min for all killing assays.

After samples were illuminated or kept in the dark for 30 min, 30 µl of each sample was added to 270 µl of phosphate buffer in a separate 96-well plate. Further 10-fold serial dilutions of the samples were made in phosphate buffer to give samples ranging from 10^1-10^5 in dilution factor. From each dilution, 50 µl was removed and spread on an agar plate, then incubated overnight at 37^{o}C. Colonies were counted the next morning to determine the remaining CFU/mL. Plates without peptide treatment were included as a negative control for sample comparison to determine percent survival.

2.4.5 Partitioning assay

Mixtures of bacteria and peptide or PS were prepared in the same manner as the photoinactivation assays above (222 µl total volume). Samples were then centrifuged at 1500 g for 10 min, and 200 µl of supernatant was transferred to a 96-well plate. Any remaining supernatant was removed, and the pellet was resuspended in 200 µl of phosphate buffer. The fluorescence intensity of the pellets was measured with a microplate reader (Promega® Glomax-Multi®) using the green filter set (Ex 525 / Em 580-640 nm). Absorbance values were ≤ 0.100 at 525 nm to avoid the inner filter effect. To ensure that quenching was not occurring, two-fold serial dilutions of samples were performed. A linear decrease in fluorescence was observed, indicating that no quenching occurred in the resuspended pellet. Experiments were performed in triplicate.

2.4.6 Photohemolysis assay

A concentration of 0.05 % by volume of RBCs was used for hemolysis experiments. This RBC concentration gives a similar L/P ratio to that used in photoinactivation assays, where the L/P ratio is 1:1 when the peptide or PS concentration is approximately 3 μM (assuming ~ 5 x 10^8 lipids per RBC). RBCs (200 μl) were placed in a well of a 96-well plate, and 22 μl of 10 X peptide-conjugate or PS was added and mixed. RBCs were incubated for 5 minutes before illuminating (or keeping in darkness) for 30 min using the halogen lamp setup described above. The extent of hemolysis was determined by centrifuging samples at 1500 g for 10 min, then reading the absorbance of hemoglobin in the supernatant at 450 nm. Untreated RBCs were included as a negative control for both dark and illuminated samples. RBCs treated with 0.1% Triton X-100 were used as a positive control for 100% lysis. The data represent experiments in triplicate with their respective standard deviations.

Mixed RBC and bacteria samples were prepared similarly, with 200 μl of bacteria (10^8 CFU/mL) in PBS placed in a well of a 96-well plate, then 11 μl of 20 X RBCs added and mixed together. Peptide-conjugate or PS (11 μl of 20 X stock solution) was added only after the RBCs and bacteria were mixed to ensure equal opportunity for binding of the peptide to either the RBCs or bacteria. Illumination by halogen lamp and measurement of hemolysis was carried out in the same manner. In order to determine the amount of bacteria killed after illumination, parallel samples were included to determine the CFU/mL remaining by performing serial dilutions on agar plates, as described for bacteria killing assays. Experiments were performed in triplicate.

For imaging of RBCs or mixed RBC and bacteria samples, a 384-well plate with a glass bottom was used to enable use of the 100X oil-immersion objective. Samples were prepared in the same manner as above, but scaled down from 220 µl to 55 µl total volume because of the well size. Cells were imaged before and after illumination for 30 min under the halogen lamp to observe binding and/or killing. SYTOX® Blue was incubated for 15 min at room temperature before imaging as an indicator of bacterial cell death. Intact erythrocytes have a dark contrast in the bright field image while lysed ghosts do not.[69]

2.4.7 Microscopy

Imaging was performed on an inverted epifluorescence microscope (Model IX81, Olympus, Center Valley, PA). The microscope is equipped with a heating stage maintained at 37°C. Images were captured with a Rolera-MGI Plus back-illuminated EMCCD camera (Qimaging, Surrey, BC, Canada). Imaging was performed using bright field imaging and the following fluorescence filter sets: DAPI (Ex = 360 ± 20 nm / Em = 460 ± 30 nm), FITC (Ex = 488 ± 10 nm / Em = 520 ± 20 nm), and RFP (Ex = 560 ± 20 nm / Em = 630 ± 35 nm). Fluorescence excitation was achieved with a 100 W mercury lamp (Leeds Precision Instruments # L202 Osram) and with neutral density filters (ND 1, 2, 3 and 4 on the instrument, corresponding to 100, 25, 12.5 and 5% transmittance). Images were captured with SlideBook 4.2 software (Olympus, Center Valley, PA).

2.4.8 Cell-based assays

Mammalian cells were cultured in Dulbecco's Minimum Essential Media (DMEM) supplemented with 10% fetal bovine serum (FBS) and maintained at 37°C in a humidified environment with 5% CO_2. For viability experiments cells were plated in sterile 96-well plate so that the cells were approximately 80% confluent after 24 or 48 h. Cells were washed twice with PBS and once with Leibovitz's L-15 medium, before addition of the desired concentration of eosin-$(KLAKLAK)_2$ in L-15. The cells were then kept in the dark or illuminated for 30 min in the same manner as the bacterial inactivation experiments. Afterwards, the cells were washed out with PBS twice and once with L-15 before incubation with SYTOX® Green and Hoechst in L-15 media according to the manufacturer's instructions. SYTOX® Green is cell-impermeable and only stains cells with a compromised plasma membrane while Hoechst stains all cells. Cells were imaged with a 20X objective using bright field and fluorescence in DAPI and FITC channels. Ten to twenty images were acquired in the green and blue channels for each experiment. The total number of cells in a given image was determined from the blue channel image (Hoechst) by counting the number of blue nuclei present. The number of dead cells was determined by identifying cells containing a green fluorescent nucleus stained by SYTOX® green. Cell viability was determined by establishing a ratio of dead cells/total number of cells for each sample (at least 1000 cells were counted in each experiment and each experiment was repeated 3 times).

For comparison of cellular uptake between eosin-TAT and eosin-$(KLAKLAK)_2$, cells were plated in 8-well glass bottom dishes (Lab-Tek) 24 or 48 h prior to

experiments. Cells were washed twice with PBS and once with L-15, then incubated with 1 μM eosin-TAT or eosin-$(KLAKLAK)_2$ in L-15 for 30 min. After incubation cells were washed twice with PBS and once with L-15. Fluorescence (IRFP channel) and bright field images were captured at 100X. For comparison of uptake, the fluorescence intensity per cell was determined with the Slidebook software by measuring the total fluorescence intensity present in each cell. This was performed by first creating outlines for each cell, which were converted to masks of the whole cell with the software. Background removal was performed by subtracting the highest background value from the IRFP channel, then using the software to calculate the sum intensity of the endocytic organelles that remained visible within the masks and above the background. The intensities of all endocytic organelles were then added to obtain the total fluorescence intensity per cell. Approximately 50 representative cells were imaged for each condition.

3. MECHANISTIC INSIGHTS INTO EOSIN-$(KLAKLAK)_2$ ACTIVITY

3.1 Introduction

In this section I describe the use of a novel application of TEM methods to visualize eosin-$(KLAKLAK)_2$ in *E. coli* and *S. aureus* samples. We take advantage of the PS for photo-oxidation of 3,3-diaminobenzidine (DAB) to produce an osmiophilic polymer at the location of the PS-AMP conjugate. Secondly, the location of the PS-AMP is further confirmed by scanning transmission electron microscopy with electron dispersal X-ray spectroscopy (STEM-EDS) to locate bromine atoms that are present only in the eosin moiety. To our knowledge this is the first application of these methods to peptides, specifically an AMP in this case. This work demonstrates the usefulness of these methods for direct visualization of peptides in biological samples for TEM without the requirement of immunogold labeling. After TEM results demonstrated, perhaps not surprisingly, that the bacterial membrane was the primary location for eosin-$(KLAKLAK)_2$ binding in the dark, we turned to lipid membrane models to study the activity of the PS-AMP conjugate, and the respective roles of the PS and AMP.

3.2 Results

3.2.1 Eosin-$(KLAKLAK)_2$ localizes to the outer surface of *E. coli* and *S. aureus* in the dark, and subsequent light excitation causes membrane disruption

To investigate the mechanism of eosin-$(KLAKLAK)_2$ activity, we first sought to determine likely molecular targets. Since AMPs have been shown to localize to both the

cell exterior and interior in different cases, we probed the location of eosin-$(KLAKLAK)_2$ during PDI experiments by TEM. To do this, we took advantage of eosin as part of the conjugate to visualize samples using a DAB photooxidation method. Suitable PS have been used to label antibodies and proteins to oxidize 3,3-diaminobenzidine (DAB) for the formation of an osmiophilic DAB polymer at the site of PS activity. The enrichment of osmium staining at the site of the polymer provides a heightened contrast by electron microscopy.[17,9]

Figure 3-1a depicts the DAB polymerization caused by singlet oxygen or superoxide production from the triplet state of eosin Y.[86] To perform this reaction we followed the sequence shown in Figure 1b. The first illumination step in this process was carried out for only 0, 2, or 5 min to limit the damage caused by eosin-$(KLAKLAK)_2$. This allowed us to examine the early stages of localization and activity. Fixation of the peptide with cells did not prevent eosin-$(KLAKLAK)_2$ from polymerizing DAB during the second illumination step (evidenced by enhanced osmium staining in Figure 3-1b). Neither did the second illumination step appear to damage cells, since samples with eosin-$(KLAKLAK)_2$ that were not irradiated before the fixation showed little structural difference compared to untreated cells by EM (Figure 3-2a). This implies that this method is suitable for observing the location of the eosin-$(KLAKLAK)_2$ conjugate before and after the PDI process. Before light irradiation, the peptide is clearly localized to the exterior of the cell surface of *E. coli* and *S. aureus* (Figure 3-2a, second column). However, light irradiation of eosin-$(KLAKLAK)_2$ in solution with each strain, results in membrane damage and lysis of the cell wall in many cases. The 2 and 5 min irradiation

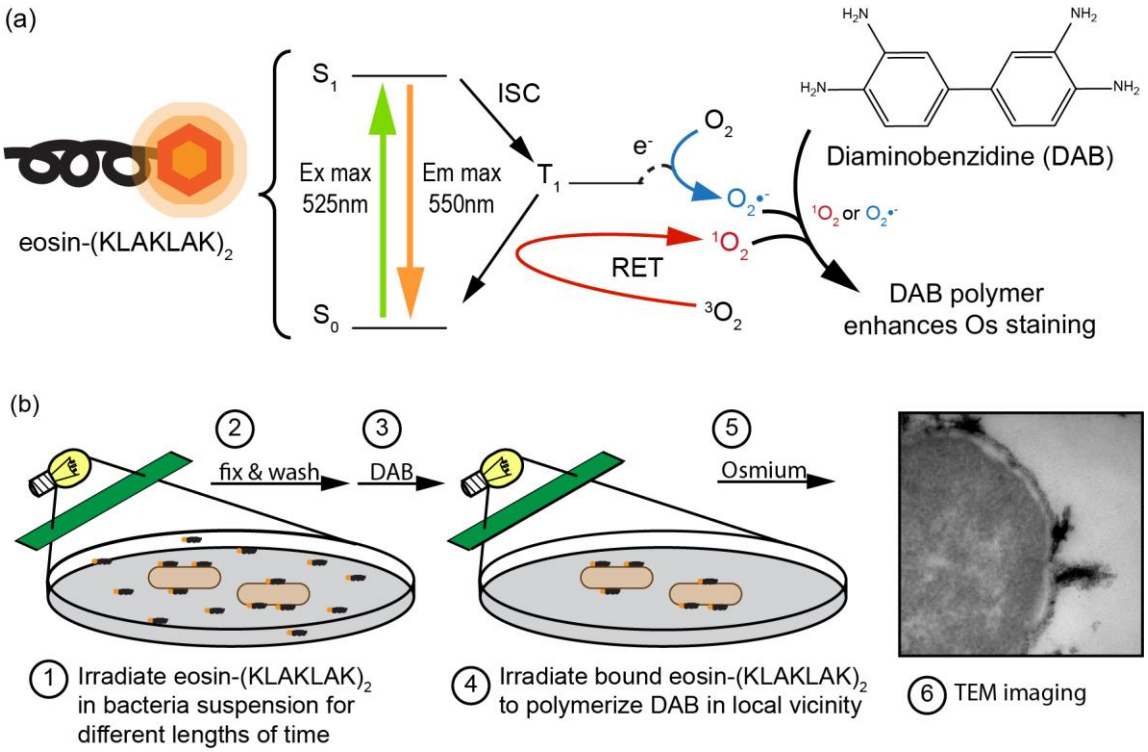

Figure 3-1: Experimental design of DAB photo-oxidation and visualization by TEM. (a) Light excitation of eosin-$(KLAKLAK)_2$ results in production of singlet oxygen and superoxide, which can polymerize DAB to provide an enhanced staining of osmium at the location of eosin-$(KLAKLAK)_2$. (b) Light irradiation has two purposes in this experiment, 1) to excite eosin-$(KLAKLAK)_2$ for photodynamic activity, then following fixation of samples, 2) to polymerize DAB at the location of the PS-AMP conjugate.

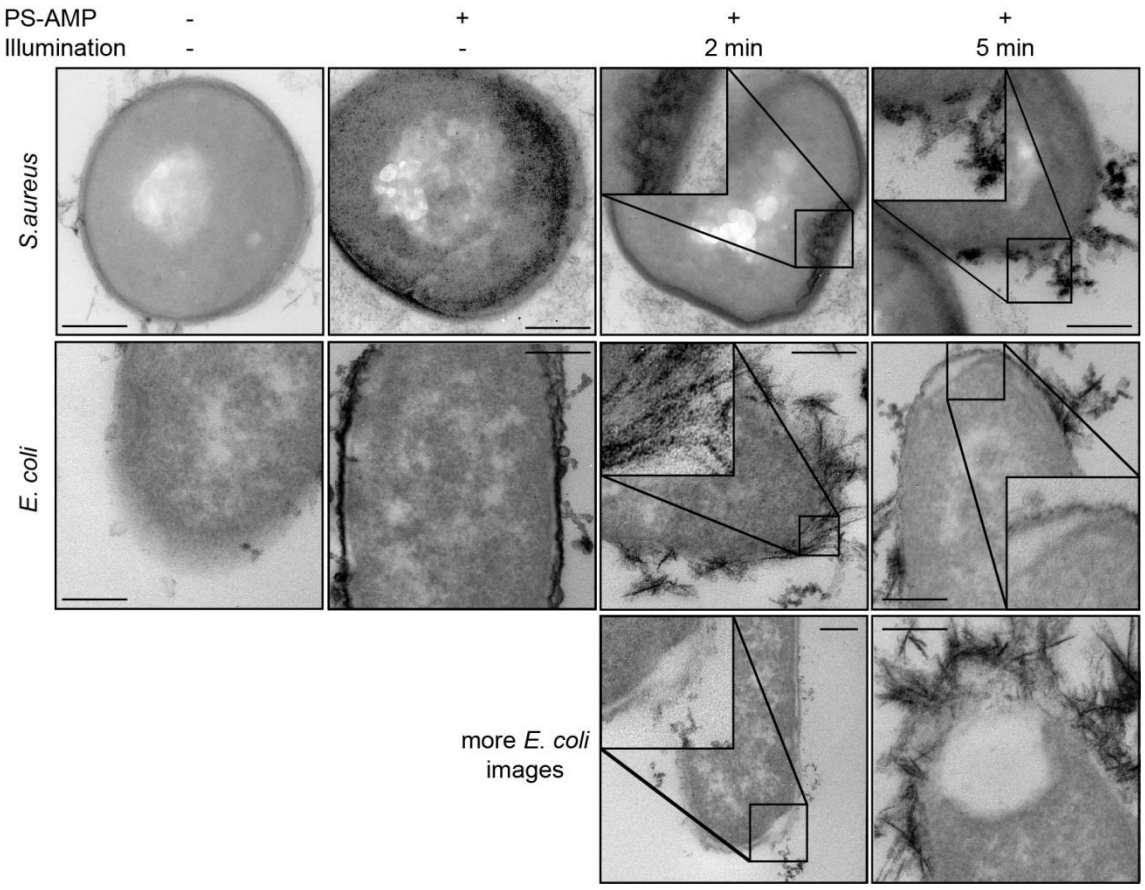

Figure 3-2: Localization of eosin-(KLAKLAK)$_2$ in *E. coli* and *S. aureus* samples determined by DAB photooxidation. Untreated samples are shown in the left column. Eosin-(KLAKLAK)$_2$ was incubated with cells, then irradiated for 0, 2, or 5 min before fixation with acrolein to anchor eosin-(KLAKLAK)$_2$ in place. Cells were then washed and a second illumination was performed in the presence of DAB (1 mg/ml), producing an osmiophilic polymer for enhanced contrast by TEM at the site of eosin-(KLAKLAK)$_2$. Scale bars are 0.2 μm in all images.

times represent approximately 50% and 90% cell death as shown in the previous section.[10] The membrane deformation and lysis seen here correlates with the cell death in section 2 and indicates a likely mechanism for cell death caused by eosin-$(KLAKLAK)_2$.

In order to validate that the enhanced osmium staining at the cell surface of bacteria was in fact the result of the presence and activity of eosin-$(KLAKLAK)_2$, STEM-EDS was used to positively identify the location of the conjugate. Scanning TEM (STEM) with energy dispersive X-ray spectroscopy (EDS) can be used for elemental analysis of biological samples to study the distribution of different atoms. Eosin Y contains four bromine atoms per molecule, making bromine a unique marker for the location of eosin-$(KLAKLAK)_2$. Furthermore, since the presence of bromine is rare among bacterial species, generally limited to specialized marine bacteria,[87] there is no background signal to specifically interfere with detection by STEM-EDS in *E. coli* or *S. aureus*, and would not be expected for most other species. In Figure 3-3a an image of a *S. aureus* cell treated with eosin-$(KLAKLAK)_2$ is shown, with a line and square depicting the paths of a line and area scan, respectively, for STEM-EDS analysis (Figure 3-3b,c). The intensity of bromine content is depicted along the path of the line scan in the plot to the right. The bromine intensity is greatest at the cell membrane and at the location of what appears to be adjacent membrane debris in the media. These results support the distribution made apparent by DAB polymerization and also demonstrate the capability of STEM-EDS to identify unique atoms on a small peptide in the context of a biological sample. Together, the DAB and STEM-EDS images suggest that eosin-

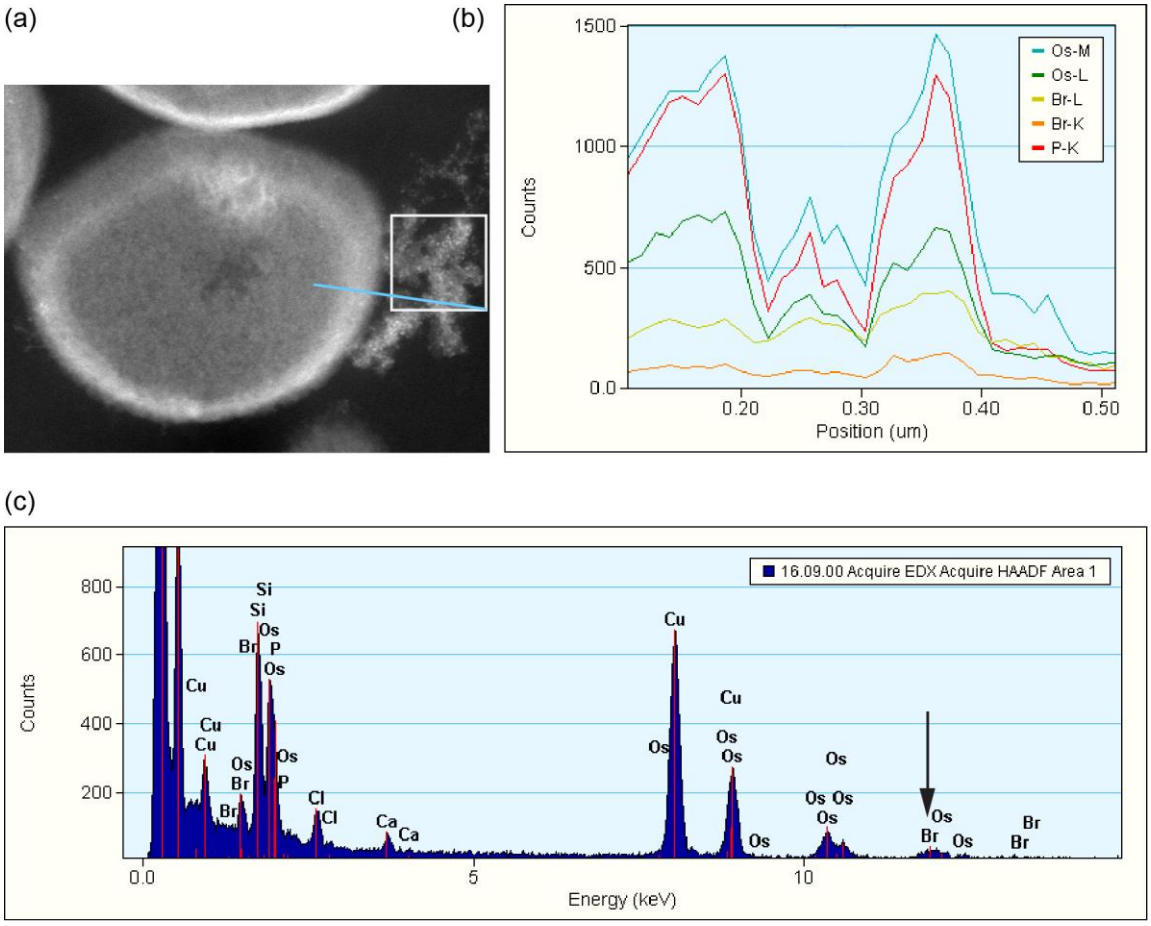

Figure 3-3: Bromine atoms in eosin-(KLAKLAK)$_2$ serve as a marker of the peptide for detection by STEM-EDS in bacteria samples. (a) STEM backscatter image of S. aureus treated with eosin-(KLAKLAK)$_2$ and light for 2 min. (b) EDS element profiles of the line scan depicted in (a) from left to right, showing the coincident intensities of Os, Br, and P elements at the cell wall and in extracellular material, possibly removed from the cell during irradiation with eosin-(KLAKLAK)$_2$. (c) Elemental analysis by EDS for the square area indicated in (a), showing the distinct presence of Br from eosin-(KLAKLAK)$_2$ among the many other elements expected for a biological sample.

$(KLAKLAK)_2$ localizes to the cell membrane in the dark, and upon light irradiation, causes membrane deformation and without light, and eosin Y alone is not toxic to cells in the light.[10]

3.2.2 Conjugation of eosin Y to $(KLAKLAK)_2$ alters the production of ROS

We previously demonstrated that eosin Y alone showed no toxicity towards *E. coli* and *S. aureus* under conditions where an equivalent amount of bound eosin-$(KLAKLAK)_2$ caused extensive killing. To examine why this difference in toxicity exists, we tested the hypothesis that the production of ROS might be altered after conjugation of eosin Y to $(KLAKLAK)_2$, which has been previously observed after conjugation of another PS to polyethyleneimine.[37] Eosin Y is reported to produce both $^1O_2$ and $O_2^{\bullet -}$,[86] which have each been shown to participate in PDI of bacteria and other microbes.[88] To compare the production of $^1O_2$ for eosin Y and eosin-$(KLAKLAK)_2$, we used the RNO assay, which reports on the oxidation of RNO in the presence of imidazole as a result of $^1O_2$ production.[89,90] Comparison of $O_2^{\bullet -}$ was achieved using the NBT assay, which detects the reduction of NBT to a formazan in the presence of NADH.[91,37] These assays are suitable to use during the production of both $^1O_2$ and $O_2^{\bullet -}$ since the RNO reaction occurs by an oxidation mechanism, while the NBT detects a reduction, so there is not a mixed detection in either case.

Figure 3-4a shows that there is a decrease in the production of singlet oxygen from eosin-$(KLAKLAK)_2$ relative to eosin Y alone. The effect of the $^1O_2$ quencher NaN_3 is shown in the extension of the Figure 3-4a, and significantly reduces the bleaching of

RNO. Surprisingly, the NBT assay in Figure 3-4b shows a dramatic increase in the production of superoxide for eosin-$(KLAKLAK)_2$ compared to eosin Y. The observed decrease in $^1O_2$ and accompanying increase in $O_2^{\bullet-}$ after conjugation to $(KLAKLAK)_2$ demonstrate altered triplet state reaction properties for eosin Y after conjugation. These changes are consistent with that observed for the PS Ce6 after conjugation to PEI,[92] although it is unclear whether this response to conjugation is a general characteristic for PS, or whether the particular response is dependent on the PS and/or peptide used. These results suggest a possible mechanism for the enhanced PDI activity of eosin-$(KLAKLAK)_2$ compared to eosin Y when equal amounts of either molecule are present at the membrane.

3.2.3 Role of ROS in PDI of *E. coli* and *S. aureus*

In order to study the role of $^1O_2$ and $O_2^{\bullet-}$ in the killing of bacteria by eosin-$(KLAKLAK)_2$, we examined the effect of quenchers upon the survival of the Gram negative *E. coli* and Gram positive *S. aureus* in the presence of light (Figure 3-5). The relative survival fraction of cultures is shown in the presence and absence of eosin-$(KLAKLAK)_2$ to distinguish any toxicity by the quencher alone from the activity of eosin-$(KLAKLAK)_2$. Since the generation of both $^1O_2$ and $O_2^{\bullet-}$ by PS is oxygen-dependent, we first examined the role of oxygen by displacing oxygen as well as we could with a N_2 environment. A completely protective effect was likely not possible since sample handling required a limited exposure to air, allowing re-entry for some

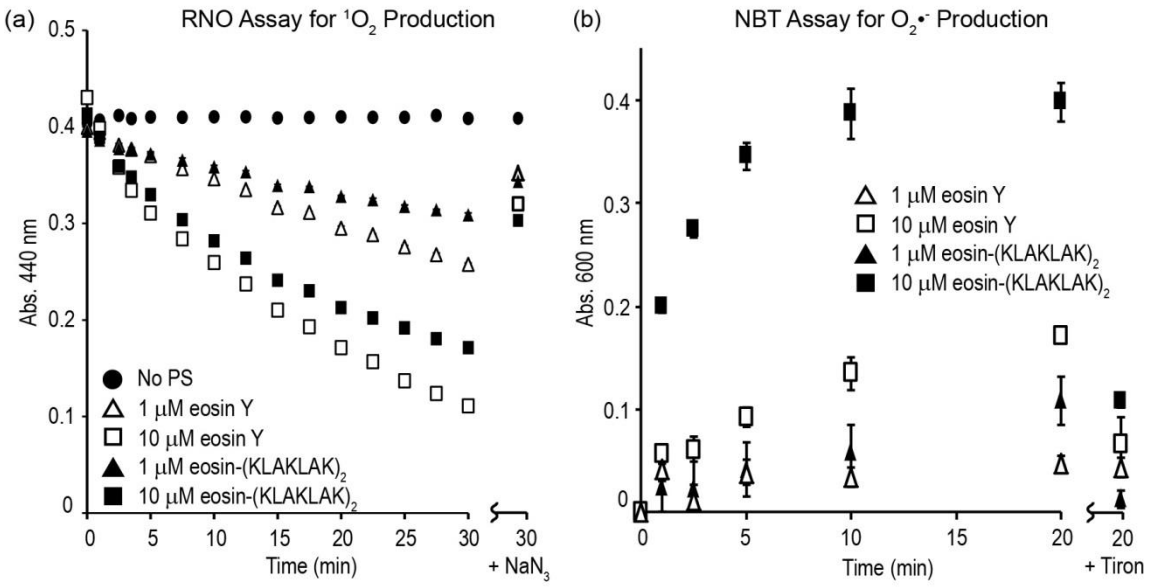

Figure 3-4: Conjugation of eosin Y to $(KLAKLAK)_2$ alters $^1O_2$ and $O_2^{\bullet-}$ production. Relative production of $^1O_2$ from eosin Y and eosin-$(KLAKLAK)_2$ detected by oxidation of RNO in the presence of imidazole. Addition of NaN3, a quencher of $^1O_2$, results in a large reduction of the response (a). Relative production of $O_2^{\bullet-}$ from eosin Y and eosin-$(KLAKLAK)_2$ detected by reduction of NBT to blue formazan in the presence of NADH, and specific quenching of $O_2^{\bullet-}$ by Tiron (b).

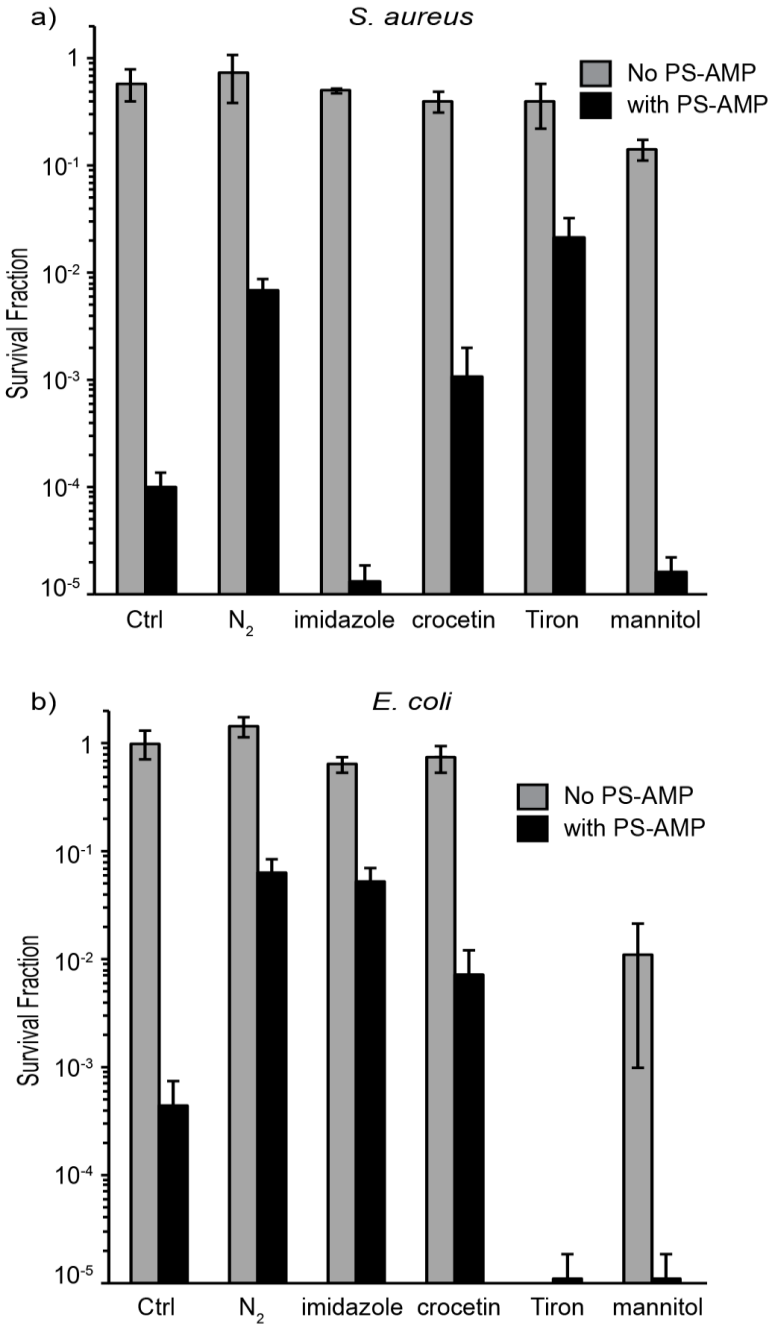

Figure 3-5: The role of different ROS in eosin-(KLAKLAK)$_2$ ("PS-AMP")-mediated killing of *S. aureus* and *E. coli*. Samples (10^8 CFU/ml) of *S. aureus* (a) and *E. coli* (b) were irradiated with light for 30 min. Serial dilutions were made for colony counting and the survival fraction determined by comparison with non-irradiated controls. Samples without the PS-AMP are included to indicate the toxicity of the quenchers alone.

level of oxygen into the sample before irradiation. Nonetheless, our N_2 environment resulted in a ~2-log protection of both strains, demonstrating a clear role for O_2 in the PDI activity of eosin-$(KLAKLAK)_2$.

In Figure 3-5, the soluble $^1O_2$ quencher imidazole (50 mM) showed no protective effect for *S. aureus*, although, *E. coli* obtained considerable protection from the same quencher. Imidazole actually enhanced the PDI against *S. aureus*, which is likely the quencher preventing some degree of PS self-bleaching that normally occurs, thus enhancing the life of the PS and its effects. In contrast, the membrane soluble $^1O_2$ quencher, crocetin (50 μM), was able to protect both strains. For *S. aureus*, this suggests that singlet oxygen is produced mostly within the membrane where only crocetin can quench its damaging activity. However, for *E. coli*, singlet oxygen produced by eosin-$(KLAKLAK)_2$ occurs in both solvent accessible and inaccessible regions, implying multiple binding sites and/or orientations for the conjugate.

The superoxide quencher Tiron (10 mM) showed extensive protection for *S. aureus*, demonstrating a significant role for superoxide in the PDI mechanism for eosin-$(KLAKLAK)_2$. However, Tiron was toxic to *E. coli*. Tiron has been shown to chelate some metals,[93] a known mechanism for disrupting LPS of Gram negative bacteria,[94] which is likely the cause of toxicity in this case. Although we cannot draw definite conclusions for the extent of damage caused to *E. coli* by superoxide, it is clear that superoxide is produced at high levels by eosin-$(KLAKLAK)_2$ (Figure 3-4b), and is playing a significant role in the cell death of *S. aureus* (Figure 3-5a), which does not contain LPS. Since both Gram positive and negative strains share the structural features

of peptidoglycan and lipids as parts of their cell wall, it is likely then that superoxide also plays a role in the death of *E.coli*.

To further establish that the PDI effects of eosin-$(KLAKLAK)_2$ are primarily due to singlet oxygen and superoxide, we tested for the possible involvement of another ROS, the highly reactive hydroxyl radical ($HO^{\bullet}$), by using mannitol, a soluble $HO^{\bullet}$ quencher (Figure 3-5). There was no protective effect of mannitol observed for either strain, although some toxicity was observed. Along with the extent of protection provided by quenchers of $^1O_2$ and $O_2^{\bullet-}$, this suggests that $HO^{\bullet}$ is not a significant contributor to the PDI activity of eosin-$(KLAKLAK)_2$. Along with results from EM and *in vitro* assays, this data suggests that both $^1O_2$ and $O_2^{\bullet-}$ are significant contributors to the PDI activity of eosin-$(KLAKLAK)_2$ at the membrane surface of bacteria. In particular, the quenching activity of crocetin, a lipid-soluble quencher, towards both strains suggests that the lipid bilayer is a common target of eosin-$(KLAKLAK)_2$ activity between the two strains.

3.2.4 Eosin-$(KLAKLAK)_2$ shows greater levels of binding and leakage towards liposomes of bacterial lipid composition

After results from EM and ROS-quenching experiments supported the lipid membrane as a target for eosin-$(KLAKLAK)_2$ activity, we hypothesized that the particular membrane composition of bacteria might provide a basis for the preferential binding and activity that we observed previously for eosin-$(KLAKLAK)_2$ towards bacteria over mammalian cells.[10] Also, since eosin-$(KLAKLAK)_2$ binds to and kills both

Gram positive and negative strains, it seemed reasonable to test a common component of the two membranes, namely, the lipids. To test this hypothesis, we performed LUV leakage assays using liposomes of different lipid composition to model the bacterial and mammalian lipid membranes. LUVs contained self-quenching concentrations of calcein (60 μM), allowing for detection of content leakage by the increase in calcein fluorescence after un-quenching. LUVs (200 μM total lipid) with or without eosin-$(KLAKLAK)_2$ present in solution (10 μM), were irradiated for 30 min under the same conditions as bacterial killing assays, after which, 0.1% Triton X-100 was added to determine the remaining fluorescent signal still encapsulated (shown at 31 min).

Figure 3-6a shows that light alone or Eosin Y alone (10 μM) does not cause leakage for either type of LUV. On the other hand, eosin-$(KLAKLAK)_2$ has only a slight effect on mammalian (Mam) LUVs, while bacterial (Bac) LUVs show early and continued leakage (Figure 3-6b). After the addition of Triton X-100, it is apparent that the total fluorescence of LUVs treated with eosin-$(KLAKLAK)_2$ is significantly diminished compared to LUVs alone or with eosin Y, indicating significant bleaching of calcein caused by eosin-$(KLAKLAK)_2$ during irradiation. This means that the apparent fluorescence of calcein throughout the irradiation process is actually underestimated for eosin-$(KLAKLAK)_2$ in this assay, although this signal still provides us with a lower limit of leakage. The greater bleaching of calcein by eosin-$(KLAKLAK)_2$ compared to eosin Y suggests a closer proximity to the membrane, or an enhancement of bleaching resulting from the altered ROS production for the conjugate, or both. The effect of both $^1O_2$ and $O_2^{\bullet-}$ quenchers for Bac LUVs with eosin-$(KLAKLAK)_2$ was a reduction in

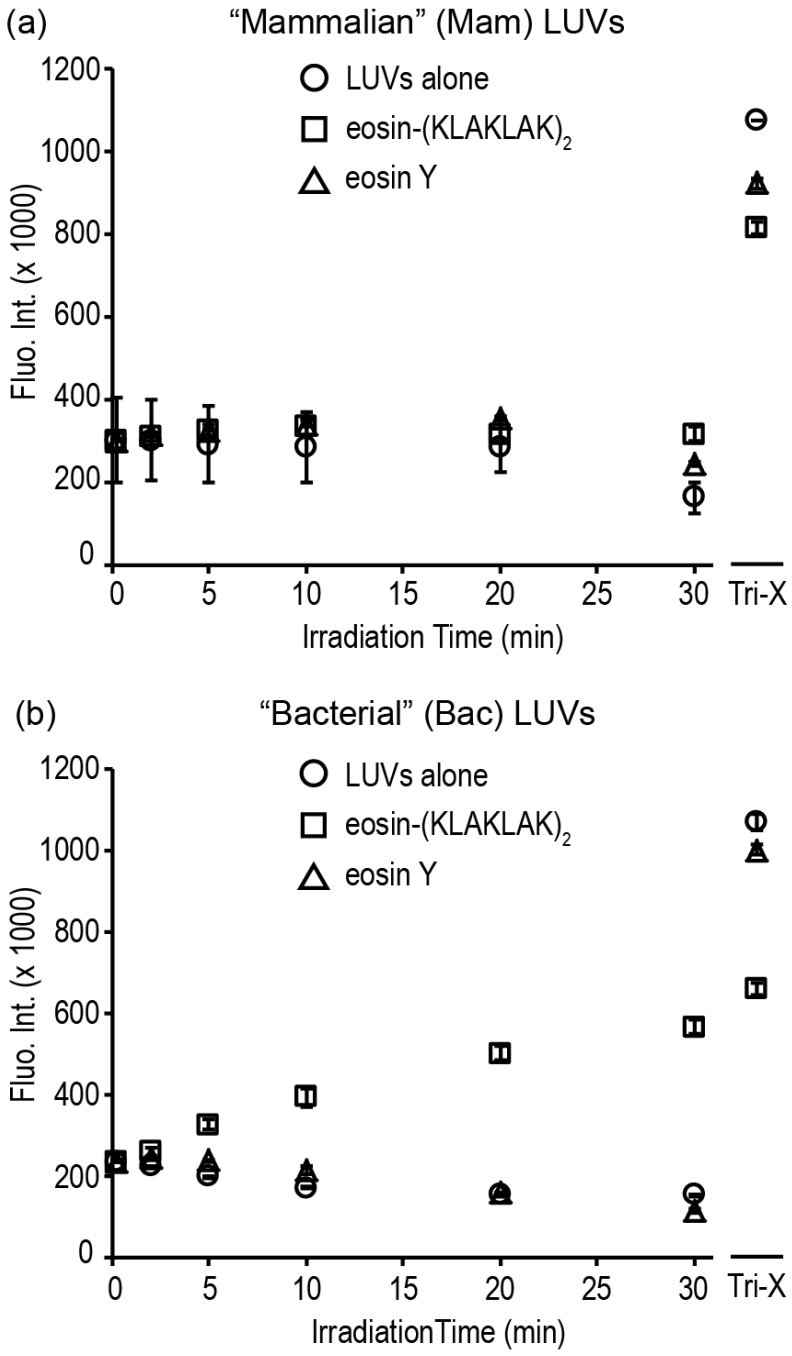

Figure 3-6: Eosin-(KLAKLAK)$_2$ lyses LUVs of bacterial lipid composition, but not of mammalian composition. Eosin-(KLAKLAK)$_2$ (10mM) with "Mammalian" (Mam) LUVs (50/30/20 PC/Chol/SM; 200mM total lipid) (a), and "Bacterial" (Bac) LUVs (75/20/5 PE/PG/CA; 200mM total lipid) (b). Samples were irradiated with the same conditions used for bacterial killing assays.

leakage (Figure 3-7), indicating a role for each of these ROS in lipid disruption. NaN_3 has a greater quenching effect than crocetin in this system, suggesting that the PS is solvent exposed.

One interesting observation was the formation of precipitates seen at the earliest time points with Bac LUVs (indicated by arrows in magnified images), while precipitates do not form with Mam LUVs (Figure 3-8a). Investigation of these precipitates by fluorescence microscopy (Figure 3-8b) reveals extensive aggregates of LUVs, ranging broadly in size, with a typical aggregate pictured here at ~90 μm across. This distance corresponds to the width of roughly one thousand intact LUVs. While it is unclear what proportion of the aggregate contains intact LUVs, the fluorescence image shows fluorescence throughout the aggregate (sample had 10 min irradiation), which could be from either eosin-$(KLAKLAK)_2$ or calcein in this case, since both are excited by the FITC filter cube used for imaging. While the presence of eosin-$(KLAKLAK)_2$ in solution is significantly diminished after 10 min, the aggregates in the samples are clearly still pink in color, indicating the presence of eosin-$(KLAKLAK)_2$ within the aggregates (since the LUV solutions are only pink after addition of eosin-$(KLAKLAK)_2$). It is unclear whether the apparent decrease of eosin-$(KLAKLAK)_2$ in solution is only the result of co-precipitation with the LUV aggregates, or whether a significant bleaching of the PS may also be occurring. Nonetheless, taken together, these results suggest that the lipid composition of bacteria may provide a sufficient basis for the preferential targeting of eosin-$(KLAKLAK)_2$ to bacteria over mammalian cells. In addition, the isolated lipid component is susceptible to lysis and aggregation in the

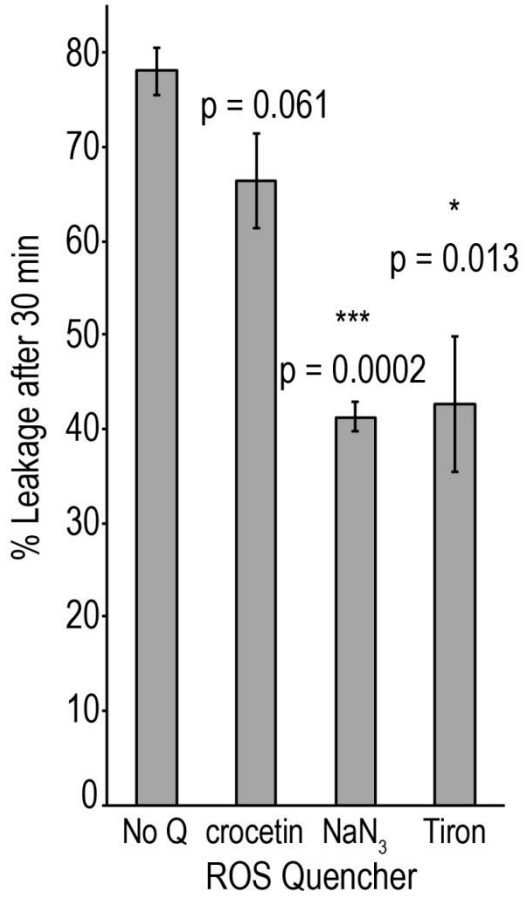

Figure 3-7: Effect of $^1O_2$ and $O_2^{\bullet-}$ quenchers on leakage of LUVs with bacterial lipid composition. The soluble $O_2^{\bullet-}$ quencher Tiron, and the soluble $^1O_2$ quencher NaN_3 inhibit leakage from Bac LUVs (two-tailed t-test, * = p <0.05, ** = p< 0.01, *** = p< 0.001).

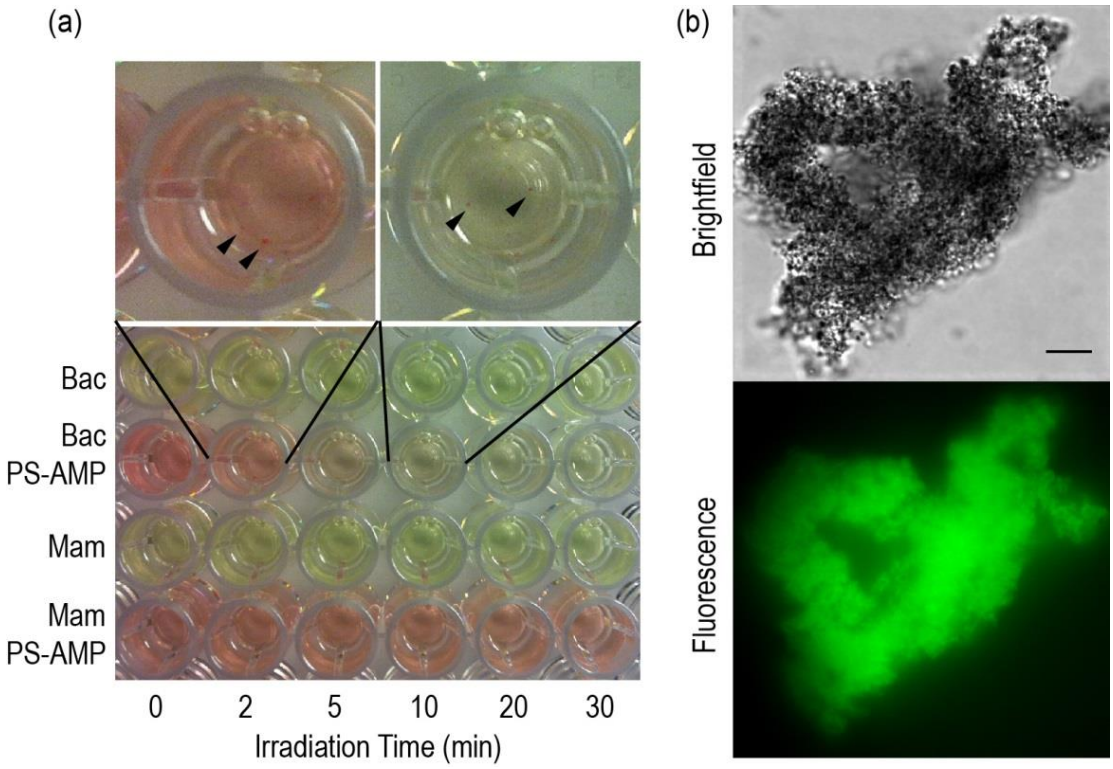

Figure 3-8: Eosin-$(KLAKLAK)_2$ causes aggregation of LUVs with bacterial lipid composition, but not with mammalian lipid composition. Isolated wells depicted above demonstrate significant bleaching of eosin-$(KLAKLAK)_2$ during irradiation with Bac LUVs, and the accompanying precipitates indicated by arrows (a). Bright field and fluorescence images of a typical precipitate from Bac LUVs after 10 min of irradiation (b). Scale bar = 10µm.

presence of eosin-$(KLAKLAK)_2$ and light.

3.2.5 The AMP component of the eosin-$(KLAKLAK)_2$ conjugate actively participates in membrane lysis

Although bacteria killing experiments have shown that eosin-$(KLAKLAK)_2$ in the presence of light can kill bacteria efficiently below 1 μM, the peptide without the PS is inactive at these concentrations (Figure 2-1). Since the PS-AMP conjugate shows much greater activity than the PS alone, this implies that $(KLAKLAK)_2$ at least plays a targeting role for the PS. Up to this point, however, it had been unclear whether $(KLAKLAK)_2$ also participated in membrane lysis, and if so, to what extent. In order to assess the role of the peptide in the PDI process, we needed to uncouple photosensitization by the PS from the potential membrane disruption by the peptide. To achieve this, we co-incubated LUVs with unconjugated $(KLAKLAK)_2$ and a free photosensitizer, chlorin e6 (Ce6), which can bind and sensitize LUVs on its own in the light. The absorbance spectrum of Ce6 and the transmittance of the red filter used during irradiation are shown in Figure 3-9. Although absorbance of Ce6 is high at 400 nm, the peaks at ~655 and 705 nm likely dominate the absorbance of light in the experiment due to the transmittance of the red filter and the output of typical quartz-halogen lamps both being relatively low at shorter wavelengths (our lamp spectrum is limited to 500 nm, but resembles typical spectra from other quartz-halogen lamps).

Figure 3-10a shows the percent leakage from Bac LUVs alone or with Ce6 (10 μM) in the presence or absence of $(KLAKLAK)_2$ after a 10 min irradiation. The leakage

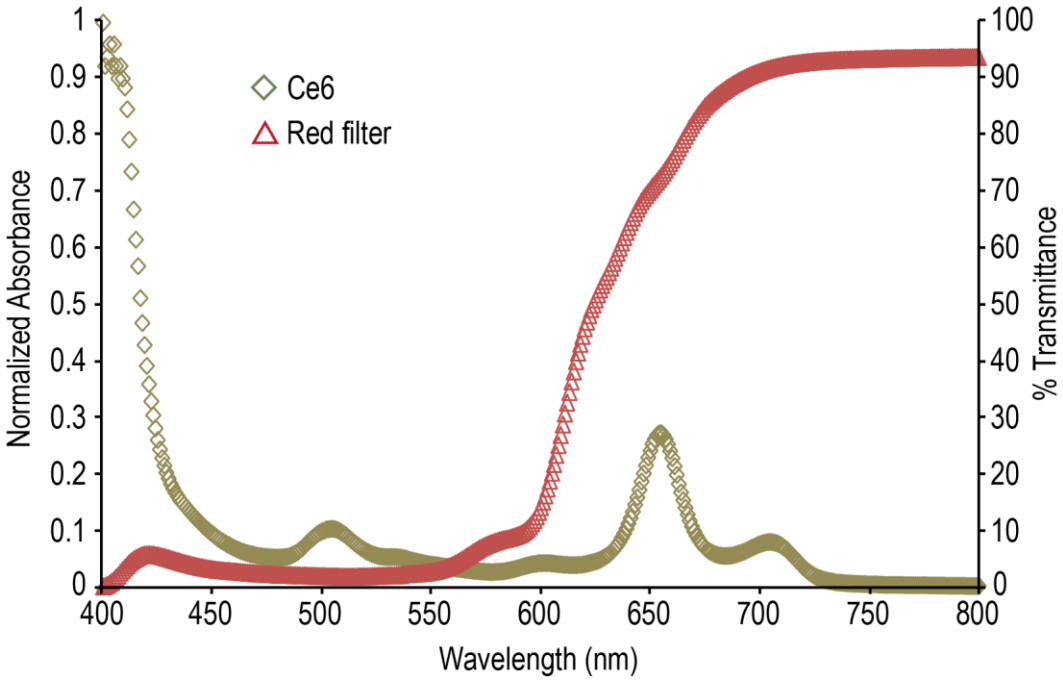

Figure 3-9: Overlay of the absorbance spectrum of Ce6 and transmittance of the red filter used for irradiation of Ce6. Absorbance was determined at ~10 µM Ce6.

of LUVs in the presence of both the PS and AMP is significantly greater for each concentration of AMP tested. In order to determine whether the increase in leakage for samples with both Ce6 and $(KLAKLAK)_2$ indicated an additive or synergistic effect, the potential synergy was calculated with the equation: Synergy = L_{Ce6+K} / (L_{Ce6} + L_K), where L_{Ce6}, L_K, and L_{Ce6+K}, represent the percent leakage in the presence of Ce6 alone, $(KLAKLAK)_2$ alone, and with co-incubation of Ce6 and $(KLAKLAK)_2$, respectively. Where synergy exists, there should be greater leakage with co-incubation, than seen for the sum of the two molecules alone, resulting in a value greater than 1. The results of the calculation for each concentration of $(KLAKLAK)_2$ are shown in Figure 3-10b. Under these conditions, the addition of $(KLAKLAK)_2$ results in a synergistic response for vesicle leakage, which increases with peptide concentration for the range tested.

While the above results were suggestive of a synergistic enhancement of leakage by $(KLAKLAK)_2$, we thought the enhanced leakage could possibly be due to a recruitment of greater amounts of the negatively charged Ce6 by the positively charged $(KLAKLAK)_2$ to the lipid membrane. To ensure that oxidation of lipids could facilitate disruption by $(KLAKLAK)_2$, we used H_2O_2 as an oxidizing agent to mimic the photooxidative damage caused by a PS. Using the same LUVs as the prior experiment, leakage was monitored during a pre-oxidation step with H_2O_2 and after addition of $(KLALKAK)_2$ or a blank. The resulting leakage and synergy calculations are shown in Figure 3-11.

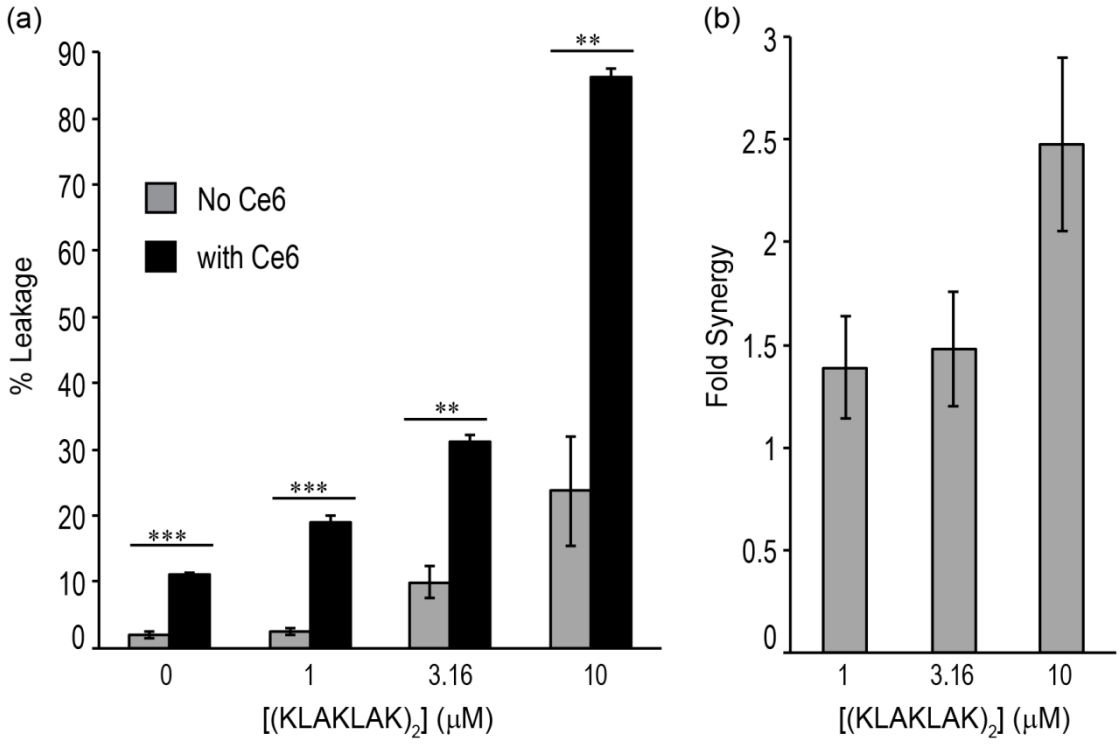

Figure 3-10: $(KLAKLAK)_2$ shows synergistic leakage activity towards LUVs of bacterial lipid composition when co-incubated with Ce6 in the presence of light. (a) Leakage of Bac LUVs in the presence of $(KLAKLAK)_2$ alone (■), or with co-incubation of $(KLAKLAK)_2$ and Ce6 (10 μM) (■) for 10 min with light. Significant differences for samples +/- Ce6 determined by two-tailed t-test, * = $p < 0.05$, ** = $p < 0.01$, *** = $p < 0.001$. (b) Fold synergy of $(KLAKLAK)_2$ activity calculated from leakage values in (a).

3.2.6 The retro-inverso $(KLAKLAK)_2$ peptide and retro-inverso eosin-$(KLAKLAK)_2$ conjugate maintain similar LUV leakage activity

Retro-inverso peptides possess amino acid enantiomers of the original peptide and a reversed amino acid sequence. These changes result in the same spatial orientation of the amino acid side chains, but with the N and C termini at opposite ends from the original peptide. The advantage of such constructs is that they often possess similar activity to the original peptide with decreased potential for degradation by proteases since D-amino acids are less susceptible to proteolytic degradation. It should be noted that a consequence of the N- and C-termini switching ends with respect to the sidechains in the retro inverso construct, is that the conjugation of the PS to the N-terminus also changes the relative position of the PS to the opposite end with respect to the original sequence.

To test whether the retro-inverso construct of eosin-$(KLAKLAK)_2$, called RI-eosin-$(KLAKLAK)_2$, might possess similar membrane disruption activity, we performed preliminary assays for comparison. The absorbance spectra of RI-eosin-$(KLAKLAK)_2$ is shown in Figure 3-12, along with eosin Y, 5(6)-carboxy-eosin Y, and eosin-$(KLAKLAK)_2$ for comparison. The retro inverso construct shows the same spectral shift observed for eosin-$(KLAKLAK)_2$. LUV leakage assays in Figure 3-13 show that RI-eosin-$(KLAKLAK)_2$ also has the same selectivity for LUVs of bacterial lipid composition as seen for the original peptide, with slightly more activity towards bacterial LUVs. Additionally, the peptide alone, RI-$(KLAKLAK)_2$, showed a similar appearance

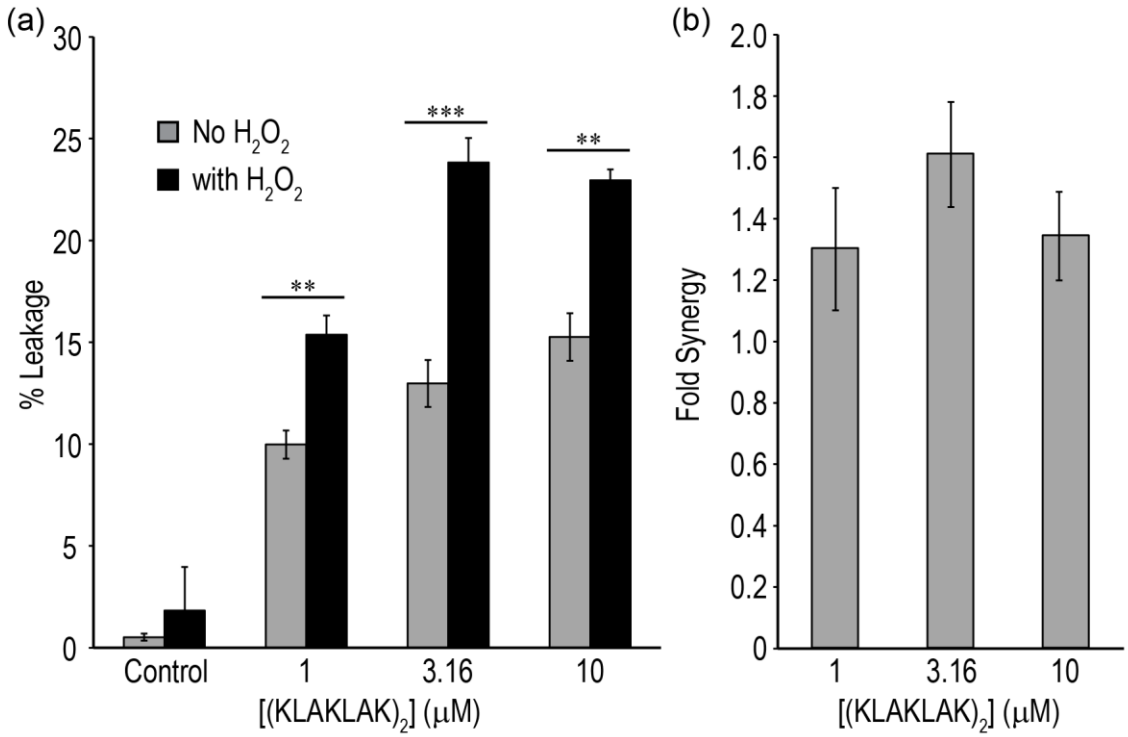

Figure 3-11: $(KLAKLAK)_2$ shows synergistic leakage activity towards LUVs of bacterial lipid composition after pre-oxidation with H_2O_2. (a) Leakage of Bac LUVs in the presence of $(KLAKLAK)_2$ alone (■), or with co-incubation of $(KLAKLAK)_2$ and H_2O_2 (13%) (■). Significant differences for samples +/- H_2O_2 determined by two-tailed t-test, * = $p < 0.05$, ** = $p < 0.01$, *** = $p < 0.001$. (b) Fold synergy of $(KLAKLAK)_2$ activity calculated from leakage values in (a).

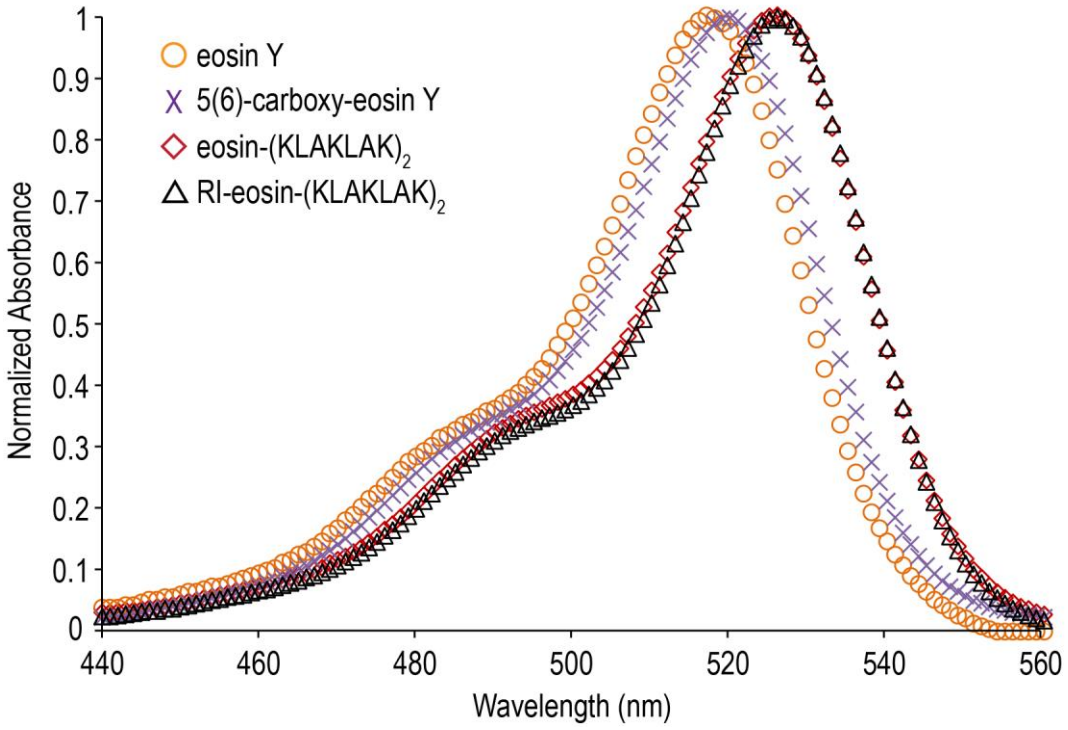

Figure 3-12: The absorbance of RI-eosin-$(KLAKLAK)_2$ is the same as eosin-$(KLAKLAK)_2$. RI-eosin-$(KLAKLAK)_2$ shows the same shift observed relative to either of the free eosin Y molecules.

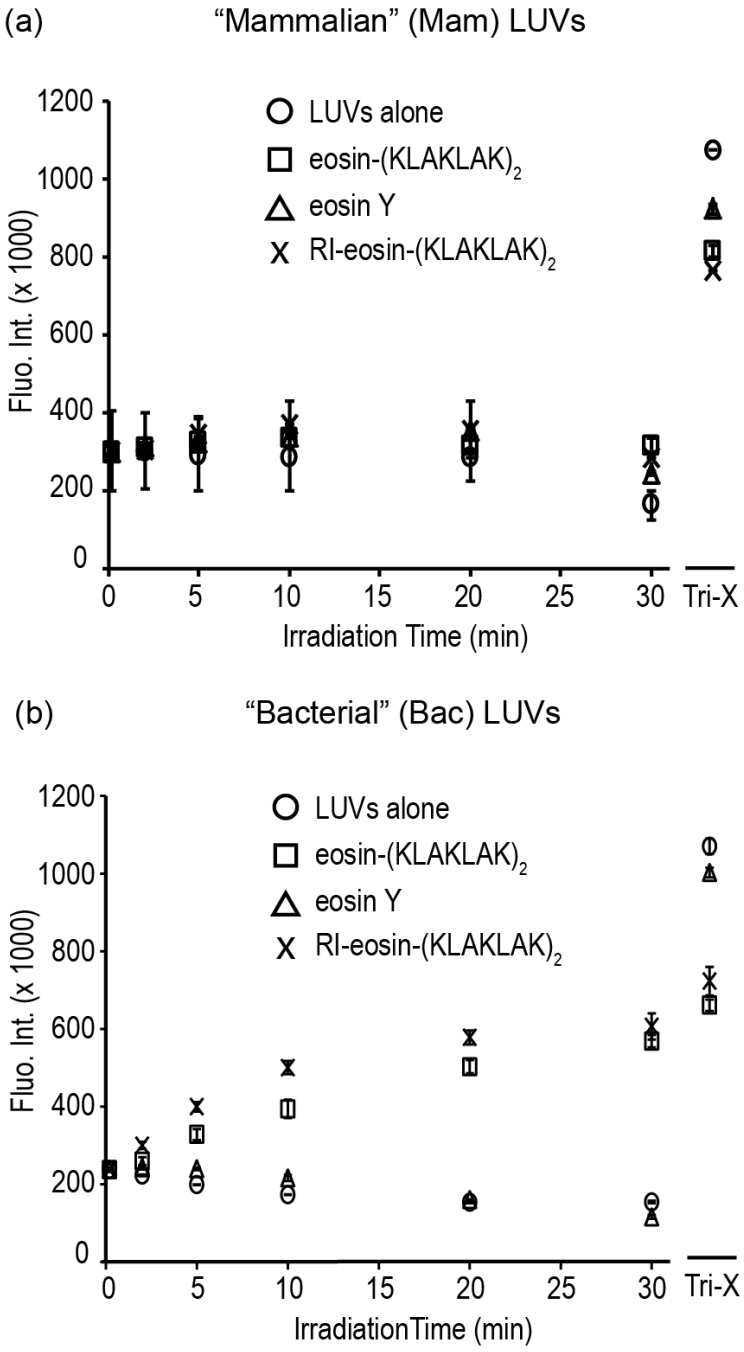

Figure 3-13: RI-eosin-(KLAKLAK)$_2$ lyses LUVs of bacterial lipid composition, but not of mammalian lipid composition. (a) RI-eosin-(KLAKLAK)$_2$ (10mM) with "Mammalian" (Mam) LUVs (50/30/20 PC/Chol/SM; 200mM total lipid), and (b) "Bacterial" (Bac) LUVs (75/20/5 PE/PG/CA; 200mM total lipid). Samples were irradiated with the same conditions used for bacterial killing assays. Data reproduced from Figure 3-6 for comparison with eosin-(KLAKLAK)$_2$.

of synergy as seen for $(KLAKLAK)_2$ when co-incubated with Ce6, towards bacterial LUVs (Figure 3-14).

3.3 Discussion

Since the widespread use of antibiotics, visualizing the effects of antibacterial agents by EM has been limited to observing morphological changes in cells. Recently, a significant progression in the field of AMPs was achieved when small helical A-AMPs were visualized with bacteria by TEM for the first time using immunogold labeling.[95] While this approach to study AMPs was indeed novel, experimental conditions were not ideal. In particular, the concentration of AMP used was ~600 µM, 10-fold greater than the concentration required to kill 85% of the culture. Despite the high peptide concentration, few peptides were observed on the cell membrane or inside *S. aureus*, which is puzzling when membrane interaction is required in all reported cases for A-AMPs.[96] The small number of peptides (gold labels) observed may be the result of incomplete labeling by the immunogold approach. Due to the vast difference in size between the peptides and a gold-labeled antibody, the immunolabel might not be able to gain access to locations that are accessible to a peptide within a cell.[17] Fixation of the samples might further diminish the ability of the immunolabel to diffuse through the resulting matrix, in order reach the peptide.[17]

An alternative approach to immunogold labeling, used in this study, is the DAB photooxidation reaction, first described by Deerinck et al. This method uses a chemical reaction with small molecules to create a localized osmiophilic polymer for enhanced

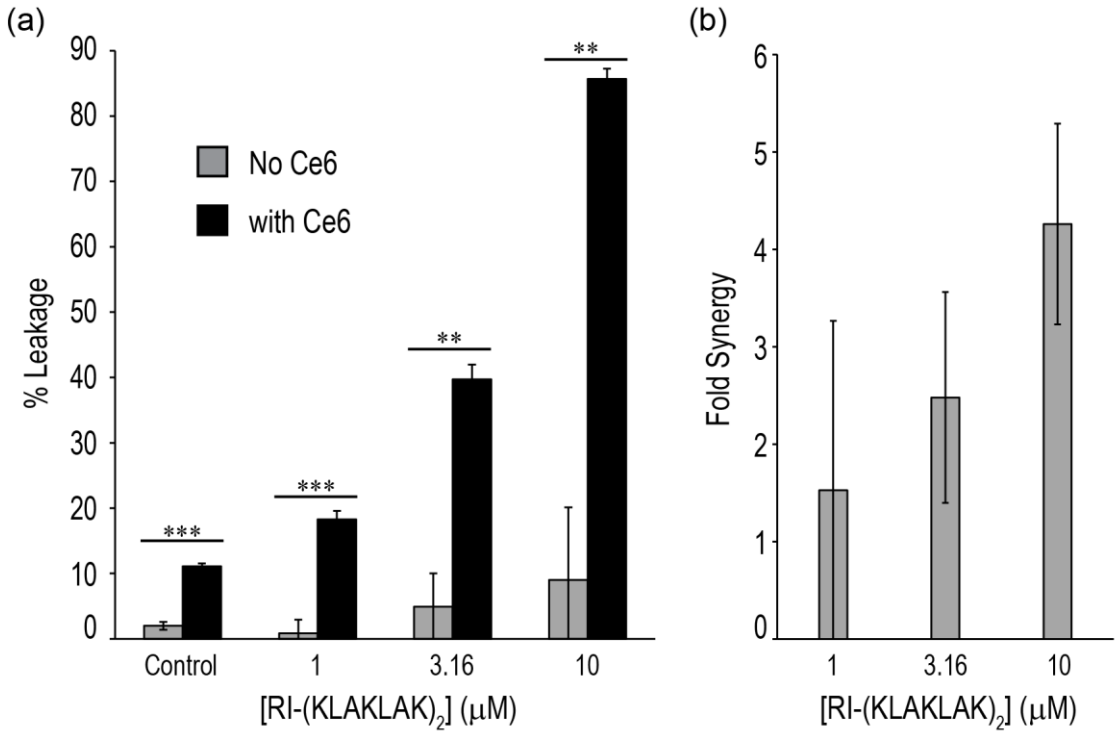

Figure 3-14: Co-incubation of Ce6 with RI-(KLAKLAK)$_2$ shows similar leakage activity towards LUVs of bacterial lipid composition as observed for Ce6 and (KLAKLAK)$_2$ in the presence of light. (a) Leakage of Bac LUVs in the presence of RI-(KLAKLAK)$_2$ alone (■), or with co-incubation of RI-(KLAKLAK)$_2$ and Ce6 (10 μM) (■) for 10 min with light. Significant differences for samples +/- Ce6 determined by two-tailed t-test, * = $p < 0.05$, ** = $p < 0.01$, *** = $p < 0.001$. (b) Fold synergy of (KLAKLAK)$_2$ activity calculated from leakage values in (a).

contrast by EM.[9, 17, 97] The minute size of the DAB monomer in comparison to an antibody should allow for a drastic increase in access to peptide locations, and thus maximize signal sensitivity. We therefore saw the DAB method as a superior approach to gain mechanistic insight into the interaction of an AMP with bacteria. TEM and STEM/EDS experiments show that eosin-$(KLAKLAK)_2$ localizes to the cell membrane of bacteria in the dark, and upon irradiation, results in significant damage to cell membranes. The initial buildup of eosin-$(KLAKLAK)_2$ upon membranes at sub-lethal concentrations in the dark is consistent with models for helical amphipathic AMPs in the literature.[62]

While the DAB method might be suitable to distinguish individual proteins in biological samples,[9] the small size of A-AMPs may not make it possible to quantify the number of peptides present. However, in the second *S. aureus* sample in Figure 3-2 (PS-AMP, no light) many individual spots can be seen in high density, which may indicate an upper limit for detection of individual AMPs. Due to the chemical nature of DAB polymer formation by ROS, a short diffusion distance is possible, and could possibly result in the generation of more than one site of DAB polymer formation and staining by osmium tetroxide (OsO_4), resulting in an overestimation of AMPs present. While the high density of spots remains consistent with membrane models for A-AMPs, an approach which can directly identify the presence of the peptide could more accurately depict the number and density of AMPs.

Direct identification of eosin-$(KLAKLAK)_2$ could be achieved by STEM/EDS, where positive identification is enabled by the presence of Br in the structure of eosin Y.

The localization of Br was isolated to the cell membrane and cellular debris, in agreement with the localization seen with the DAB method. This supports the use of DAB for visualization of small AMPs, and demonstrates the usefulness of STEM/EDS for direct identification of molecules containing an appropriate label for EDS detection within a biological sample. Current detection limits for STEM/EDS are around 0.5% of atomic presence in the sample. This may require relatively high local concentrations for molecules of interest, however, for AMPs which are expected to accumulate at the membrane surface, this may not be a significant issue, as shown in this work. DAB and STEM/EDS can be valuable for determining the location of AMPs or other molecules over time, which could lead to a better understanding of mechanisms for cellular penetration and intracellular localization.

Although PS are most often characterized by their singlet oxygen generation in the literature, it is clear that eosin Y produces superoxide to a significant extent.[86] The production of superoxide is surprisingly enhanced by conjugation of eosin Y to $(KLAKLAK)_2$ (Figure 3-4), which suggests that superoxide could play an important role in PDI mechanisms. The first sign that $(KLAKLAK)_2$ might alter the properties of eosin Y came from the red-shifted absorbance of eosin-$(KLAKLAK)_2$ compared to either eosin Y or 5(6)-carboxy-eosin Y (Figure 2-2a). It may stand to reason then, that observation of shifted PS absorbance spectra should caution the user of potentially altered triplet state properties of the PS, and thus altered ROS production.

The particular significance of superoxide in PDI is demonstrated in Figure 3-5a, where the superoxide quencher Tiron results in greater protection of *S. aureus* than any

other quencher tested. These results suggest that superoxide may actually be a more effective product for killing bacteria. While singlet oxygen has the advantage of a short lifetime which could limit non-specific damage, superoxide damage might also be sufficiently limited to reaction at its sight of production if it can be sufficiently targeted. Indeed, we previously showed that eosin-$(KLAKLAK)_2$ in mixed cultures of RBCs and bacteria could cause a 3-log reduction of bacteria without lysis of RBCs, demonstrating sufficient restriction for ROS activity to bacterial cells, where the peptide was bound.[10] In the future it will be interesting to examine the relative efficiency of bacterial killing from targeted PS which generate primarily singlet oxygen or superoxide.

Given the different membrane structures of Gram negative and positive bacteria, it is not surprising to see differing protection from quenchers, which may have differing degrees of access amongst the two membrane surfaces. DAB experiments with *E. coli* show that the majority of the peptide is bound at the outer membrane before irradiation, while *S. aureus* samples show a less restricted distribution, possibly indicating some degree of cellular penetration in the dark. Despite potential differences in binding sites, the PDI activity is similar for both strains, implying that the exact molecular binding targets may not be particularly important. The only importance may be that eosin-$(KLAKLAK)_2$ is in sufficient proximity to the surface, demonstrated by the fact that the soluble eosin Y alone has no PDI effect at even 10-fold the concentration of eosin-$(KLAKLAK)_2$ required to achieve a 5-log reduction in bacterial cultures. The attraction to bacterial cells over mammalian cells provided by $(KLAKLAK)_2$ supports the use of short A-AMPs as targeting agents to achieve localized damaged with PS. A-AMPs may

hold a distinct advantage over previously used poly-lysine or arginine-rich peptides, which are known to also bind mammalian cells, thereby decreasing specificity.

The attraction of AMPs to bacterial over mammalian membrane components may come from negatively charged LPS and peptidoglycan layers, as well as from lipids. However, AMPs must encounter and interact with a lipid layer at some point to achieve pore formation or passage through the membrane for their activity, and a lipid layer is common to both Gram types. Furthermore, PS-based strategies are known to act via lipid oxidation mechanisms. In this light, we examined whether the differences in lipid composition between mammalian cells and bacteria might be sufficient to explain differences in membrane disruption activity after treatment with eosin-$(KLAKLAK)_2$. Leakage of encapsulated calcein from liposomes was clearly evident with a bacterial lipid composition, while little effects could be observed from the mammalian lipid counterparts (Figure 3-6), suggesting that the differences in lipid composition could indeed be sufficient for differences in lipid disruption during photodynamic processes. Another distinction of bacterial lipid membranes is the apparent bleaching of eosin-$(KLAKLAK)_2$ (Figure 3-8), which does not occur with mammalian LUVs. This could be indicative of increased self-bleaching from either higher peptide concentration at the membrane, or perhaps insertion of the PS into the membrane where oxygen is approximately four times more soluble. However, the fact that leakage from bacterial LUVs is only significantly inhibited with the soluble quenchers NaN_3 and Tiron (Figure 3-7), suggests that membrane insertion of the PS is not significant in this model system.

Leakage of Bac LUVs caused by eosin-$(KLAKLAK)_2$ leads to massive aggregation that is not seen before irradiation (Figure 3-8). This suggests that peptide binding at the surface of LUVs is not sufficient to interact with other LUVs in solution to achieve aggregation, and thus the observed aggregation must be due to photodynamic effects. These results imply a mechanism for the killing of bacteria, where lipid damage leads to disruption and aggregation of lipid components. While disruption and aggregation of Bac LUVs was clearly light dependent, we could not rule out a contribution from $(KLAKLAK)_2$, which aside from targeting to bacteria, has its own antibacterial activity and may therefore participate in the lipid disruption. As seen in Figure 3-10, when $(KLAKLAK)_2$ is uncoupled from the PS in the membrane (Ce6 was used here for its natural membrane affinity), the leakage in the presence of both PS and AMP is greater than PS alone in each condition. While a greater leakage might be expected, a synergistic effect is also observed from the presence of $(KLAKLAK)_2$, indicating that $(KLAKLAK)_2$ plays a significant role in the lipid disruption caused by PS activity. One weakness of this assay is that Ce6 has a negative charge, so it is possible that the presence of $(KLAKLAK)_2$ at the membrane could actually recruit larger amounts of Ce6 to the membrane than would otherwise be present. In Figure 3-11 we addressed this issue by oxidizing LUVs in a manner independent of a PS, namely, pre-treatment of LUVs with H_2O_2 before addition of $(KLAKLAK)_2$. This assay also showed the same synergistic activity from the peptide, suggesting that the results from co-incubation with Ce6 did, in fact, reflect synergy from the peptide. It is unclear from this data, however, whether additional Ce6 may have also been recruited to the membrane by

$(KLAKLAK)_2$. From these results we can infer that similar peptide synergy effects are likely to take place when $(KLAKLAK)_2$ is directly connected to the PS, as is the case for the eosin-$(KLAKLAK)_2$ conjugate. These results support a model where $(KLAKLAK)_2$ and eosin Y act in synergy for the disruption of lipid bilayers by combining photochemical and physical disruption mechanisms.

In systems consisting of peptide reagents or components, retro inverso peptides can be synthesized to reduce the proteolytic degradation that occurs with the typical L-amino acid peptides. The RI-eosin-$(KLAKLAK)_2$ conjugate and RI-$(KLAKLAK)_2$, respectively, showed improved leakage toward bacterial LUVs (Figure 3-13) as well as an increase in apparent synergy with a PS (Figure 3-14). These data indicate that the RI-eosin-$(KLAKLAK)_2$ might be a better reagent for bacterial killing, although this remains to be tested.

Overall, our results demonstrate that eosin-$(KLAKLAK)_2$ is an effective antibacterial agent for PDI, which utilizes a synergistic interaction between PS and AMP. The properties of the PS are affected by conjugation, and may enhance the activity of the PS by altering ROS production. This design may serve as the basis for the future rational design of PS-AMP compounds with enhanced activity. The use of PS yielding greater levels of ROS, or AMPs with greater membrane disruption activity may provide for significant improvements in activity and bacterial specificity. The use of eosin Y as a dual marker for determining the location of AMPs or other small peptides in a biological context with the DAB method and STEM/EDS is also demonstrated in this work. One might envision of course, that the DAB and STEM/EDS approaches might be

separated, requiring only a PS for the DAB approach, or only a unique atomic label for STEM/EDS. We anticipate that the STEM/EDS approach may be of particular use for peptidomimetics, which often include atoms such as fluorine, which have little presence (background signal) in biological environments. In this case fluorine could serve as an intrinsic label, not requiring further modification of the molecule. While we have demonstrated these principles here, further tests are needed to validate these ideas.

3.4 Materials and methods

3.4.1 Materials

Fmoc amino acids and HBTU were purchased from Novabiochem, while all solvents and chemicals were purchase from Sigma. One exception was 5(6)-carboxy eosin Y, which was purchased from Marker Gene Technologies. Lipids and cholesterol were purchased from Avanti Lipids.

3.4.2 Solid phase peptide synthesis

Same as in section 2, except retro-inverso $(KLAKLAK)_2$ was synthesized using D-amino acids, which were also ordered from Novabiochem.

3.4.3 Spectroscopy

Same as in section 2, except Ce6 was used at 10 μM.

3.4.4 Light source for photodynamic experiments

Same as in section 2.

3.4.5 Photooxidation, fixation, and DAB polymerization in bacteria samples

Samples of *E. coli* or *S. aureus* were prepared in the same manner used previously for phototoxicity experiments.[10] Cultures were grown overnight in LB broth and fresh subcultures were prepared in the morning. After growth to O.D.600 ~0.6, the cells were pelleted and resuspended in phosphate buffer (100 mM NaCl, 10 mM Na_2HPO_4, pH 7.4), and this wash procedure repeated once more. The stock suspension was diluted to an O.D. which gave approximately 10^8 CFU/ml for each strain. Eosin-$(KLAKLAK)_2$ (22 µl of 10µM), or water as a blank, was added to wells of a 96 well plate before addition of 200 µl of bacteria suspension in phosphate buffer (10^8 CFU/ml). Samples were then kept in the dark for 2 min or illuminated under the halogen lamp assembly mentioned above for 2 or 5 min. Acrolein (100 µl of 2% solution) was then added to samples and incubated at room temperature for 20 min to fix the bacteria and any bound eosin-$(KLAKLAK)_2$. To remove unbound eosin-$(KLAKLAK)_2$, the samples were transferred to microcentrifuge tubes and pelleted in a small benchtop centrifuge for 5 min. The supernatant was removed and samples were washed twice with 100 µl of cold 0.1 M cacodylate buffer. The pellets were then resuspended in the same buffer supplemented with 0.1 M glycine to react with any remaining acrolein in solution, and allowed to incubate for 20 min before addition of 100 µl of diaminobenzidine (DAB) buffer (1 mg/ml DAB in cacodylate buffer). These suspensions were transferred to a 96

well plate for 15min illumination to polymerize DAB specifically in the locations where the peptide was fixed, followed by an additional 100 µl of DAB buffer and 15 min of illumination. Samples were then transferred back to microcentrifuge tubes and washed twice with cacodylate buffer, followed by suspension in cacodylate buffer containing 1% (wt/vol) osmium tetroxide.

3.4.6 Electron microscopy sample preparation and imaging

After suspension of cells in osmium tetroxide, samples were dehydrated with 10% steps of methanol to (10%-100%), infiltrated overnight, and embedded in Quetol 651-Spurr epoxy resin[98] and polymerized overnight. Thin sections (200-250 nm) were cut with a Microstar diamond knife, (Huntsville, TX) using an AO Ultracut ultramicrotome picked up on grids and examined in a FEI Tecnai Field emission electron microscope at 200 kV accelerating voltage after carbon stabilizing the grids with approximately 10 nm of carbon using a Cressington 308 evaporative coater. Elemental analysis was performed on a TECNAI F20 (scanning) transmission electron microscope (TEM/STEM) fitted with a Schottky field emission gun, a high angle annular dark field (HAADF) detector, and an EDAX instrument ultrathin window energy dispersive X-ray spectroscopy (EDS) detector. The combination of STEM and EDS allows direct imaging of a nanoscale area and *in situ* identification of component elements. An EDS spectrum at each spot in the area of interest was collected at a 200 kV accelerating voltage and a ~15° tilting angle with a stationary electron probe in STEM mode. An elemental map

was then acquired after choosing a proper energy window for an element-specific transition along with STEM-HAADF images.

3.4.7 In vitro detection of singlet oxygen and superoxide production

Detection of singlet oxygen from eosin Y or eosin-$(KLAKLAK)_2$ was achieved by irradiation in the presence of imidazole and RNO (p-nitrosodimethylaniline).[89] Production of singlet oxygen from eosin Y leads to reaction with imidazole to form a peroxide intermediate, which subsequently reacts with RNO to cause bleaching of RNO absorbance. A total reaction volume of 200 µl was obtained by addition of 20 µl each of 10X solutions for RNO, imidazole, quencher (or H_2O blank), PS or PS-AMP (or H_2O blank), and 120 µl phosphate buffer (10 mM phosphate, pH 7.4, 100mM NaCl). Final concentrations were 50 µM RNO, 8 mM imidazole, 100 mM sodium azide, and eosin Y or eosin-$(KLAKLAK)_2$ at 1 or 10 µM. Illumination was carried out in the same manner as bacterial killing experiments to ensure relevant results. Bleaching of RNO was detected at 450nm using a Glomax Multi + Plate reader.

Detection of superoxide was achieved by excitation of eosin Y and eosin-$(KLAKLAK)_2$ in the presence of NADH and NBT (nitro blue tetrazolium). A total reaction volume was obtained with 10X stock solutions in the manner mentioned above for the RNO assay. Final concentrations for eosin Y or eosin-$(KLAKLAK)_2$ were 1 or 10 µM, 10mM NADH, and 80 µM NBT. Illumination was carried out in the same manner as bacterial killing experiments. Reduction of NBT resulting in the production of a formazan was detected by absorbance at 600nm using a plate reader. Since the RNO

and NBT reactions proceed by oxidation and reduction, respectively, there is no cross talk between the assays.[37, 91]

3.4.8 Bacterial killing experiments with ROS quenchers

Bacterial killing experiments were carried out in the same manner as described in section II, but using 11 µl of 20X quencher and 11 µl of 20X eosin-$(KLAKLAK)_2$, before addition of 200 µl of 10^8 CFU/ml bacteria culture. Crocetin was used from a 100X in DMSO, requiring only 2.2 µl of stock in a total volume of 222 µl.

3.4.9 Liposomes

Large unilamellar vesicles (LUVs) of two compositions were prepared to represent lipids of bacterial[99] and mammalian membranes. The mammalian composition was 50/30/20 of PC/Chol/SM, (PC = 1-stearoyl-2-oleoyl-sn-glycero-3-phosphocholine; Chol = cholesterol, SM = choline sphingomyelin from stearic acid). The bacterial composition was 75/20/5 of PE/PG/CA (PE = dioleoyl-phosphatidyl ethanolamine, PG = L-α-Phosphatidyl-DL-Glycerol from chicken egg, CA = cardiolipin). Stock lipids in chloroform were mixed in a scintillation vial for the required molar ratios and the solvent evaporated under a nitrogen stream. These lipid mixtures were placed in a vacuum desiccator for a minimum of 2 hrs. before addition of swelling buffer. The lipids were then put through ten freeze-thaw cycles between liquid nitrogen and a water bath at 42^{o}C to obtain multi-lamellar vesicles (MLVs). These MLVs were extruded twenty one times using an Avanti extruder with a 100 nm polycarbonate membrane. For leakage

studies LUVs were prepared with a swelling buffer of 60 mM calcein in phosphate buffer (10 mM NaH_2PO_4, 100 mM NaCl, pH 7.4). After extrusion the free dye was excluded by running the LUVs through a Sephadex G-50 column in phosphate buffer. The calcein-loaded LUV preparations for both lipid compositions used for this manuscript were stable for approximately three weeks when kept at 4°C. This stability varies with lipid composition, however, and should be carefully noted in each case. We monitored stability over time by measuring the increase in fluorescence after addition of 0.1% Triton X-100 (final concentration), using a 200 µl sample of 200 µM total lipid. Samples were placed in a 96 well plate and fluorescence determined with a Promega® Glomax Multi® microplate reader. Ten-fold dilutions were made where needed to ensure that no self-quenching remained in the detergent samples, allowing for a linear comparison between samples.

3.4.10 Leakage assays

For leakage experiments, stock solutions of calcein-loaded LUVs were diluted as needed in phosphate buffer to obtain working solutions of 200 µM total lipid. Wells of a 96 well plate were first filled with 11 µl of 20X quencher or H_2O blank, followed by 11 µl of 20X eosin-$(KLAKLAK)_2$, RI-eosin-$(KLAKLAK)_2$, or H_2O blank. A volume of 200 µl of the 200 µM LUV working solution was then added to each well. This mixture provides a 1X concentration of quencher and eosin-$(KLAKLAK)_2$ or RI-eosin-$(KLAKLAK)_2$ with 90% of the total lipid concentration in the final solution. Samples were irradiated using the light source described above, and calcein release was

monitored by fluorescence with the plate reader (Ex 490, Em 510-570). Readings of all samples were taken before irradiation for a value at "0 min." An estimate of fluorescence for 100% lysis was obtained by addition of 10X Triton X-100 (0.1% final concentration) to each sample after the last time point. For experiments examining the influence of membrane oxidation upon the activity of free $(KLAKLAK)_2$ or RI-$(KLAKLAK)_2$, LUVs were co-treated with 10 μM Ce6 and varying concentrations of $(KLAKLAK)_2$ or RI-$(KLAKLAK)_2$. Alternatively, LUVs were pre-treated with H_2O_2 for 15 min before addition of free $(KLAKLAK)_2$.

4. CONCLUSION

Due to the unique broad-spectrum targeting of bacteria preferentially over mammalian cells, I propose that the eosin-$(KLAKLAK)_2$ conjugate can serve as an effective antibacterial agent for PDI, as well as a model platform for the enhancement of PS by conjugation to AMPs, and vice versa. In section 2, I showed that conjugation of the soluble PS, eosin Y, to the AMP, $(KLAKLAK)_2$, resulted in the targeting of eosin Y to bacterial membranes, even in mixed RBC and bacteria cultures. Furthermore, the eosin-$(KLAKLAK)_2$ conjugate could achieve a 5-log reduction in both *E. coli* and *S. aureus* cultures under conditions showing no toxicity to RBCs or mammalian cell lines. Intriguingly, when eosin Y and eosin-$(KLAKLAK)_2$ were bound to bacterial cells to the same extent (requiring 10-fold excess of eosin Y), eosin-$(KLAKLAK)_2$ was toxic to bacteria, while eosin Y was not, suggesting a role for $(KLAKLAK)_2$ beyond simple targeting. To address these observations, in section 3, I tested the respective roles for eosin Y and $(KLAKLAK)_2$ in the conjugate. DAB and STEM/EDS methods, which have never been used for AMPs before, revealed a localization of eosin-$(KLAKLAK)_2$ at the membrane before irradiation, and expanding to extracellular debris after irradiation, accompanied by alteration of membrane morphology and lysis. It was shown that eosin-$(KLAKLAK)_2$ demonstrates a strong preference for disruption of liposomes with bacterial lipid composition, resulting in significant leakage and aggregation, and suggesting a plausible cause of preferential attraction for bacterial over mammalian cells. A synergistic affect was revealed for both $(KLAKLAK)_2$ and RI-$(KLAKLAK)_2$ in

the presence of a PS for lipid membrane disruption, demonstrating that the nature of the peptide chosen for targeting a PS may be able to significantly enhance any damage achieved by the PS alone. Overall, the use of biochemical and microscopy techniques with mammalian cell lines, RBCs, and bacterial cells, has led to a mechanistic understanding of eosin-$(KLAKLAK)_2$ in PDI. The results here have established the PS-AMP approach as a working platform for PDI and may serve as the basis for the rational design of future PDI agents.

REFERENCES

(1) Dai, T., Huang, Y. Y., and Hamblin, M. R. (2009) Photodynamic therapy for localized infections - state of the art. *Photodiagnosis and Photodynamic Therapy 6*, 170-88.

(2) Moghissi, K. (2010) Can Surgical Site Infection (SSI) be treated by photodynamic therapy (PDT)? *Photodiagnosis and Photodynamic therapy 7*, 1-2.

(3) Downes, A., and Blunt, T. P. (1877) Researches on the effect of light upon bacteria and other organisms. *Proceedings of the Royal Society of London 26*, 488-500.

(4) Raab, O. (1900) Ueber diewirkung fluoreszierender stoffe auf infusori. *Z. Biol. 39*, 524-536.

(5) Meyer-Betz, F. (1913) Research on the biological (photodynamic) action of hematoporphyrin and other derivatives of blood and bile pigments. *Deutsches Archiv. fur Kinische. Medizin. 112*, 476-503.

(6) Valenzeno, D. P., and Pooler, J. P. (1987) Photodynamic action. *BioScience 37*, 270-276.

(7) Redmond, R. W., and Gamlin, J. N. (1999) A compilation of singlet oxygen yields from biologically relevant molecules. *Photochemistry and Photobiology 70*, 391-475.

(8) Calzavara-Pinton, P., Rossi, M. T., Sala, R., and Venturini, M. (2012) Photodynamic antifungal chemotherapy. *Photochemistry and Photobiology 88*, 512-22.

(9) Shu, X., Lev-Ram, V., Deerinck, T. J., Qi, Y., Ramko, E. B., Davidson, M. W., Jin, Y., Ellisman, M. H., and Tsien, R. Y. (2011) A genetically encoded tag for correlated light and electron microscopy of intact cells, tissues, and organisms. *PLoS Biology 9*, e1001041.

(10) Johnson, G. A., Muthukrishnan, N., and Pellois, J. P. (2013) Photoinactivation of Gram positive and Gram negative bacteria with the antimicrobial peptide $(KLAKLAK)_2$ conjugated to the hydrophilic photosensitizer eosin Y. *Bioconjugate Chemistry 24*, 114-23.

(11) Sharma, S. K., Mroz, P., Dai, T., Huang, Y. Y., St Denis, T. G., and Hamblin, M. R. (2012) Photodynamic therapy for cancer and for infections: what is the difference? *Israel Journal of Chemistry 52*, 691-705.

(12) Hamblin, M. R., O'Donnell, D. A., Murthy, N., Rajagopalan, K., Michaud, N., Sherwood, M. E., and Hasan, T. (2002) Polycationic photosensitizer conjugates: effects of chain length and Gram classification on the photodynamic inactivation of bacteria. *Journal of Antimicrobial Chemotherapy 49*, 941-951.

(13) Valenzeno, D. P., and Pooler, J. P. (1982) Cell membrane photomodification: relative effectiveness of halogenated fluoresceins for photohemolysis. *Photochemistry and Photobiology 35*, 343-50.

(14) Pooler, J. P. (1989) Photooxidation of cell membranes using eosin derivatives that locate in lipid or protein to study the role of diffusible intermediates. *Photochemistry and Photobiology 50*, 55-68.

(15) Mojzisova, H., Bonneau, S., Maillard, P., Berg, K., and Brault, D. (2009) Photosensitizing properties of chlorins in solution and in membrane-mimicking systems. *Photochemical & Photobiological Sciences 8*, 778-787.

(16) Valenzeno, D. P. (1987) Photomodification of biological membranes with emphasis on singlet oxygen mechanisms. *Photochemistry and Photobiology 46*, 147-160.

(17) Deerinck, T. J., Martone, M. E., Lev-Ram, V., Green, D. P., Tsien, R. Y., Spector, D. L., Huang, S., and Ellisman, M. H. (1994) Fluorescence photooxidation with eosin: a method for high resolution immunolocalization and in situ hybridization detection for light and electron microscopy. *The Journal of Cell Biology 126*, 901-910.

(18) Hamblin, M. R., and Hasan, T. (2004) Photodynamic therapy: a new antimicrobial approach to infectious disease? *Photochemical & Photobiological Sciences 3,* 436-450.

(19) Maisch, T., Szeimies, R. M., Jori, G., and Abels, C. (2004) Antibacterial photodynamic therapy in dermatology. *Photochemical and Photobiological Sciences 3,* 907-17.

(20) Wainwright, M., Smalley, H., and Flint, C. (2011) The use of photosensitisers in acne treatment. *Journal of Photochemistry and Photobiology B: Biology 105,* 1-5.

(21) Bethea, D., Fullmer, B., Syed, S., Seltzer, G., Tiano, J., Rischko, C., Gillespie, L., Brown, D., and Gasparro, F. P. (1999) Psoralen photobiology and photochemotherapy: 50 years of science and medicine. *Journal of Dermatological Science 19*, 78-88.

(22) Ravic-Nikolic, A., Radosavljevic, G., Jovanovic, I., Zdravkovic, N., Mitrovic, S., Pavlovic, S., and Arsenijevic, N. (2011) Systemic photochemotherapy decreases the expression of IFN-gamma, IL-12p40 and IL-23p19 in psoriatic plaques. *European Journal of Dermatology 21*, 53-7.

(23) Bliss, J. M., Bigelow, C. E., Foster, T. H., and Haidaris, C. G. (2004) Susceptibility of *Candida* species to photodynamic effects of photofrin. *Antimicrobial Agents and Chemotherapy 48*, 2000-2006.

(24) Dai, T., Fuchs, B. B., Coleman, J. J., Prates, R. A., Astrakas, C., St Denis, T. G., Ribeiro, M. S., Mylonakis, E., Hamblin, M. R., and Tegos, G. P. (2012) Concepts and principles of photodynamic therapy as an alternative antifungal discovery platform. *Frontiers in Microbiology 3*, 120-136.

(25) Wainwright, M. (2000) Methylene blue derivatives — suitable photoantimicrobials for blood product disinfection? *International Journal of Antimicrobial Agents 16*, 381-394.

(26) Tanaka, M., Kinoshita, M., Yoshihara, Y., Shinomiya, N., Seki, S., Nemoto, K., Hirayama, T., Dai, T., Huang, L., Hamblin, M. R., and Morimoto, Y. (2012)

Optimal photosensitizers for photodynamic therapy of infections should kill bacteria but spare neutrophils. *Photochemistry and Photobiology 88,* 227-32.

(27) Mohr, H., Lambrecht, B., and Selz, A. (1995) Photodynamic virus inactivation of blood components. *Immunological Investigations 24*, 73-85.

(28) Braham, P., Herron, C., Street, C., and Darveau, R. (2009) Antimicrobial photodynamic therapy may promote periodontal healing through multiple mechanisms. *Journal of Periodontology 80*, 1790-8.

(29) Lauro, F. M., Pretto, P., Covolo, L., Jori, G., and Bertoloni, G. (2002) Photoinactivation of bacterial strains involved in periodontal diseases sensitized by porphycene-polylysine conjugates. *Photochemical & Photobiological Sciences 1*, 468-470.

(30) Maisch, T., Hackbarth, S., Regensburger, J., Felgentrager, A., Baumler, W., Landthaler, M., and Roder, B. (2011) Photodynamic inactivation of multi-resistant bacteria (PIB) - a new approach to treat superficial infections in the 21st century. *Journal of the German Society of Dermatology 9*, 360-6.

(31) Vera, D. M., Haynes, M. H., Ball, A. R., Dai, T., Astrakas, C., Kelso, M. J., Hamblin, M. R., and Tegos, G. P. (2012) Strategies to potentiate antimicrobial photoinactivation by overcoming resistant phenotypes. *Photochemistry and Photobiology 88,* 3: 498-511.

(32) Demidova, T. N., and Hamblin, M. R. (2004) Photodynamic therapy targeted to pathogens. *International Journal of Immunopathology and Pharmacology 17,* 245-54.

(33) Bourre, L., Giuntini, F., Eggleston, I. M., Mosse, C. A., MacRobert, A. J., and Wilson, M. (2010) Effective photoinactivation of Gram-positive and Gram-negative bacterial strains using an HIV-1 Tat peptide-porphyrin conjugate. *Photochemical & Photobiological Sciences 9*, 1613-1620.

(34) Hamblin, M. R., O'Donnell, D. A., Murthy, N., Rajagopalan, K., Michaud, N., Sherwood, M. E., and Hasan, T. (2002) Polycationic photosensitizer conjugates: effects of chain length and Gram classification on the photodynamic inactivation of bacteria. *Journal of Antimicrobial Chemotherapy 49*, 941-51.

(35) Polo, L., Segalla, A., Bertoloni, G., Jori, G., Schaffner, K., and Reddi, E. (2000) Polylysine-porphycene conjugates as efficient photosensitizers for the inactivation of microbial pathogens. *Journal of Photochemistry and Photobiology B 59*, 152-8.

(36) Soukos, N. S., Ximenez-Fyvie, L. A., Hamblin, M. R., Socransky, S. S., and Hasan, T. (1998) Targeted antimicrobial photochemotherapy. *Antimicrobial Agents and Chemotherapy. 42*, 2595-2601.

(37) Tegos, G. P., Anbe, M., Yang, C., Demidova, T. N., Satti, M., Mroz, P., Janjua, S., Gad, F., and Hamblin, M. R. (2006) Protease-stable polycationic photosensitizer conjugates between polyethyleneimine and chlorin(e6) for broad-spectrum antimicrobial photoinactivation. *Antimicrobial Agents and Chemotherapy 50*, 1402-1410.

(38) Vaara, M., and Vaara, T. (1983) Polycations as outer membrane-disorganizing agents. *Antimicrobial Agents and Chemotherapy 24*, 114-22.

(39) Sara, M., and Sleytr, U. B. (1987) Molecular sieving through S layers of *Bacillus stearothermophilus* strains. *Journal of Bacteriology 169*, 4092-8.

(40) Sharma, S. K., Chiang, L. Y., and Hamblin, M. R. (2011) Photodynamic therapy with fullerenes in vivo: reality or a dream? *Nanomedicine 6*, 1813-25.

(41) Nisnevitch, M., Nakonechny, F., and Nitzan, Y. (2010) Photodynamic antimicrobial chemotherapy by liposome-encapsulated water-soluble photosensitizers. *Russian Journal of Bioorganic Chemistry 36*, 363-369.

(42) Tsai, T., Yang, Y. T., Wang, T. H., Chien, H. F., and Chen, C. T. (2009) Improved photodynamic inactivation of gram-positive bacteria using hematoporphyrin encapsulated in liposomes and micelles. *Lasers in Surgery and Medicine 41*, 316-22.

(43) Foote, C. S. (1991) Definition of type I and type II photosensitized oxidation. *Photochemistry and Photobiology 54*, 659.

(44) Vera, D. M., Haynes, M. H., Ball, A. R., Dai, T., Astrakas, C., Kelso, M. J., Hamblin, M. R., and Tegos, G. P. (2012) Strategies to potentiate antimicrobial photoinactivation by overcoming resistant phenotypes. *Photochemistry and Photobiology 88*, 499-511.

(45) Ochsner, M. (1997) Photophysical and photobiological processes in the photodynamic therapy of tumours. *Journal of Photochemistry and Photobiology B: Biology 39*, 1-18.

(46) Redmond, R. W., and Kochevar, I. E. (2006) Symposium in print: singlet oxygen invited review. *Photochemistry and Photobiology 82,* 1178-1186.

(47) Albert W, G. (2001) Photosensitized oxidation of membrane lipids: reaction pathways, cytotoxic effects, and cytoprotective mechanisms. *Journal of Photochemistry and Photobiology B: Biology 63*, 103-113.

(48) Girotti, A. W. (1998) Lipid hydroperoxide generation, turnover, and effector action in biological systems. *Journal of Lipid Research 39*, 1529-1542.

(49) Lambrechts, S. A., Demidova, T. N., Aalders, M. C., Hasan, T., and Hamblin, M. R. (2005) Photodynamic therapy for *Staphylococcus aureus* infected burn wounds in mice. *Photochemical and Photobiological Sciences 4*, 503-9.

(50) Vecchio, D., Dai, T., Huang, L., Fantetti, L., Roncucci, G., and Hamblin, M. R. (2012) Antimicrobial photodynamic therapy with RLP068 kills methicillin-resistant *Staphylococcus aureus* and improves wound healing in a mouse model of infected skin abrasion PDT with RLP068/Cl in infected mouse skin abrasion. *Journal of Biophotonics* Sep 14. doi: 10.1002/jbio.201200121. [Epub ahead of print].

(51) Soukos, N. S., Hamblin, M. R., and Hasan, T. (1997) The effect of charge on cellular uptake and phototoxicity of polylysine chlorin(e6) conjugates. *Photochemistry and Photobiology 65*, 723-9.

(52) Schastak, S., Ziganshyna, S., Gitter, B., Wiedemann, P., and Claudepierre, T. (2010) Efficient photodynamic therapy against Gram-positive and Gram-negative bacteria using THPTS, a cationic photosensitizer excited by infrared wavelength. *PLoS ONE 5*, e11674.

(53) Maisch, T. (2007) Anti-microbial photodynamic therapy: useful in the future? *Lasers in Medical Science 22*, 83-91.

(54) Zasloff, M. (1987) Magainins, a class of antimicrobial peptides from *Xenopus* skin: isolation, characterization of two active forms, and partial cDNA sequence of a precursor. *Proceedings of the National Academy of Sciences USA 84*, 5449-5453.

(55) Zasloff, M. (2002) Antimicrobial peptides of multicellular organisms. *Nature 415*, 389-95.

(56) Nguyen, L. T., Haney, E. F., and Vogel, H. J. (2011) The expanding scope of antimicrobial peptide structures and their modes of action. *Trends in Biotechnology 29*, 464-472.

(57) Fjell, C. D., Hiss, J. A., Hancock, R. E. W., and Schneider, G. (2012) Designing antimicrobial peptides: form follows function. *Nature Reviews in Drug Discovery 11*, 37-51.

(58) Perron, G. G., Zasloff, M., and Bell, G. (2006) Experimental evolution of resistance to an antimicrobial peptide. *Proceedings of the Royal Society B: Biological Sciences 273*, 251-256.

(59) Lipsky, B. A., Holroyd, K. J., and Zasloff, M. (2008) Topical versus systemic antimicrobial therapy for treating mildly infected diabetic foot ulcers: A randomized, controlled, double-blinded, multicenter trial of pexiganan cream. *Clinical Infectious Diseases 47*, 1537-1545.

(60) Gottler, L. M., and Ramamoorthy, A. (2009) Structure, membrane orientation, mechanism, and function of pexiganan - a highly potent antimicrobial peptide designed from magainin. *Biochimica et Biophysica Acta - Biomembranes 1788*, 1680-1686.

(61) Findlay, B., Zhanel, G. G., and Schweizer, F. (2010) Cationic amphiphiles, a new generation of antimicrobials inspired by the natural antimicrobial peptide scaffold. *Antimicrobial Agents and Chemotherapy 54*, 4049-4058.

(62) Brogden, K. A. (2005) Antimicrobial peptides: pore formers or metabolic inhibitors in bacteria? *Nature Reviews in Microbiology 3*, 238-250.

(63) Yeaman, M. R., and Yount, N. Y. (2003) Mechanisms of antimicrobial peptide action and resistance. *Pharmacological Reviews 55*, 27-55.

(64) Park, C. B., Kim, H. S., and Kim, S. C. (1998) Mechanism of action of the antimicrobial peptide buforin II: buforin II kills microorganisms by penetrating the cell membrane and inhibiting cellular functions. *Biochemical and Biophysical Research Communications 244*, 253-7.

(65) Wimley, W., and Hristova, K. (2011) Antimicrobial peptides: successes, challenges and unanswered questions. *Journal of Membrane Biology 239*, 27-34.

(66) Huang, H. W. (2006) Molecular mechanism of antimicrobial peptides: the origin of cooperativity. *Biochimica et Biophysica Acta - Biomembranes 1758*, 1292-1302.

(67) Liu, F., Soh Yan Ni, A., Lim, Y., Mohanram, H., Bhattacharjya, S., and Xing, B. (2012) Lipopolysaccharide neutralizing peptide-porphyrin conjugates for effective photoinactivation and intracellular imaging of gram-negative bacteria strains. *Bioconjugate Chemistry 23*, 1639-47.

(68) Dosselli, R., Tampieri, C., Ruiz-Gonzalez, R., De Munari, S., Ragas, X., Sanchez-Garcia, D., Agut, M., Nonell, S., Reddi, E., and Gobbo, M. (2013) Synthesis, characterization, and photoinduced antibacterial activity of porphyrin-type photosensitizers conjugated to the antimicrobial peptide apidaecin 1b. *Journal of Medicinal Chemistry 56*, 1052-63.

(69) Srinivasan, D., Muthukrishnan, N., Johnson, G. A., Erazo-Oliveras, A., Lim, J., Simanek, E. E., and Pellois, J.-P. (2011) Conjugation to the cell-penetrating peptide TAT potentiates the photodynamic effect of carboxytetramethylrhodamine. *PLoS ONE 6*, e17732.

(70) Javadpour, M. M., Juban, M. M., Lo, W.-C. J., Bishop, S. M., Alberty, J. B., Cowell, S. M., Becker, C. L., and McLaughlin, M. L. (1996) De novo antimicrobial peptides with low mammalian cell toxicity. *Journal of Medicinal Chemistry 39*, 3107-3113.

(71) Brogden, K. A. (2005) Antimicrobial peptides: pore formers or metabolic inhibitors in bacteria? *Nature Reviews in Microbiology 3*, 238-50.

(72) Ellerby, H. M., Arap, W., Ellerby, L. M., Kain, R., Andrusiak, R., Rio, G. D., Krajewski, S., Lombardo, C. R., Rao, R., Ruoslahti, E., Bredesen, D. E., and Pasqualini, R. (1999) Anti-cancer activity of targeted pro-apoptotic peptides. *Nature Medicine 5*, 1032-8.

(73) Dathe, M., Meyer, J., Beyermann, M., Maul, B., Hoischen, C., and Bienert, M. (2002) General aspects of peptide selectivity towards lipid bilayers and cell membranes studied by variation of the structural parameters of amphipathic helical model peptides. *Biochimica et Biophysica Acta - Biomembranes 1558*, 171-186.

(74) Frolov, A. A., and Gurinovich, G. P. (1992) The laws of delayed photohaemolysis sensitized by chlorin e6. *Journal of Photochemistry and Photobiology B: Biology 13*, 39-50.

(75) Valenzeno, D. P., and Pooler, J. P. (1982) Cell membrane photomodification: relative effectiveness of halogenated fluoresceins for photohemolysis. *Photochemistry and Photobiology 35*, 343-350.

(76) Segalla, A., Borsarelli, C. D., Braslavsky, S. E., Spikes, J. D., Roncucci, G., Dei, D., Chiti, G., Jori, G., and Reddi, E. (2002) Photophysical, photochemical and antibacterial photosensitizing properties of a novel octacationic Zn(II)-phthalocyanine. *Photochemical and Photobiological Sciences 1*, 641-8.

(77) Usacheva, M. N., Teichert, M. C., and Biel, M. A. (2001) Comparison of the methylene blue and toluidine blue photobactericidal efficacy against gram-positive and gram-negative microorganisms. *Lasers in Surgery and Medicine 29*, 165-73.

(78) Maisch, T., Bosl, C., Szeimies, R. M., Lehn, N., and Abels, C. (2005) Photodynamic effects of novel XF porphyrin derivatives on prokaryotic and eukaryotic cells. *Antimicrobial Agents and Chemotherapy 49*, 1542-52.

(79) Nakase, I., Niwa, M., Takeuchi, T., Sonomura, K., Kawabata, N., Koike, Y., Takehashi, M., Tanaka, S., Ueda, K., Simpson, J. C., Jones, A. T., Sugiura, Y.,

and Futaki, S. (2004) Cellular uptake of arginine-rich peptides: roles for macropinocytosis and actin rearrangement. *Molecular Therapy 10*, 1011-22.

(80) Ryser, H. J., and Hancock, R. (1965) Histones and basic polyamino acids stimulate the uptake of albumin by tumor cells in culture. *Science 150*, 501-3.

(81) Shen, W. C., and Ryser, H. J. (1978) Conjugation of poly-L-lysine to albumin and horseradish peroxidase: a novel method of enhancing the cellular uptake of proteins. *Proceedings of the National Academy of Sciences U S A 75*, 1872-6.

(82) Berg, K., and Moan, J. (1994) Lysosomes as photochemical targets. *International Journal of Cancer 59*, 814-822.

(83) Choi, Y., McCarthy, J. R., Weissleder, R., and Tung, C. H. (2006) Conjugation of a photosensitizer to an oligoarginine-based cell-penetrating peptide increases the efficacy of photodynamic therapy. *ChemMedChem 1*, 458-63.

(84) Takeuchi, T., Kosuge, M., Tadokoro, A., Sugiura, Y., Nishi, M., Kawata, M., Sakai, N., Matile, S., and Futaki, S. (2006) Direct and rapid cytosolic delivery using cell-penetrating peptides mediated by pyrenebutyrate. *ACS Chemical Biology 1*, 299-303.

(85) Angeles-Boza, A. M., Erazo-Oliveras, A., Lee, Y. J., and Pellois, J. P. (2010) Generation of endosomolytic reagents by branching of cell-penetrating peptides: tools for the delivery of bioactive compounds to live cells in cis or trans. *Bioconjugate Chemistry 21*, 2164-7.

(86) Natera, J. E., Massad, W. A., Amat-Guerri, F., and García, N. A. (2011) Elementary processes in the eosin-sensitized photooxidation of 3,3′-diaminobenzidine for correlative fluorescence and electron microscopy. *Journal of Photochemistry and Photobiology A: Chemistry 220*, 25-30.

(87) Gribble, G. (2000) The natural production of organobromine compounds. *Environmental Science & Pollution Research 7*, 37-49.

(88) Wang, M., Maragani, S., Huang, L., Jeon, S., Canteenwala, T., Hamblin, M. R., and Chiang, L. Y. (2013) Synthesis of decacationic [60]fullerene decaiodides

giving photoinduced production of superoxide radicals and effective PDT-mediation on antimicrobial photoinactivation. *European Journal of Medicinal Chemistry 63C*, 170-184.

(89) Kraljić, I., and Mohsni, S. E. (1978) A new method for the detection of singlet oxygen in aqueous solutions. *Photochemistry and Photobiology 28*, 577-581.

(90) Kochevar, I. E., and Redmond, R. W. (2000) Photosensitized production of singlet oxygen, in *Methods in Enzymology* (Lester Packer, H. S., Ed.) pp 20-28, Academic Press, Waltham, MA.

(91) Yamakoshi, Y., Umezawa, N., Ryu, A., Arakane, K., Miyata, N., Goda, Y., Masumizu, T., and Nagano, T. (2003) Active oxygen species generated from photoexcited fullerene (C60) as potential medicines: $O_2^{-\bullet}$ versus $^1O_2$. *Journal of the American Chemical Society 125*, 12803-12809.

(92) Tegos, G. P., Anbe, M., Yang, C., Demidova, T. N., Satti, M., Mroz, P., Janjua, S., Gad, F., and Hamblin, M. R. (2006) Protease-stable polycationic photosensitizer conjugates between polyethyleneimine and chlorin(e6) for broad-spectrum antimicrobial photoinactivation. *Antimicrobial Agents and Chemotherapy 50*, 1402-10.

(93) Domingo, J. L., de la Torre, A., Bellés, M., Mayayo, E., Llobet, J. M., and Corbella, J. (1997) Comparative effects of the chelators sodium 4,5-dihydroxybenzene-1,3-disulfonate (Tiron) and diethylenetriaminepentaacetic acid (DTPA) on acute uranium nephrotoxicity in rats. *Toxicology 118*, 49-59.

(94) Belfiore, C., Castellano, P., and Vignolo, G. (2007) Reduction of *Escherichia coli* population following treatment with bacteriocins from lactic acid bacteria and chelators. *Food Microbiology 24*, 223-9.

(95) Azad, M. A., Huttunen-Hennelly, H. E. K., and Ross Friedman, C. (2011) Bioactivity and the first transmission electron microscopy immunogold studies of short de novo-designed antimicrobial peptides. *Antimicrobial Agents and Chemotherapy 55*, 2137-2145.

(96) Jenssen, H., Hamill, P., and Hancock, R. E. W. (2006) Peptide antimicrobial agents. *Clinical Microbiology Reviews 19*, 491-511.

(97) Martell, J. D., Deerinck, T. J., Sancak, Y., Poulos, T. L., Mootha, V. K., Sosinsky, G. E., Ellisman, M. H., and Ting, A. Y. (2012) Engineered ascorbate peroxidase as a genetically encoded reporter for electron microscopy. *Nature Biotechnology 30*, 1143-1152.

(98) Ellis, E. A. (2006) Epoxy resin embedding media. *Microscopy Today 14*, 50.

(99) Cronan, J. E. (2003) Bacterial membrane lipids: where do we stand? *Annual Review of Microbiology 57*, 203-224.